

Institute of Molecular Immunology, Helmholtz Center Munich

Group leader: Prof. Dr. Elfriede Nöbner



***Double strike approach for tumor attack: Engineering T cells
using CD40L:CD28 chimeric co-stimulatory proteins for
enhanced tumor targeting in adoptive cell therapy.***

Dissertation to obtain the Doctorate in Natural Sciences

at the Faculty of Medicine

Ludwig-Maximilian-University Munich

Submitted by

Luis Felipe Olguín Contreras

from

Durango, México

2021

"It always seems impossible until it is done"

Nelson Mandela

**In loving memory of my Father
Francisco Olguin**

All this effort and everything it represents
goes to you.

You are and will always be by my side.

**Printed with permission of the Faculty of Medicine
Ludwig-Maximilian-University Munich**

Supervisor: Prof. Dr. rer. nat. Elfriede Nöbner

Co-supervisor: Prof. Dr. rer. nat. Gerhild Wildner

Dean of the Faculty: Prof. Dr. med. Thomas Gudermann

Date of oral examination: 04.10.2021

Table of content

Table of content	4
Zusammenfassung	7
Abstract	9
List of abbreviations	10
1. Introduction	14
1.1 Immunity, T cell receptors and co-stimulatory signals	14
1.2 Adoptive cell therapy (ACT) using TCRs for cancer treatment.....	16
1.3 Immunosuppressive factors and cancer immunoescape	18
1.4 Chimeric proteins to improve ACT	19
1.5 Mechanisms of CD40/CD40L action in the immune system	21
1.6 Antitumor effect of CD40 ligation as a promising therapeutic approach	23
2. Objective of the Thesis	25
3. Materials	27
3.1 Equipment.....	27
3.2 Consumables	29
3.3 Reagents, kits and bacteria	31
3.3.1 Reagents.....	31
3.3.2 Kits	34
3.3.3 Bacteria	35
3.4 Media	35
3.4.1 Media and buffers	35
3.4.2 Prepared media and buffers	36
3.5 Plasmids, primers and restriction enzymes	39
3.5.1 Plasmids.....	39
3.5.2 Primers.....	51
3.5.3 Restriction enzymes.....	53
3.6 Chimeric protein sequences	54
3.7 Antibodies	58
3.7.1 Antibodies for cell culture.....	58
3.7.2 Antibodies for flow cytometry.....	58
3.7.3 Staining combinations.....	61
3.7.4 Antibodies for western blot.....	62
3.8 Primary cells and cell lines.....	63
3.9 Blood samples	64
3.10 Mice.....	64
4. Methods	65
4.1 Density gradient centrifugation for isolation of peripheral blood mononuclear cells (PBMC)	65
4.2 Cell counting, cryopreservation and thawing	65

4.3	Cultivation of human cell lines	66
4.4	Transient transfection of human T cells and HEK293 cell line using <i>ivt</i> -RNA	67
4.4.1	<i>In vitro</i> transcribed RNA (<i>ivt</i> -RNA) generation	67
4.4.2	Electroporation of cells with <i>ivt</i> -RNA	68
4.5	Retroviral transduction of Human T cells	68
4.6	Protein detection (Western Blot)	71
4.7	Molecular biology methods	73
4.7.1	Cloning CCP sequences into vectors for retroviral transduction and <i>in vitro</i> transcription	73
4.7.2	RNA isolation and quantitative reverse transcription PCR (qRT-PCR)	76
4.7.3	RNA isolation	76
4.7.4	cDNA synthesis	77
4.7.5	qRT-PCR analysis	78
4.8	Functional assays	79
4.8.1	Activation of antigen-specific T cells	79
4.8.2	Co-culture set up for analysis of T cell function	79
4.8.3	B cell activation assay	80
4.8.4	DC maturation assay	80
4.8.5	Enzyme-linked-immunosorbent assays (ELISA)	81
4.8.6	Chromium release assay	81
4.9	Flow cytometry	82
4.9.1	FACS analysis principle	82
4.9.2	Cell surface and intracellular markers FACS staining	83
4.9.3	Flow cytometry staining of phosphorylated signaling proteins	84
4.10	Mouse experiments	85
4.10.1	Human melanoma xenograft NSG model	85
4.10.2	Matriplug assay	86
4.10.3	Preparation of cell suspensions from NSG mice melanoma xenografts	87
4.11	Statistical analyses	88
5.	Results	89
5.1	CD40L:CD28 CCP design	89
5.2	Surface expression capability of the CD40L:CD28 CCPs	92
5.3	Culture conditions influence surface expression of the CD40L:CD28 CCPs	97
5.4	Downregulation of CD40L:CD28 CCPs by CD40 ligation.	104
5.5	Biological functionality of CD40L and CD28 domains in the CD40L:CD28 CCPs	107
5.5.1	Biological activity of the extracellular CD40L domain	107
5.5.2	Biological activity of the intracellular CD28 signaling domain	113
5.6	CD40L:CD28 CCPs improve T cell function	117
5.7	<i>In vivo</i> performance of CCPs composed of PD-1 extracellular domain and intracellular signaling domain CD28 (PD-1:CD28 CCP)	120
6.	Discussion	125
6.1	Chimeric protein design	127
6.2	Impact of chimeric protein design on protein expression	130
6.3	CCP surface expression is upregulated upon activation	132

6.4	CD40L:CD28 CCPs are biologically active.....	134
6.4.1	B cell activation assay.....	134
6.4.2	DC maturation assay	134
6.4.3	CD28 signaling assay	135
6.4.4	Cytokine secretion and cytotoxicity.....	136
6.5	<i>In vivo</i> studies and the role of CCPs for adoptive cell therapy	137
6.6	Outlook.....	138
	References	140
	Acknowledgements.....	151
	List of publications	153
	Affidavit	154

Zusammenfassung

Die Aktivierung von Kostimulationssignalen in zytotoxischen T-Zellen, die mit chimären Antigenrezeptoren (CAR) ausgestattet wurden, steigerte deren Effektoraktivität und Langzeitpersistenz, und verbesserte die Tumorabstoßung. Effektor-T-Zellen, die anstelle von CAR mit T-Zellrezeptoren (TZR) ausgestattet wurden, exprimieren oft keine Kostimulationsproteine, so dass sie keine Kostimulation erhalten können. Das Fehlen der Kostimulation steht einer robusten antitumoralen Antwort entgegen und schränkt die klinische Effektivität des adoptiven T-Zelltransfers mit TZR-transgenen T-Zellen ein. In soliden Tumoren stellt das Tumorstroma eine weitere Hürde dar, indem es das Eindringen der T-Zellen in den Tumor und die Aktivität der T-Zellen im Tumor vermindert. Ziel dieser Dissertation war es, chimäre Kostimulationsproteine (CCPs) herzustellen, die eine intrazelluläre signalgebende Domäne (ICD) eines Kostimulationsproteins mit der extrazellulären Domäne (ECD) eines anderen Proteins verbinden, für welches im Tumormilieu stimulierende Liganden exprimiert werden. Mit solchen CCPs sollen die Hürden einer effektiven Antitumorantwort bei soliden Tumoren überwunden werden, indem durch die CCPs die T-Zellaktivität verstärkt und gleichzeitig das Tumorstroma angegriffen wird.

In dieser Arbeit wurde die ECD des CD40L Proteins gewählt und mit der ICD von CD28 in einem chimären Protein vereinigt. Die Erwartung war, dass das CD40L:CD28 CCP sowohl die Kostimulationskaskade in T-Zellen initiiert und damit das TZR-Signal verstärkt, als auch über die CD40L ECD tumor-residente antigenpräsentierende Zellen (APC) aktiviert, das Tumorendothel verändert, so dass verstärkt T-Zellen transmigrieren und in den Tumor eindringen können, und TZR-MHC unabhängige Apoptose von Tumorzellen auslöst.

Die Kombination der ECD von CD40L mit der ICD von CD28 in einem Protein gestaltete sich schwierig, weil die Donorproteine unterschiedliche Membranorientierung besaßen. In dieser Arbeit werden verschiedene Lösungsmöglichkeiten für diese Herausforderung vorgestellt. Es wurden verschiedene Domänenverknüpfungen hergestellt und die Expression der CCP in T-Zellen gemessen. Es wurde beobachtet, dass das strukturelle Design, d.h. die Art und Weise wie die beiden Domänen verknüpft wurden, die Intensität der Expression auf der T-Zelloberfläche beeinflusste. Die Oberflächenexpression der CD40L:CD28 CCP zeigte weiterhin eine durch Aktivierung und antigenspezifische Stimulation regulierbare Dynamik. Die Ligation der CCP im Kontext einer TZR-Stimulation löste entsprechend der Erwartung den Signalweg des CD28 aus, welcher anhand der Phosphorylierung von AKT, mTOR und RPS6 gemessen werden konnte. T-Zellen, die ein CD40L:CD28 CCP exprimierten, sezernierten bei TZR-Stimulation mit

gleichzeitiger CCP-Ligation mehr Zytokin und zeigten verstärkte Zytotoxizität gegenüber Tumorzellen. In Kokulturrexperimenten von T-Zellen mit APC (B-Zellen, dendritische Zellen) induzierten T-Zellen, die CD40L:CD28 CCP exprimierten, die Maturierung der dendritischen Zellen und Aktivierung der B-Zellen, womit gezeigt wurde, dass die ECD des CD40L in den chimären Proteinen funktionell integriert war. Zum Nachweis, ob CCP *in vivo* Aktivität zeigen, wurde ein anderes CCP verwendet, welches ebenfalls die CD28 ICD besaß, diese aber mit der ECD von PD-1 verknüpft war. T-Zellen, die PD-1:CD28 exprimierten, zeigten nach adoptivem Transfer in ein humanes Melanomxenograft deutlich stärkere Proliferation, und das Wachstum des Xenografts wurde verzögert. Sollten sich in zukünftigen *in vivo*-Experimenten die positiven Ergebnisse des PD-1:CD28 CCP auch für das CD40L:CD28 CCP zeigen lassen, so wäre die Inklusion des CD40L:CD28 CCP in den T-Zell-Engineeringprozess äußerst vielversprechend, weil es die T-Zellen für den adoptiven T-Zelltransfer mit komplementären Eigenschaften aufrüsten wird, die sowohl Unterstützung der T-Zellfunktion als auch Angriff auf das Tumorstroma in Aussicht stellen.

Abstract

Activation of co-stimulatory pathways in cytotoxic T lymphocytes expressing chimeric antigen receptors (CARs) have proven to boost effector activity, tumor rejection and long-term T cell persistence. When using antigen-specific T cell receptors (TCR) instead of CARs, the lack of co-stimulatory signals hampers robust antitumoral response, limiting clinical efficacy. In solid tumors, tumor stroma poses an additional hurdle through hindrance of infiltration and active inhibition. Our project aims at generating chimeric co-stimulatory proteins (CCPs) consisting of an intracellular co-stimulatory domain (ICD) fused to an extracellular protein domain (ECD) for which ligands are expressed in solid tumors. These CCPs should help bypass the limited antitumoral response by boosting T cell effector functions and stromal attack.

In this thesis, the ECD of CD40L protein was selected for combination with the ICD from CD28 protein in different formats. It was expected that the CD40L:CD28 CCPs will not only provide co-stimulation and strengthen the TCR signaling, but also, through the CD40L ECD, facilitate the activation of tumor-resident antigen-presenting cells (APCs), modulate tumor endothelium for improved T cell transmigration and tumor infiltration and induce TCR-MHC independent apoptotic effect on tumor cells.

It was a challenge to combine the ECD of CD40L with the ICD of CD28 in one chimeric protein sequence due to the different membrane orientations of the donor proteins. In the thesis, I present solutions to this challenge and describe different CCP formats that were successfully expressed in human T cells along with an antigen-specific TCR.

It was observed that the structural design of the CCP strongly influenced intensity and dynamics of surface expression, which showed regulation through activation or antigen-specific stimulation. Ligation of the CCP in the context of TCR-stimulation modulated intracellular signaling cascades along the CD28 pathway including stronger phosphorylation of AKT, mTOR and RPS6, and led to improved TCR-induced cytokine secretion as well as cytotoxicity. Moreover, the CD40L ECD exhibited activity as evidenced by effective maturation and activation of APCs (dendritic cells and B cells).

Using a PD-1:CD28 CCP, adoptive T cells transfer was performed in a human melanoma xenograft mouse model. In the solid tumor environment, T cells expressing the PD-1:CD28 CCP showed improved persistence and stronger proliferation, which allowed better tumor control. Based on these results, CD40L:CD28 CCPs constitute a promising tool to be included in the engineering process of T cells to endow them with complementary features, i.e. T cell support and stromal attack, for improved performance in the tumor microenvironment.

List of abbreviations

Abbreviations	
7AAD	7-Aminoactinomycin D
aa	Amino acid
ACT	Adoptive cell therapy
ADCC	Antibody-dependent cell-mediated cytotoxicity
AICD	Activation-induced cell death
AKT (PKB)	Also known as protein kinase b
APC	Antigen presenting cell
APC	Allophycocyanin
APC-Cy7	Allophycocyanin – Cyanine 7
bp	Base pairs
BSA	Bovine serum albumin
BV421	Brilliant violet 421
Ca	Calcium
CAF	Cancer-associated fibroblasts
CAR	Chimeric antigen receptor
CCP	Chimeric co-stimulatory protein
CD	Cluster of differentiation
CD28i	CD28 inverted
CD40L	CD40 ligand
cDNA	Complementary desoxyribonucleic acid
CFDA-SE	Carboxyfluorescein diacetate succinimidyl ester
CFSE	Carboxyfluorescein succinimidyl ester
CML	Cell mediated lysis assay
Cq	PCR cycle number at which the samples reaction intersect the threshold line
CSR	Chimeric switch receptor
CTL	Cytotoxic T cell
DC	Dendritic cells
DCregs	Regulatory dendritic cells

DEPC	Diethylpyrocarbonate
DMEM	Dulbecco´s modified eagle medium
DMSO	Dimethyl sulfoxide
DNA	Desoxyribonucleic acid
ECD	Extracellular domain
EDTA	Ethylenediaminetetraacetic acid
eGFP	Enhanced green fluorescent protein
ELISA	Enzyme-linked immunosorbent assay
ER	Endoplasmic reticulum
FACS	Fluorescence activated cell sorting
FBS	Fetal bovine serum
FDA	Food and Drug administration
Fil3	Filamin 3 repeat
FITC	Fluorescein isothiocyanate
FSC	Forward side scatter
GAPDH	Glyceraldehyde 3-phosphate dehydrogenase
Gly	Glycine
HBSS	Hank´s buffered salt solution
HEK293 cells	Human embryonic kidney 293 cells
Hepes	4-(2-Hydroxyethyl)-1-piperazine-ethanesulfonic acid
HLA	Human leukocyte antigen
HRP	Horseradish peroxidase
HS	Human serum
i.p.	Intra peritoneal
ICD	Intracellular domain
iDCs	Immature dendritic cells
IFN-γ	Interferon-gamma
IgG	Immunoglobulin
IgGFc	Immunoglobulin Fc region
IL-	Interleukin-
Ivt-RNA	<i>In vitro transcribed</i> -RNA

JNK	C-Jun N-terminal kinase
kDa	Kilo Daltons
LB	Luria Broth
Lck	Leukocyte C-terminal sarcoma kinase
mDCs	Mature dendritic cells
MDSC	Infiltrating myeloid-derived suppressor cells
Mg	Magnesium
Min	Minutes
MMLV	Moloney murine leukemia virus reverse transcriptase
mRNA	Messenger Ribonucleic acid
ms	milliseconds
MSC	Mesenchymal stem cells
mTOR	Mammalian target of rapamycin
nCD40L	Native CD40 ligand
NK cells	Natural killer cells
nm	Nanometer
NOD	Non-obese diabetic
NSG mice	NOD/scid IL2Rgnull mice
PB	Pacific blue
PBL	Peripheral blood lymphocytes
PBMC	Peripheral blood mononuclear cells
PBS	Phosphate buffered saline
PCR	Polymerase chain reaction
PD-1	Programmed cell death protein-1
PE	Phycoerythrin
PE-Cy7	Phycoerythrin – Cyanine 7
PerCP-Cy5.5	Peridinin chlorophyll protein – Cyanine 5.5
PFA	paraformaldehyde
pg	picogram
PGE₂	Prostaglandin E2
PKC	Protein kinase C

PLCγ	Phospholipase Cgamma
pMHC	Peptide-major histocompatibility complex
pmol	picomolar
qPCR	Quantitative polymerase chain reaction
RCC	Renal cell carcinoma
RPMI-1640	Roswell Park Memorial Institute-1640 medium
RPS6	Ribosomal protein S6
RT	Room temperature
RT-PCR	Real time polymerase chain reaction
s	Seconds
s.c.	Subcutaneously
sCD40L	Soluble CD40 ligand
SCID	Severe combined immunodeficiency
Ser	Serine
SSC	Side scatter
TAA	Tumor associated antigens
TAM	Tumor-associated macrophages
TBS	Tris Buffered Saline
TCM	T cell medium
TCR	T cell receptor
TGF-β	Transforming growth factor-beta
TIL	Tumor infiltrating lymphocytes
TNF	Tumor necrosis factor
TRAF	TNF receptor-associated factor
Treg	Regulatory T cells
Tyr	Tyrosinase
VLE	Very low endotoxin

1. Introduction

1.1 Immunity, T cell receptors and co-stimulatory signals

The defense against different types of pathogens consists of more than just structural and chemical barriers. The main line of defense is accomplished by the immune system with its two branches, the innate and the adaptive immunity. The first response, which develops within minutes or hours after an aggression, corresponds to the innate immunity and doesn't generate immunologic memory. The other fundamental axis corresponds to the adaptive immunity, which is characterized as being antigen-dependent and specific. This grants the capacity to create memory, meaning that the organism will be able to mount a more rapid and efficient response upon later encounter with the antigen (1).

Specificity is the main characteristic of the adaptive immune response, consisting mainly of a cellular response guided by T cells and B cells expressing T cell (TCRs) and B cell (BCR, or immunoglobulin) receptors, respectively. The TCR is a heterodimer, which is for the majority of T cells, formed by an alpha (TCR- α) and a beta (TCR- β) chain. The TCR heterodimer interacts with CD3 chains in order to assemble the complete TCR structure capable of recognizing specific parts of an antigen (peptide) that is presented by a protein of the major histocompatibility complex (MHC). The interaction of the TCR-CD3 complex on the surface of a T cells with the peptide/MHC on the target cell initiates a complex signaling pathway that involves the phosphorylation of the CD3 chains and downstream activation of second messengers and kinases. This antigen-specific signaling, also described as signal 1, initiates T cell activation, but it is not enough for T cells to develop a sustained T cell functionality. For this, complementary signaling through other receptors on the cell surface, known as co-stimulatory receptors, are required (signal 2). The co-stimulation provides anti-apoptotic signals to unlock the proliferation capacity, it activates, amongst others, the transcription factor NF κ B for cytokine production and the AKT/mTOR pathway for effector activity, cell cycle progression and the ability to develop immunological memory. If co-stimulatory signals are missing T cells will be unable to respond to antigen-specific stimulation properly and become anergic, meaning that the T cells will not respond to subsequent antigen encounter. This state of

unresponsiveness is thought to be a control mechanism to avert T cell activation in non-dangerous situations (2).

Different molecules have been described to participate in this co-stimulatory process, like 4-1BB and members of the CD28 T cell co-stimulatory receptor family and also cytotoxic T lymphocyte antigen 4 (CTLA-4/CD152), inducible co-stimulatory (ICOS), OX40 (CD134), CD40 ligand (CD40L/CD154) and programmed death 1 (PD-1). Each molecule performs different functions, depending on the cellular context of their triggering. For example, 4-1BB activates cytokine induction in APCs, it prevents activation-induced cell death (AICD) and increases survival and CD8⁺ cytotoxic T cell (CTL) activity (3). CD28 mediated co-stimulation not only increases T cell activity by preventing anergy and increasing cytokine secretion, but in addition drives long lasting T cell activity. ICOS is known to stimulate IFN- γ production and activate CD4⁺ T cells. OX40/OX40L interaction drives memory development at a late activation point and extends the production of IL-2. At late time points after activation, T cells express molecules that will decrease effector function as a control mechanism to prevent exacerbated responses. Examples of these co-inhibitory molecules are CTLA-4 and PD-1 (4,5). CTLA-4 and CD28 bind to the same ligands, B7-1 and B7-2, also known as CD80 and CD86. Thereby, they support either inhibition or activation, respectively. Since CTLA-4 and CD28 are expressed at different activation states of the T cells, interaction with the same ligands has opposing outcome depending on the T cell activation stage with the late expressed CTLA-4/CD80/CD86 interaction causing inhibition and the early expressed CD28/CD80/CD86 interaction enabling activation (6). Typically, the strongest activation of CD8⁺ T cells results from stimulation through CD28 (7).

The basic principle of co-stimulation led to the concept of “checkpoints” for T cells. Different targeted approaches have been developed to either block the co-inhibitory receptors, PD-1 or CTLA-4 (checkpoint inhibitors) or boost co-stimulatory receptor signals with CD28 agonists. Both strategies aim to generate higher antitumor responses by T cells, since poor immunogenicity detected in many tumors could be caused by inappropriate delivery of signal 2 and an altered balance of T cell co-stimulation versus co-inhibition (Fig. 1) (8).

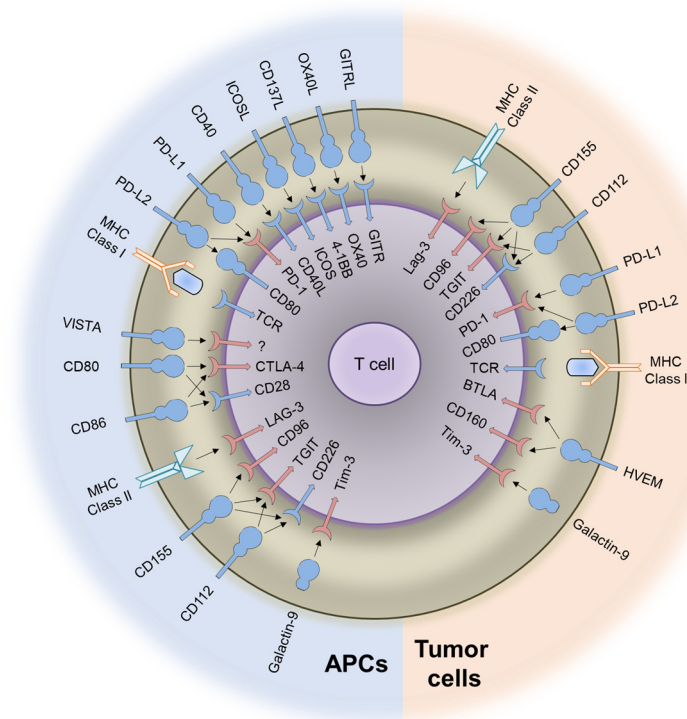


Figure 1. Co-inhibitory and co-stimulatory receptors expressed by T cells and their interaction partners expressed by antigen-presenting cells (left) and tumor cells (right). Inhibitory signaling is indicated by red symbols, stimulatory signals are displayed by blue symbols. Figure based on Zarour H. M., Clin. Cancer Res. 2016 (9).

1.2 Adoptive cell therapy (ACT) using TCRs for cancer treatment

Adoptive cell therapy (ACT) involves lymphocytes that are isolated from the patient. These cells are modified and expanded *ex vivo* to later be reinfused back into the patient. It has developed into a promising immunotherapy approach taking advantage of either the already existing antitumoral response of T cells or using engineering technology to redirect the T cells specifically against tumor cells (10,11). To allow T cell recognition of tumor cells, tumor cells need to express antigen that is different from normal cells. Antigenicity does occur since individual human tumors arise due to a combination of genetic and epigenetic changes that facilitate cell immortality by activation of genes that stimulate proliferation and protection against cell death, and inactivation of genes that normally inhibit proliferation (tumor suppressor genes) (12,13). As a consequence of these changes, these cells produce antigenic epitopes inform proteins that are normally expressed by cells of a given cell lineage (tumor-associated antigens – TAA), or new epitopes arise from proteins that are

exclusively expressed by the mutated cells (neo-antigens). These antigens can potentially be recognized by the immune system through TCR-MHC interaction and can be targets for cell destruction (**14**).

Various treatments exist to fight cancer, including surgery, radiation therapy or chemotherapy, monoclonal antibodies, targeted drugs or stem cell transplantation. Surgery achieves good results as long as the cancer is detected early and has not spread to other sites. Chemo- and radiotherapy lack tissue specificity and, therefore, are associated with damages of normal tissue. Targeted drugs are highly specific, but the development of drug tolerance is commonly observed. Finally, hematopoietic stem cell transplantation is effective, but selection of donors is difficult, and the graft has the propensity to be rejected (**15**).

Cancer treatment experienced an immense advance in the recent years, not only due to improved knowledge about the process of cancer development but also due to therapeutic progress including immunotherapy. The enormous benefit that immunotherapy has provided in cancer patient care was appreciated by awarding the 2018 Nobel prize in physiology and medicine to James P. Allison and Tasuku Honjo, who discovered the mechanisms how to harness the body's own immune system to fight cancer. Since then, much research has been focused on the field of how to improve the recognition and destruction of cancers by the immune system. Improvements in engineering technologies allowed the extension of using the natural ability of tumor infiltrating lymphocytes (TILs) expressing native TCRs to genetically engineered T cells that express transgenic TCRs or chimeric antigen receptors (CAR) to recognize and destroy tumor cells (**16,17**). TCR- and CAR-based adoptive cell therapy (ACT) allows the redirection of the T cell specificity in a highly specific manner thereby greatly extending the antigen range, and hence the cancer cells, that can be therapeutically targeted. While genetically engineered T cells produced promising results in hematologic disease leading to the FDA approval of two engineered T cell products (**18**), a wider application to solid tumors is still facing hurdles that require creative solutions (**19**).

1.3 Immunosuppressive factors and cancer immunoescape

Several major limitations impede clinical efficacy of ACT in solid tumors. These include the difficulty in selecting good target antigens, in isolating antigen-specific TCRs, the high diverse HLA restriction regarding antigens and patients, as well as diminished infiltration and T cell response in the tumor microenvironment (TME). Different mechanisms of immune escape and immunosuppression are present within the TME (**20**).

Cancer-induced immunosuppression reduces the antitumor effects of immunotherapies. The inhibitory microenvironment is the result of a complex network of interactions during tumorigenesis involving cancer cells, immune cells and other stromal cells, like mesenchymal stem cells (MSCs), cancer-associated fibroblasts (CAFs), regulatory T cells (Treg), infiltrating myeloid-derived suppressor cells (MDSCs), tumor-associated macrophages (TAMs), regulatory dendritic cells (DCregs), together with a variety of immunosuppressive factors (**21,22**). Within a complex stromal environment, cancer cells manage to escape immune recognition and subsequent destruction (immunoescape), even though the immune system would be capable of recognizing the tumor cell (immunosurveillance). The tumor immunoescape allows continuous tumor expansion, albeit the composition of the tumor cell population might change over time, a process described as immunoediting (**23**).

Tumor immunoescape and immunoediting are driven by acquisition of mutations and selection of characteristics that help evade the immune system. A tumor cell population is sculpted with reduced immunogenicity or increased ability to inhibit tumor immune responses. Immunoescape may be the result of diverse mechanisms like loss of MHC class I molecules or antigen presentation causing evasion of CTL attack. Approaches that target mainly immunodominant epitopes of tumor antigens might allow the proliferation of cells with a different phenotype in its "shadow". Furthermore, immunosuppressive cytokines like TGF- β and IL-10, which are secreted by tumor cells or the tumor stroma, can curb the immune response, and a modification of cell death signals may prevent tumor cell from undergoing apoptosis (**24**).

Co-inhibitory receptors (checkpoints) have been identified as hurdles to effective antitumor response. Physiologically, they are expressed in a regulated temporary kinetics and, thereby, are crucial to avoid exacerbated immune responses by

induction of T cell exhaustion. In situations of chronic exposure to antigen, co-inhibitory molecules are constantly expressed and causes progressive loss of T cell function, including the loss of proinflammatory cytokines like TNF- α and IFN- γ , the loss of cytotoxic activity, decreased proliferation and increased T cell apoptosis. T cells progressively express various co-inhibitory receptors like PD-1, CTLA-4, LAG-3 and TIM-3, the co-expression of which marks a point of terminal exhaustion that ends in deletion of T lymphocytes with high-affinity TCRs (25,26).

The appreciation that co-inhibition is a major impediment to antitumor immunity resulted in targeting strategies that counteract inhibitory and suppressive mechanisms. They are applied as monotherapy (immune checkpoint blockade) or together with therapeutic vaccines and strategies that regulate the tumor microenvironment and ACT, providing synergy through synthetic biology (16).

1.4 Chimeric proteins to improve ACT

Knowing that tumor cells can induce antigen-specific tolerance or anergy by several different mechanisms, T cells used for ACT require support to perform effective cytotoxicity and cytokine secretion and being able to proliferate and be protected from apoptosis. All of these support signals can result from specific co-stimulation. Therefore, T cells for ACT are engineered to receive co-stimulation in various ways (27). Synthetic biology combines elements of different disciplines, including engineering, chemistry, computer science and molecular biology, to gather necessary cellular and biological tools to improve the natural function of the infused T cells (28).

Transgenic TCRs can be engineered to incorporate the transmembrane and cytoplasmic domain of the co-stimulatory receptor CD28 linked to the cytoplasmic domain of the CD3 chain, allowing TCR signaling together with co-stimulation (29). This concept of combining the antigen-recognition with co-stimulation and TCR signaling in one protein sequence is realized in the design of chimeric antigen receptors (CARs) (Fig. 2). CARs are composed of an extracellular antibody binding domain, which allows T cells to recognize cell surface antigens, fused to the CD3 zeta signaling sequence (first generation of CAR). Second generations of CAR additionally incorporate intracellular co-stimulatory domains of CD28 or 4-1BB to facilitate co-stimulation for longer persistence and decreased

exhaustion (2nd generation of CAR designs). Meanwhile, further CAR designs are being explored, some including the secretion of cytokines to locally modulate the immunosuppressive tumor microenvironment, or the disruption of the PD-1 pathway to overcome inhibitory signals (30,31).

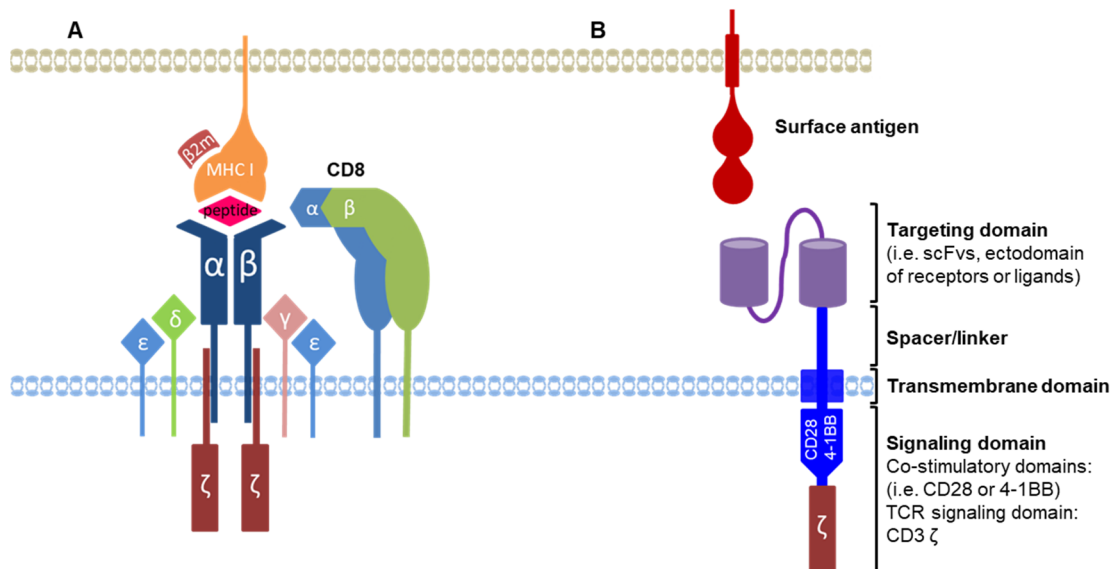


Figure 2. Comparison of T cell receptor (TCR) vs chimeric antigen receptor (CAR).

A) Schematic presentation of the TCR, showing the α and β chains in association with the different CD3 chain subunits. The TCR interacts with an MHC molecule that presents a peptide (pMHC) expressed on an antigen presenting cell. Phosphorylation of the CD3 chains upon pMHC recognition initiates an intracellular signaling cascade leading to T cell function. B) CAR is an engineered molecule designed to recognize surface antigens via a recognition domain derived from a specific antibody. The antibody targeting domain is connected through linkers and spacer with a signaling domains from co-stimulatory molecules. The main difference between TCR and CAR is the type of antigens that they can recognize, which is a surface expressed antigens in the case of CAR, while the TCR is able to recognize a wider range of antigens including intracellular antigens as long as they are presented by MHC molecules. Figure adaptation from Lee and Kim, Arch. Pharm. Res., 2019 (32)

Yet other approaches include the design of novel chimeric receptors that utilize inhibitory receptors or ligands expressed in the TME to convert them into support for T cell function. These types of receptors are commonly known as switch receptors (CSRs) or chimeric co-stimulatory proteins (CCPs). Several designs are currently explored, using the extracellular domain of an inhibitory receptor (CTLA-4, PD-1, TIGIT, CD200R, Fas) and linking it to an intracellular domain of a co-stimulatory protein like CD28, 4-1BB or OX40, obtaining activation upon engagement with an inhibitory ligand (28,33–39).

1.5 Mechanisms of CD40/CD40L action in the immune system

In addition to counteracting co-inhibition, activation of lymphocytes is also a key requirement for productive and effective adaptive immune response. Two prominent receptor/ligand pairs are the CD28/B7 (CD80 or CD86) and CD40/CD40L (CD154) interactions. In the CD40/CD40L interaction the signaling is primarily in the direction of the CD40 bearing cells, which are antigen presenting cells like DCs and B cells, leading to their activation. In contrast, the CD28/B7 interaction works in the opposite direction delivering positive co-stimulation signals to the CD28 expressing cells, which are predominantly T cells. An important link between these two pathways is that the CD40 ligation on the APCs results in upregulation of the B7 proteins, which in turn will interact with CD28 on T cells (Fig. 3) (6,40).

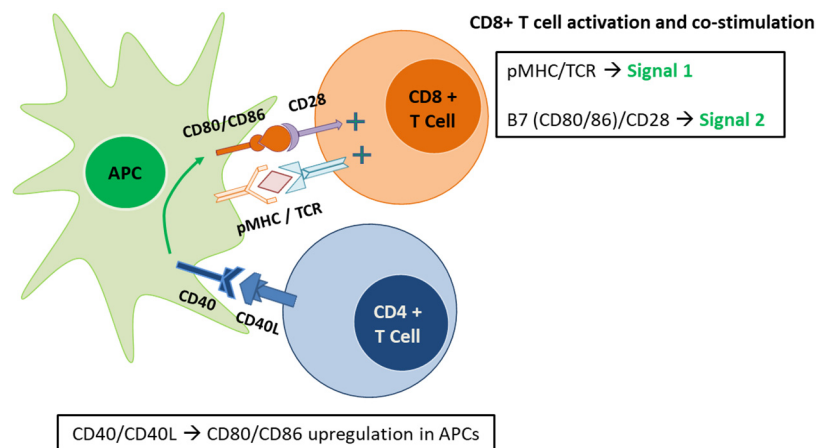


Figure 3. CD40 ligation upregulates B7 proteins (CD80/CD86) on APCs facilitating CD8⁺ T cell activation and co-stimulation by delivering signal 2 through CD28 ligation.

The CD40/CD40L pathway provoked attention within the immunology field as it is associated with both humoral and cellular immunity. The interaction between these two surface molecules influences B cell activation and expansion, and their differentiation into plasma cells capable of producing immunoglobulins. Furthermore, this interaction participates in macrophage activation enhancing their response against different types of pathogens. CD40L is known to induce strong stimulation of DCs, which allows them to robustly activate T cells and modulate T cell tolerance against self-antigens. Therefore, it has been reported

that blocking the signals derived from CD40/CD40L ligation will negatively impact important immunological responses (**41,42**). Mice lacking the expression of these molecules show an impaired innate and adaptive immunity, mainly manifested through poor licensing of APCs. (**43**).

CD40L belongs to the family of tumor necrosis factor (TNF) cell surface molecules. It is a type II membrane glycoprotein of 261 amino acid (aa), with a variable molecular weight between 32 and 39 kilo Daltons (kDa). A soluble form has been reported to have similar activities as the transmembrane form. CD40L is mainly expressed by CD4⁺ T cells, although it can also be expressed on activated B cells, platelets, and smooth muscle cells. The expression of CD40L on CD4⁺ T cells is tightly regulated with mRNA expression peaking 1 to 2 hours after stimulation. Cell surface protein is highest expressed after 4-6 hours and starts to decline at 16 hours being barely detectable or significantly reduced by 24 hours after activation (**44–46**). Although evidence suggests that the CD40/CD40L interaction directs signaling into the CD40 bearing cells, CD40L can also mediate co-stimulation via reverse signaling inducing phosphorylation of cellular proteins like Lck and phospholipase C γ (PLC γ), which further activate protein kinase C (PKC). Cross-linking with anti-CD40L antibodies was observed to trigger JNK and p38 activation, suggesting direct stimulatory function despite its short 22 aa cytoplasmatic tail (**47,48**).

CD40, the 43-50 kDa membrane receptor of the tumor necrosis factor (TNFR) superfamily, is expressed by APCs including DCs, macrophages and B cells, but expression can also extend to a variety of other normal cell types including neuronal cells, fibroblast, epithelial and endothelial cells, not to mention also expression in a wide range of carcinomas (**49**). Its expression may be induced or enhanced by various cytokines, including IFN- γ and TNF- α . The widespread expression indicates a broader role in human physiology and disease pathogenesis. Structurally, it comprises a 277 aa protein with a cytoplasmic tail that lacks intrinsic kinase activity. The signaling involves the ligand-dependent recruitment of adaptor proteins of the TNF receptor-associated factor (TRAF) family (**50**). Signaling cascades downstream of TRAFs modulate diverse survival and growth-related genes depending on the cell type with which the interaction occurs. CD40 signaling exerts profound effects on DCs by promoting their cytokine production, the induction of surface co-stimulatory molecules and

facilitating antigen presentation. Overall, CD40 signals license DCs to mature and be able to trigger T cell activation. In B cells, CD40 signals promote immunoglobulin (Ig) isotype switch, and formation of long-lived plasma cells and memory B cells (51).

1.6 Antitumor effect of CD40 ligation as a promising therapeutic approach

Multiple signals that modulate a wide range of immunological responses, including survival and cell death, cell maturation and expansion, find a common connection with CD40 expression (52,53).

In epithelia, the outcome of CD40/CD40L signaling depends on the context and intensity of the interaction. Strong CD40 signaling has been associated with cell death through apoptosis, while weak signals may cause cell growth and expansion (54). CD40 ligation has been shown to stimulate a host antitumor immune response in numerous tumor models, and CD40 expression was detected in several solid tumors including breast cancer, lung cancer, colorectal cancer, renal cell carcinoma, melanoma, bladder cancer and B-lineage malignancies. Correlations between An association with CD40 expression and patient survival has been suggested in the past, and several results obtained from lung and esophageal malignancies suggest that CD40 expression correlates with a poor prognosis. The observation that tumor tissue tends to overexpress CD40 compared to the low detection on normal tissue has further triggered interest in targeting this receptor therapeutically (55). Different approaches of stimulating the CD40/CD40L signaling are tested, including CD40L soluble molecules, agonistic monoclonal antibodies, and genetic means aiming to increase CD40L expression. Yet, it is not completely understood how CD40 causes cell apoptosis in tumor cells, since its intracellular domain is short and substantially different to death domains found in other death inducing proteins (Fas, TNFR1 and TNF-related apoptosis-inducing ligand (TRAIL)). The mechanisms by which CD40 transduces death signals may occur via autocrine/paracrine induction of death ligands such as TNF- α or functional Fas ligand (FasL), or TRAIL in apoptosis susceptible carcinoma cells. Another way could be the upregulation of the Fas-death receptor through the TRAF adaptor proteins (56). Agonistic anti-CD40 antibodies were shown to mediate antibody-dependent cell-mediated cytotoxicity

(ADCC), an activity that was strongly enhanced when the Fc end of the anti-CD40 antibody was engineered for increased Fcγ receptor (FcγR) binding (57).

Membrane-presented CD40L (mCD40L) was found to cause extensive apoptosis in situations where soluble agonist antibodies caused little apoptosis. However, the outcome of mCD40L ligation was cell context dependent and induced apoptosis and pro-inflammatory cytokine secretion in CD40 expressing malignant renal cell carcinoma while normal renal cells were completely refractory to CD40 mediated killing although they also expressed CD40 (58).

The role of CD40L in immune regulation was further explored using CD40L-modified T cells. Augmented immunogenicity of CD40⁺ tumor cells was observed by the upregulation of surface expression of co-stimulatory molecules (CD80 and CD86), adhesion molecules (CD54, CD58 and CD70) and HLA molecules (MHC I and MHCII) (59). CD40L expressing CD8⁺ T cells were able to activate tolerogenic DCs in prostate tumor draining lymph nodes leading to increased proliferation, IFN-γ secretion and T cell infiltration (60,61).

Latest advances in reprogramming T cells for improved tumor targeting in ACT led to CARs that constitutively express the immunostimulatory molecule CD40L. Results from this type of approach demonstrated that CD40L⁺ CAR T cells could circumvent tumor immune escape due to antigen loss by exerting antigen-independent CD40/CD40L-mediated cytotoxicity. In addition, induction of a sustained, endogenous immune response with superior antitumor efficacy was observed that involved licensing of APCs and enhancing recruitment of immune effectors (62). The true significance of this approach is that it not only augments the effector functions of CAR T cells in ACT, but also affects the tumor microenvironment. Thereby it promises a greater therapeutic potential in immunotherapy than the activation of the CD40/CD40L pathway alone.

2. Objective of the Thesis

Various approaches are being explored in order to prevent TCR-transgenic T cells from developing deficits in effector function at the tumor milieu and to counteract poor *in vivo* persistence. The loss of CD28 in effector T cells likely represents one of the main problems that deprives adoptively transferred T cells of proper supportive co-stimulatory signals. Co-stimulation enhances TCR signaling and effector function, but also extends the operative life span of CTLs (63). Therefore, the idea of developing a chimeric co-stimulatory protein (CCP) consisting of an intracellular co-stimulatory sequence fused with an extracellular protein domain for which ligands are expressed in the milieu of solid tumors was the aim of this dissertation. CD40L (CD154) was selected as the donor for the extracellular domain because its ligand CD40 is aberrantly expressed on many carcinoma cells. Additional antitumor benefits are expected as CD40-CD40L interactions have functional importance for a number of other cell types, such as antigen presenting cells (APCs) and endothelial cells.

CD40L:CD28-engineered T cells should support the antitumor response on four distinctive axes as shown below:

1) Strengthening the MHC/peptide-triggered TCR signaling through eliciting an intracellular co-stimulatory signaling cascade potentially allowing the T cells to overcome inhibition of effector function in the tumor milieu.

2) Activation of tumor-resident CD40-expressing DCs. Interaction of CD40 on DCs with CD40L expressed on the engineered T cells could induce signals in DCs leading to their maturation with gain in *de novo* priming capability.

3) Modulation of tumor endothelium. CD40 is expressed on neovascular endothelium and can be up-regulated by TNF- α and IFN- γ . The stimulation of CD40 activates the endothelium and has been shown to induce lymphocyte adhesion and transmigration (64–66). Targeting this stromal compartment could potentially enhance the immunotherapy effect by increasing the number of tumor-infiltrating engineered T cells.

4) Apoptotic effects on tumor cells. It is reported that tumor cells aberrantly express CD40 and that CD40 signals induce apoptotic cell death independent of MHC/peptide-specific targeting (**67,68**). Thus, CD40L:CD28-engineered T cells may kill tumor cells expressing CD40 even if they do not present the cognate TCR-MHC ligand.

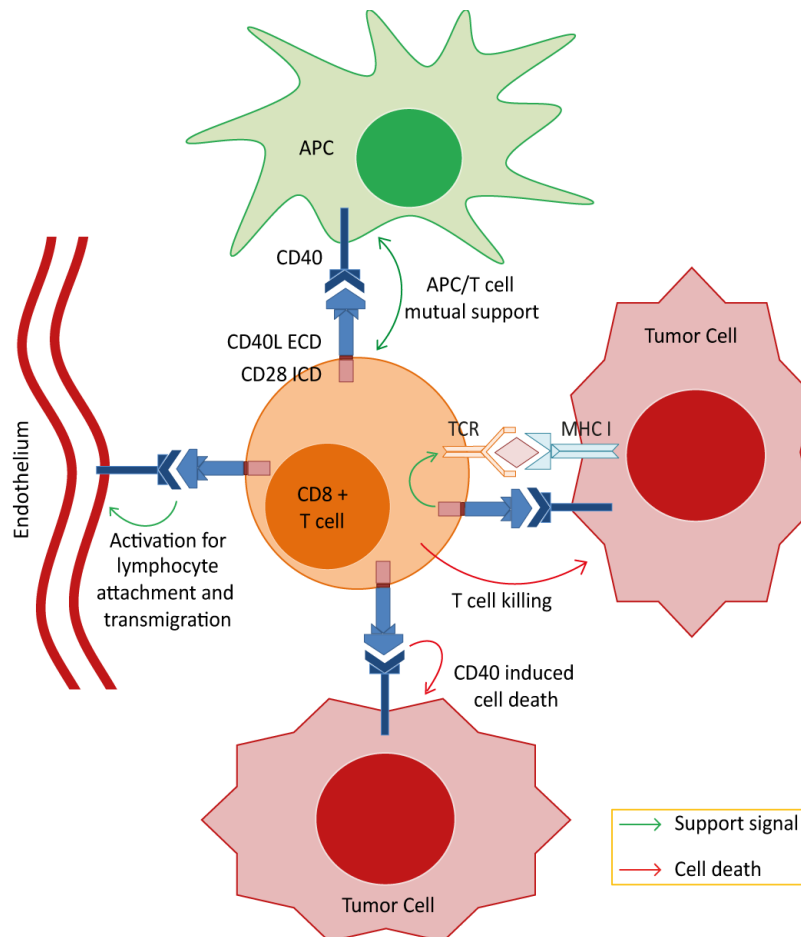


Figure 4. Postulated effector mechanisms for the CD40L:CD28 chimeric co-stimulatory protein.

Depicted are the 4 potential axes of effector mechanisms of T cells engineered with the CD40L:CD28 CCP when interacting with different components of the tumor microenvironment as described in the text.

Procedures of this thesis involved the molecular engineering of the chimeric CD40L:CD28 CCP, followed by transgenic expression in human T cells. Co-culture experiments were used to assess functional activity of the CCPs regarding the 4 postulated effector mechanisms outlined in Figure 4.

3. Materials

This thesis is embedded in the larger research topic of the group of E. Nößner. A previous doctoral thesis was performed by R. Schlenker, which is available on the webpage of the LMU (69). Therefore, overlaps in Material and Methods exist. Parts of the original work of this thesis, including the adoptive T cell transfer in human xenograft NSG mice, contributed to the publication by R. Schlenker with L. Olguin Contreras as second author (70).

3.1 Equipment

EQUIPMENT	COMPANY
Automatic X-ray Film Processor	AGFA
Balance PC 400 Delta Range	Mettler, Giessen Germany
Centrifuge 4K15	Sigma Laboratory Centrifuges
Centrifuge 5417 R	Eppendorf, Hamburg Germany
Cover glass for Neubauer counting chambers 20 x 26 mm, depth 0.4 mm	Hirschmann Laborgeräte, Eberstadt Germany
Flow Cytometer LSR II	Becton Dickinson, Heidelberg Germany
Incubator	Hereaus Instruments, Hanau Germany
Innova 4200 Shaker	New Brunswick Scientific, Edison USA
Integral water purification system Milli-Q®	Millipore, Schwalbach Germany
Light Cycler® 96 480 Multiwell Plate 96, white	Roche Diagnostics Deutschland GmbH, Mannheim, Germany
Light Cycler® 96 480 Sealing Foil	Roche Diagnostics Deutschland GmbH, Mannheim, Germany
Light Cycler® 96 Instrument	Roche Diagnostics Deutschland GmbH, Mannheim, Germany
Light microscope Leica DMLS	Leica Microsystems, Heidelberg Germany
Light microscope Zeiss Axioskop	Carl Zeiss Micro Imaging GmbH, Göttingen Germany
Magnets MACS®	MiltenyiBiotec, Bergisch Gladbach, Germany

Megafuge 2.0 R centrifuge	Heraeus Instruments, Hanau Germany
Mr Frosty™ Freezing container	ThermoFischer Scientific/Catlag, Waltham Massachusetts
Multistepper	Eppendorf, Hamburg Germany
Nanodrop ND-1000-Spektrophotometer	Peqlap Biotechnologie GmbH, Erlangen
Neubauer counting chamber depth 0.1 mm	Gesellschaft für Laborbedarf Würzburg, Germany
Nutating mixer	VWR International, Ismaning Germany
Pipettes Single- and multi-channel	Eppendorf, Hamburg Germany Thermo Scientific, Waltham USA
Pipettor Pipetus®	Hirschmann Laborgeräte, Eberstadt Germany
Polymax 1040 Shaker	Heidolph
Polymerization chain reaction machine Flex cyclor	Analytik, Jena Germany
PowerPac™ 200 electrophoresis power supply	BIO-RAD, Feldkirchen Germany
Rotanda 460R centrifuge	Hettich, Ebersberg Germany
Rotator	VWR, Darmstadt Germany
Scintillation counter TopCount NXT	Canberra-Packard, Dreieich Germany
Scissors and tweezers	NeoLab, Heidelberg Germany
Spectrophotometer	Tecan Group AG, Männedorf Switzerland
Sterile laminar flow hood	BDK Luft- und Reinraumtechnik GmbH, Sonnenbühl-Genkingen Germany
Syringes for multistepper 5ml	Eppendorf, Hamburg Germany
Thermocycler TGradient 48	Biometra GmbH, Göttingen, Germany
Thermomixer 5436	Eppendorf, Hamburg Germany
Thermomixer compact	Eppendorf, Hamburg, Germany

UV light imaging system InGenius	Syngene Bio Imaging, Cambridge UK
Vortexer MS1 Minishaker	IKA Werke GmbH & Co KG, Staufen Germany
Water bath	Köttermann Labortechnik, Uetze Germany
XCell II™ Blot Module	Thermo Fisher Scientific, Schwerte Germany
XCell SureLock Mini-Cell electrophoresis chamber	Thermo Fisher Scientific, Schwerte Germany
X-ray Film cassette	CAWO 24x30 cm

3.2 Consumables

CONSUMABLES	COMPANY
24-well plates Tissue culture treated Non-tissue culture treated	Becton Dickinson Falcon, Heidelberg Germany
96-well plates, with filter (LUMA)	Canberra Packard, Dreieich Germany
Amersham PVDF Hybond membrane	GE Healthcare, distributed by Merck
Bolt™ 4 to 12%, Bis-Tris, 1.0 mm, mini protein gel 15-well	Invitrogen, life technologies
Casted gels for WB	Invitrogen
Cell strainer 40 µm, 100 µm	Becton Dickinson Falcon Heidelberg Germany
Disposable pipette tips for pipettor 10 ml, 25 ml	Greiner bio-one, Frickenhausen Germany
Filter 0.45 µm	Millipore, Schwalbach Germany
Flow cytometry polypropylene tubes 1 ml	Greiner bio-one, Frickenhausen Germany
Flow cytometry polypropylene tubes 5 ml	Becton Dickinson Falcon, Heidelberg Germany

Freezing vials 1.5 ml	Nunc, Wiesbaden Germany
Glass Pasteur pipettes	Josef Peske GmbH & Co KG, Munich Germany
Glass pipette tips for pipettor 2 ml, 5 ml, 10 ml, 20 ml	Hirschmann Laborgeräte, Eberstadt Germany
Magnetic cell separation columns LS columns, pre-separation columns	MiltenyiBiotec, Bergisch Gladbach Germany
Needles, 26G	NeoLab, Heidelberg Germany
Nunclon™ Delta flasks	Thermo Fisher Scientific, Schwerte Germany
Parafilm®	Pechiney Plastic Packaging, Menasha USA
Pipette tips with and without filter 1-10 µl, 10 – 200 µl, 200 – 1000 µl	Eppendorf, Hamburg Germany
Polypropylene tubes 1.5 ml, 2 ml	Eppendorf, Hamburg Germany
Polypropylene tubes 15 ml, 50 ml	Becton Dickinson Falcon, Heidelberg Germany
Polystyrene petri dishes 100 mm	Becton Dickinson Falcon, Heidelberg Germany
Scalpels	Braun, Tuttlingen Germany
Sterile filtration tubes (0.2 µm) 50 ml	Becton Dickinson Falcon, Heidelberg Germany
Syringes 1 ml, 10 ml, 50 ml	Eppendorf, Hamburg Germany
Winged infusion set	Dispomed Witt oHG, Gelnhausen Germany
X-ray film	GE Healthcare, distributed by Merck

3.3 Reagents, kits and bacteria

3.3.1 Reagents

REAGENTS	COMPANY
1-Bromo-3-chloropropane	Sigma-Aldrich, Taufkirchen Germany
4-(2-Hydroxyethyl)-1-piperazine-ethanesulfonic acid (HEPES)	Biochrom AG, Berlin Germany
⁵¹Cr Sodium chromate	Hartmann Analytic, Braunschweig Germany
7-Aminoactinomycin D (7-AAD)	Sigma-Aldrich, Taufkirchen Germany
Accutase[®]	PAA Laboratories, Cölbe Germany
Acetic acid	Merck, Darmstadt Germany
Agarose, Electrophoresis grade	GIBCO, Thermo Fisher Scientific, Schwerte Germany
Amersham ECL Prime Western Blot detection reagent	GE Healthcare, distributed by Merck
Ampicillin	Sigma-Aldrich, Taufkirchen Germany
Beads for compensating fluorescence activated cell sorting (FACS) data	Becton Dickinson Pharmigen, Heidelberg Germany
Biocoll[®] separating solution (Ficoll[®])	Biochrom AG, Berlin Germany
Bovine serum albumin (BSA)	Sigma-Aldrich, Taufkirchen Germany
Carboxyfluorescein diacetate succinimidyl ester (CFDA-SE)	Invitrogen, Karlsruhe Germany
CD40L, soluble (human) (recombinant) set	Enzo Life Sciences, Lausen Switzerland
CellTracker[™] Deep Red fluorescent dye	Thermo Fisher Scientific, Schwerte Germany
Collagenase IV	Sigma-Aldrich, Taufkirchen Germany

cOmplete™ EDTA-free protease Inhibitor Cocktail	Roche, Distributed by Sigma-Aldrich
Diethylpyrocarbonate (DEPC)	Sigma-Aldrich, Taufkirchen Germany
Dimethyl sulfoxide (DMSO)	Sigma-Aldrich, Taufkirchen Germany
Disodium hydrogen phosphate	Sigma-Aldrich, Taufkirchen Germany
Dispase	Corning Life Sciences, Amsterdam Netherlands
DNA Ladder, 1kb	Thermo Fisher Scientific, Schwerte Germany
DNAloading dye 6x	Thermo Fisher Scientific, Schwerte Germany
DNase I, type IV	Sigma-Aldrich, Taufkirchen Germany
EDTA disodium	Roth, Karlsruhe Germany
Ethanol, 99%	Merck, Darmstadt Germany
Ethidium bromide 10 mg/ml	Roth, Karlsruhe Germany
Ethylenediaminetetraacetic acid (EDTA), 0.5 M	Sigma-Aldrich, Taufkirchen Germany
Fetal bovine serum (FBS)	GIBCO, ThermoFisher Scientific, Schwerte Germany
Glycine	Sigma-Aldrich, Taufkirchen Germany
Heparin-sodium	B. Braun, Melsungen Germany
Human Serum (HS)	In-house production
Ionomycin	Sigma-Aldrich, Taufkirchen Germany
Isopropanol	Sigma-Aldrich, Taufkirchen Germany
L-glutamine	GIBCO, ThermoFisher Scientific, Schwerte Germany
Linear Acrylamide	Thermo Fisher Scientific, Vilnius Lithuania
LIVE/DEAD™ Fixable Blue Dead Cell Staining Kit	Thermo Fisher Scientific/Caltag, Waltham Massachusetts USA
Luria Broth and agar powder	Roth, Karlsruhe Germany

Corning® Matrigel® Basement membrane matrix growth factor reduced, Phenol red free	Corning Life Sciences, Amsterdam Netherlands
Methanol	Merck, Darmstadt Germany
Milk powder	Roth, Karlsruhe Germany
Mucocit disinfectant cleaner	Mucocit disinfectant cleaner
Non-essential amino acids	GIBCO, ThermoFisher Scientific, Schwerte Germany
Paraformaldehyde (PFA)	Merck, Darmstadt Germany
PCR MasterMix, 2x	Promega, Mannheim Germany
Penicillin/Streptomycin	GIBCO, ThermoFisher Scientific, Schwerte Germany
PGE₂	Promokine, PromoCell, Heidelberg, Germany
Phorbol-12-myristate-13-acetate (PMA)	Sigma-Aldrich, Taufkirchen Germany
Phosphoric acid, 1M	Sigma-Aldrich, Taufkirchen Germany
PKH26 Red fluorescent linker kit	Sigma-Aldrich, Taufkirchen Germany
Potassium hydrogen carbonate	Roth, Karlsruhe Germany
Precision Plus Protein™ All blue standards	BIO-RAD, Feldkirchen Germany
Recombinant human GM-CSF	Promokine, PromoCell, Heidelberg, Germany
Recombinant human IL-15	Promokine, PromoCell, Heidelberg, Germany
Recombinant human IL-1β	Promokine, PromoCell, Heidelberg, Germany
Recombinant human IL-2	Cancernova GmbH, Reute, Germany
Recombinant human IL-4	Promokine, PromoCell, Heidelberg, Germany
Recombinant human IL-6	Sigma-Aldrich, Taufkirchen Germany
Recombinant human TNF-α	Immunotools, Friesoythe Germany
Retronectin®	Takara Bio Incorporation, Shiga Japan
RNA ladder	Thermo Scientific, Schwerte Germany

RNA loading dye, 2x	Thermo Scientific, Schwerte Germany
Roti[®]-Load 1 western blot loading buffer	Roth, Karlsruhe Germany
Saponin	Merck, Darmstadt Germany
Sodium Chloride 150mM	Sigma-Aldrich, Taufkirchen Germany
Sodium pyruvate	GIBCO, ThermoFischer Scientific, Schwerte Germany
TAE, 10x	GIBCO, ThermoFischer Scientific, Schwerte Germany
TransIT[®]-LT1 Reagent	Mirus Bio LLC, Madison USA
TRI Reagent[®]	Sigma-Aldrich, Taufkirchen Germany
Tris 50 mM, pH 8.0	United states Biomedicals
Triton X-100	MP Biomedicals
Trypan blue	Sigma-Aldrich, Taufkirchen Germany
Trypsin-EDTA	GIBCO, ThermoFischer Scientific, Schwerte Germany
Tween20	Sigma-Aldrich, Taufkirchen Germany
Water Milli-Q[®] purified	In house production
Water Nuclease-free	Promega, Mannheim, Germany
β-Mercaptoethanol	GIBCO, ThermoFisher Scientific, Schwerte Germany

3.3.2 Kits

KIT	COMPANY
AffinityScript qPCR cDNA Synthesis Kit	Agilent, Santa Clara, CA, USA
Gel extraction Kit	Quiagen, Hilden Germany
Human IFN-γ and IL-2 ELISA Kit	BD Bioscience, Heidelberg Germany
JetStar 2.0 preparation kit	Genomed GmbH, Löhne Germany

MicroBCA™ protein assay kit	Thermo Scientific, Schwerte Germany
MinElute® Reaction Cleanup kit	Quiagen, Hilden Germany
mMESSAGE mMACHINE Kit	Ambion®, Schwerte Germany
Naïve B Cell Isolation Kit II, human	Miltenyi Biotec, Bergisch Gladbach Germany
RNeasy Mini Kit	Quiagen, Hilden Germany

3.3.3 Bacteria

BACTERIA	USE	COMPANY
TOP10 and MACH1 <i>E. coli</i> (+SOC medium)	Transformation with Geneart, pGEM and pMP71 vectors	Life technologies, Schwerte, Germany

3.4 Media

3.4.1 Media and buffers

MEDIUM / BUFFER	COMPANY
BD Cytotfix/Cytoperm Fixation/Permeabilization Kit	BD Biosciences, Heidelberg Germany
BD Phosflow™ Perm Buffer III	BD Biosciences, Heidelberg Germany
Cytotfix™ Fixation Buffer	BD Biosciences, Heidelberg Germany
Dulbecco's modified eagle medium (DMEM)	Invitrogen, Karlsruhe Germany
Dulbecco's phosphate buffered saline (PBS)	GIBCO Invitrogen, Darmstadt Germany
Hank's buffered salt solution (HBSS) w/o and with Ca²⁺ Mg²⁺	GIBCO Invitrogen, Darmstadt Germany
MOPS-SDS 20x running buffer	Invitrogen, Karlsruhe Germany
NuPAGE 20x Transfer buffer	Invitrogen, Karlsruhe Germany

Opti-MEM	GIBCO Invitrogen, Darmstadt Germany
Roswell Park Memorial Institute (RPMI)-1640 medium	GIBCO Invitrogen, Darmstadt Germany
Tris Buffered Saline (TBS) 10x buffer	BIO-RAD, Feldkirchen Germany
Very low endotoxin (VLE) RPMI-1640	Biochrom AG, Berlin Germany

3.4.2 Prepared media and buffers

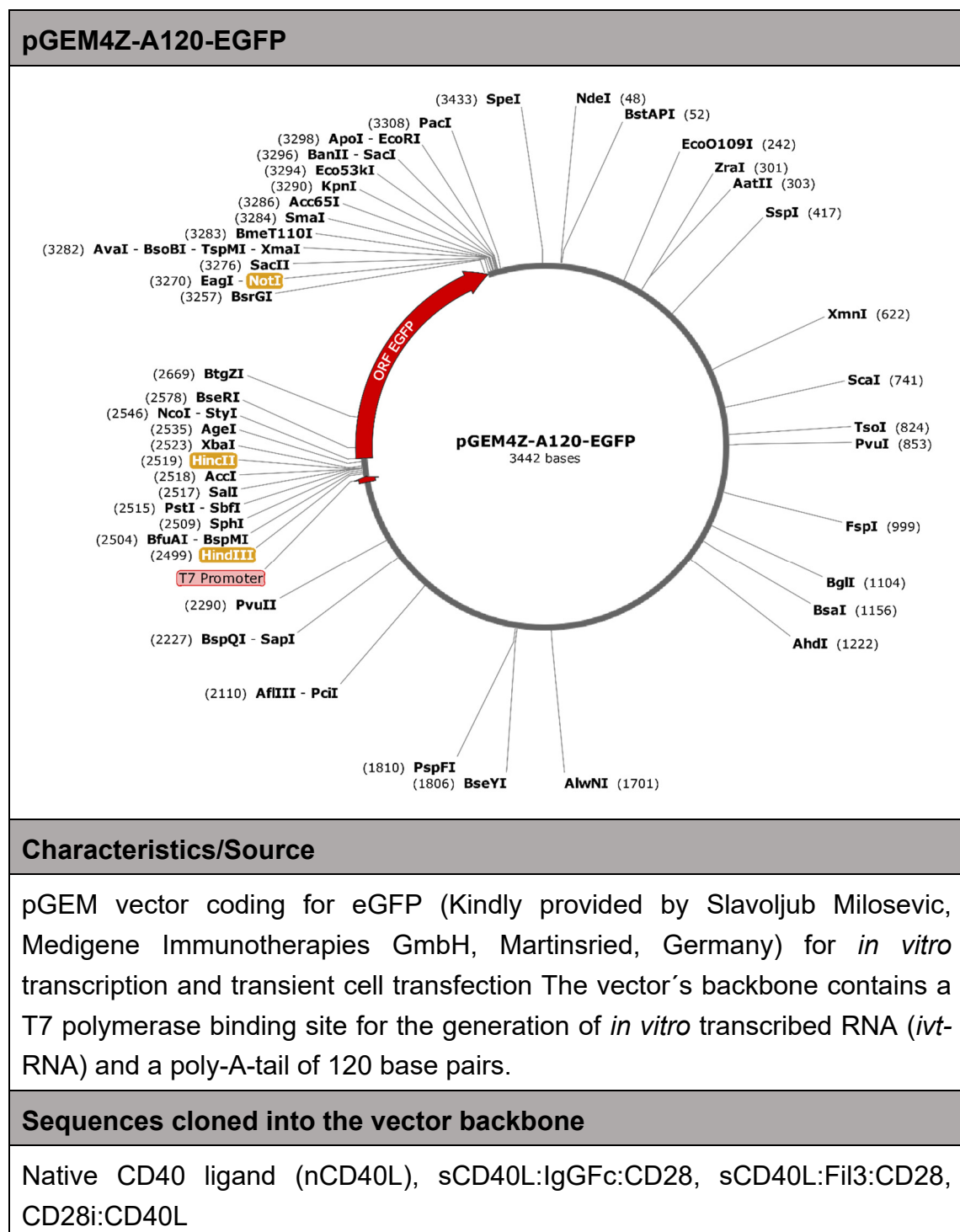
MEDIUM / BUFFER	COMPOSITION
Cell freezing medium	RPMI-1640 + 1% L-glutamine + 1% non-essential amino acids + 1% sodium pyruvate + 20% DMSO
CML medium	RPMI-1640 + 1% L-glutamine + 1% non-essential amino acids + 1% sodium pyruvate + 15% FBS
DC medium	VLE RPMI-1640 + 1.5% HS
Digestion buffer for murine tumors	RPMI-1640 + 0.1% BSA + 1% penicillin/streptomycin + 10 mM HEPES + 218 U/ml collagenase IV + 435 U/ml DNase I, type IV
ELISA coating Buffer, pH 9.5	Milli-Q® purified water + 8.4 g sodium hydrogen carbonate + 3.56 g sodium carbonate
ELISA washing buffer	PBS + 0.05% Tween20

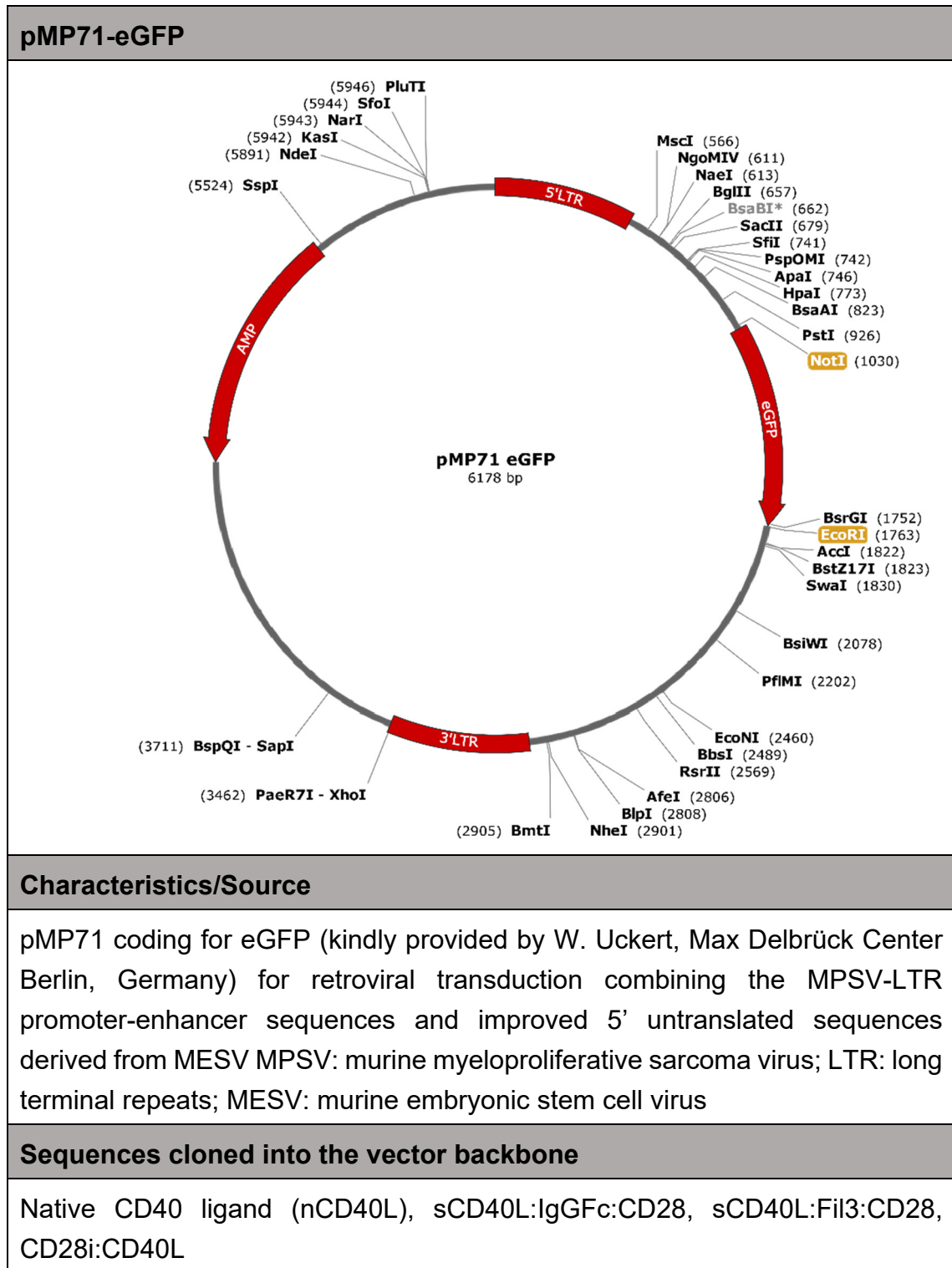
FACS fixation buffer	PBS + 1% PFA
Fluorescence activated cell sorting (FACS) buffer	PBS + 2mM EDTA + 2% HS + 0.1% sodium azide
HEK293 cell medium	DMEM + 1% L-glutamine + 1% non-essential amino acids + 1% sodium pyruvate + 12% FBS
LB Medium	500 ml Milli-Q® water + 12.5 g LB powder + 100 µg/ml ampicillin
Magnetic cell separation buffer (MACS buffer)	PBS + 0.5% FBS + 2 mM EDTA
Medium for human T cells (TCM)	RPMI-1640 + 1% L-glutamine + 1% non-essential amino acids + 1% sodium pyruvate + 10% HS
NP-40 lysis buffer	150 mM sodium chloride 1 % Triton X-100 50 mM Tris, pH 8.0
RCC medium	RPMI-1640 + 1% L-glutamine + 1% non-essential amino acids + 1% sodium pyruvate + 12% HS
RPMI 4' medium	RPMI-1640 + 1% L-glutamine + 1% non-essential amino acids + 1% sodium pyruvate + 10% FBS
Running Buffer (Western Blot)	50 ml MOPS-SDS 20x running buffer + 950 ml ultra pure Milli-Q® water

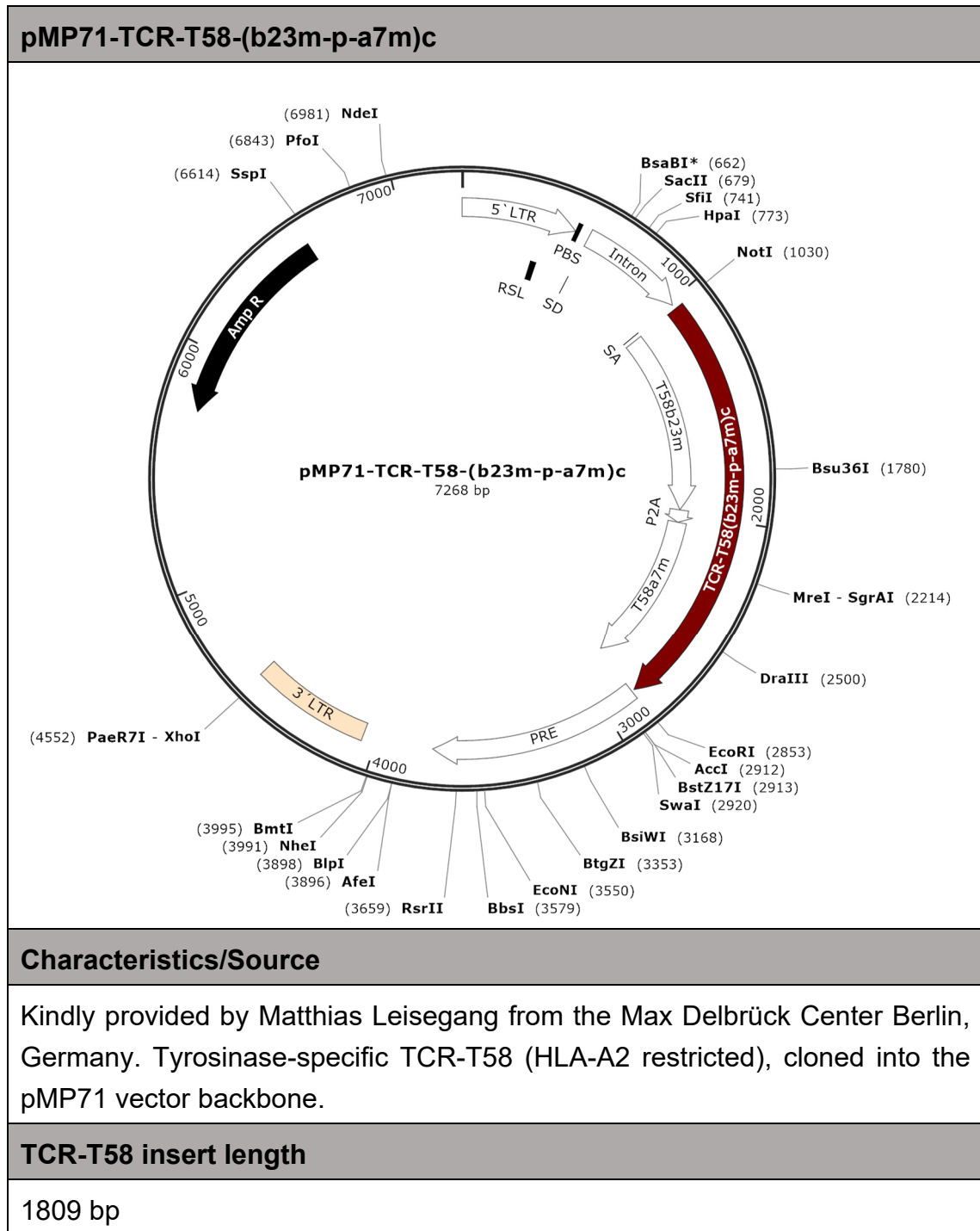
TBST (Western Blot)	100 ml of TBS 10x + 900 ml ultra-pure Milli-Q® water + 1 ml Tween20
Transfer Buffer (Western Blot)	100 ml TBS 10x + 900 ml ultra pure Milli-Q® wáter + 1 ml Tween20

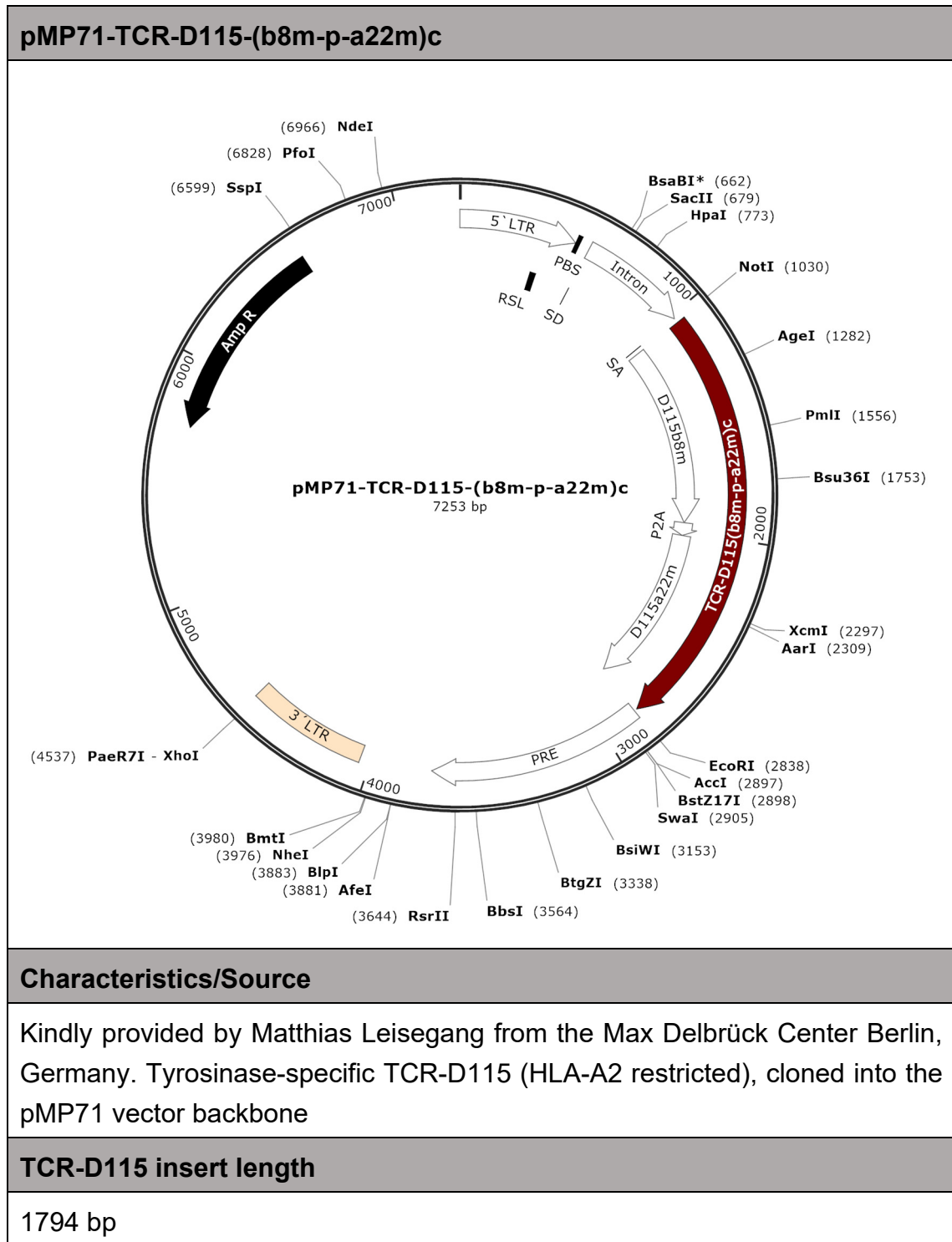
3.5 Plasmids, primers and restriction enzymes

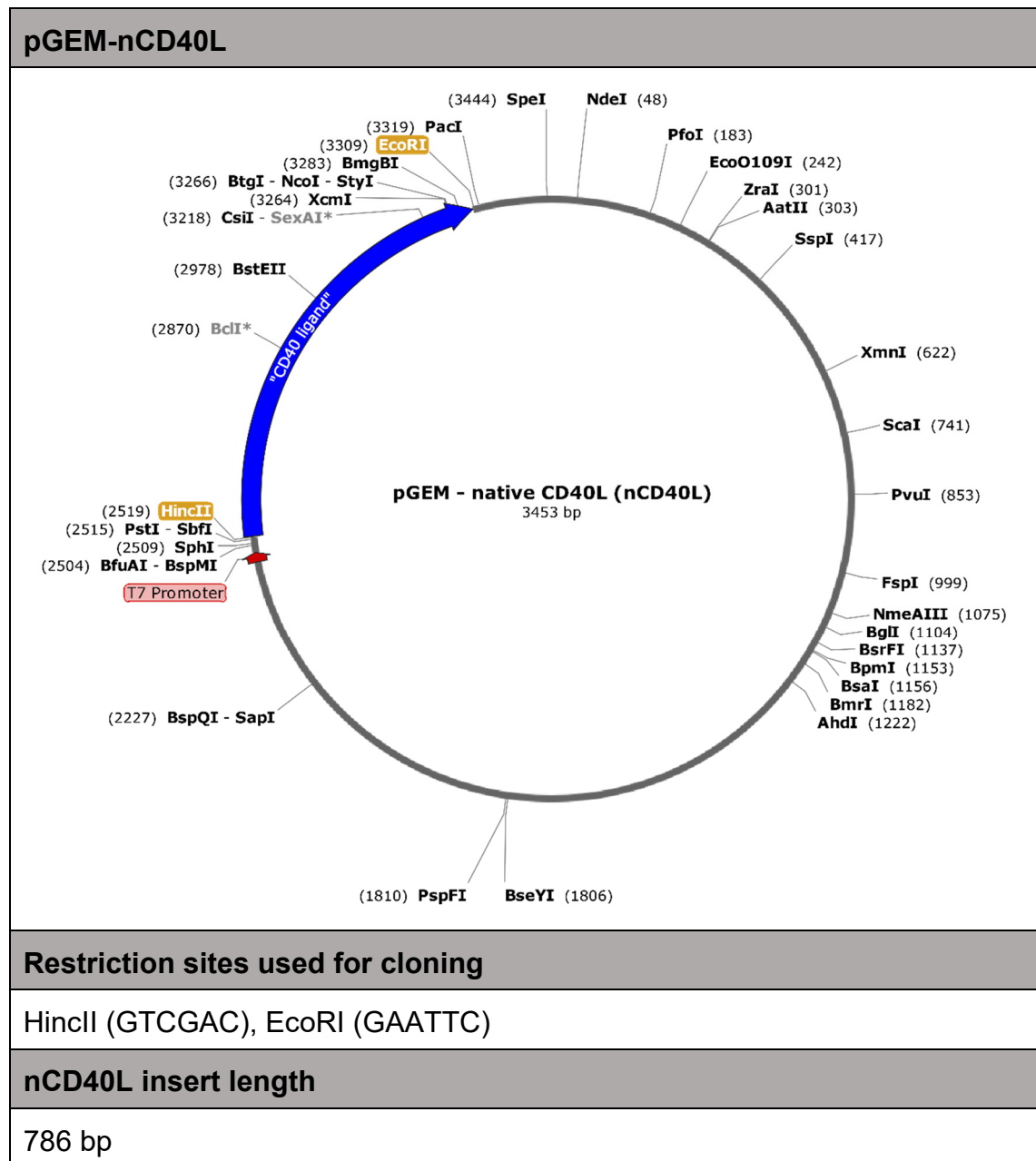
3.5.1 Plasmids

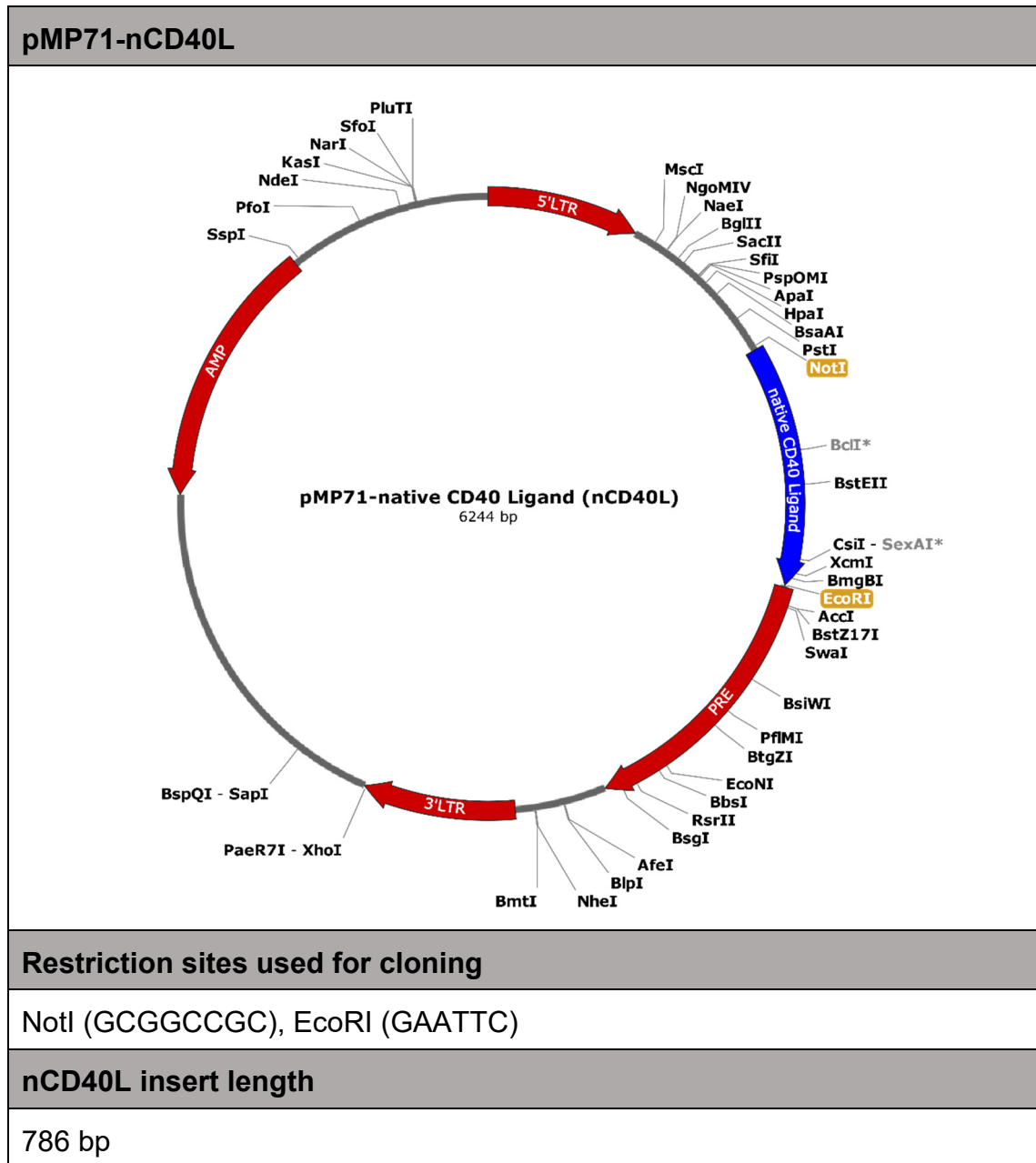


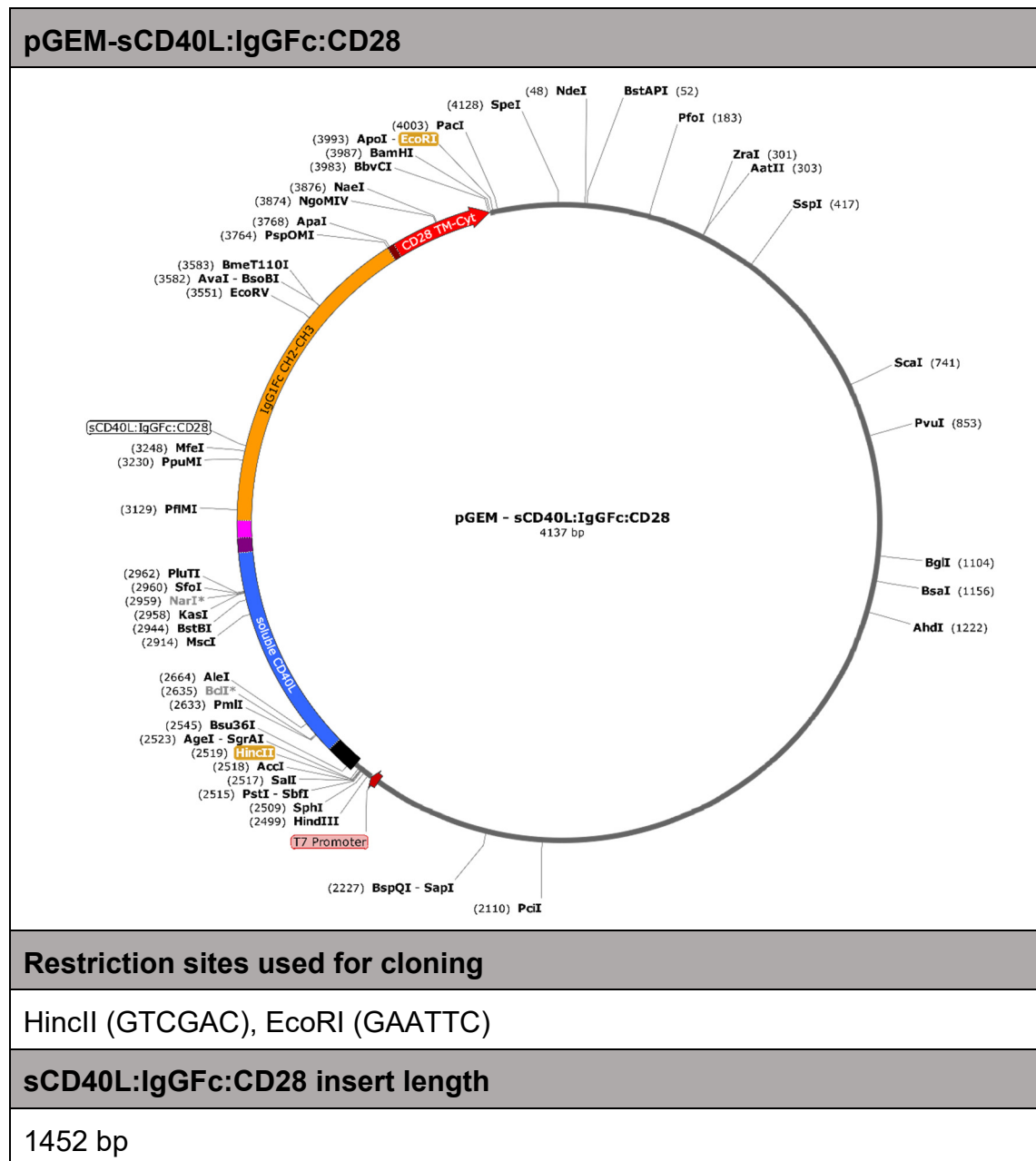


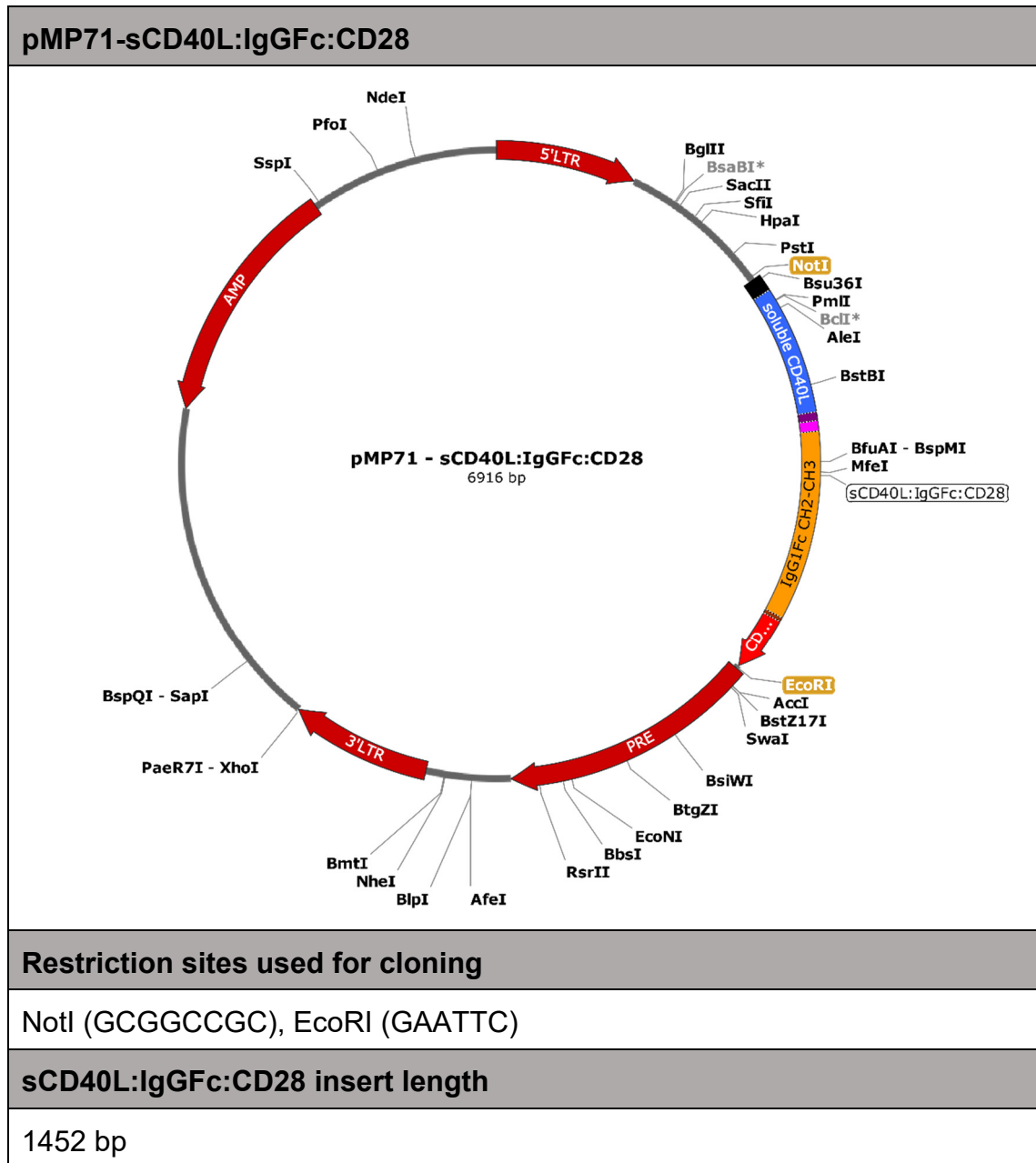


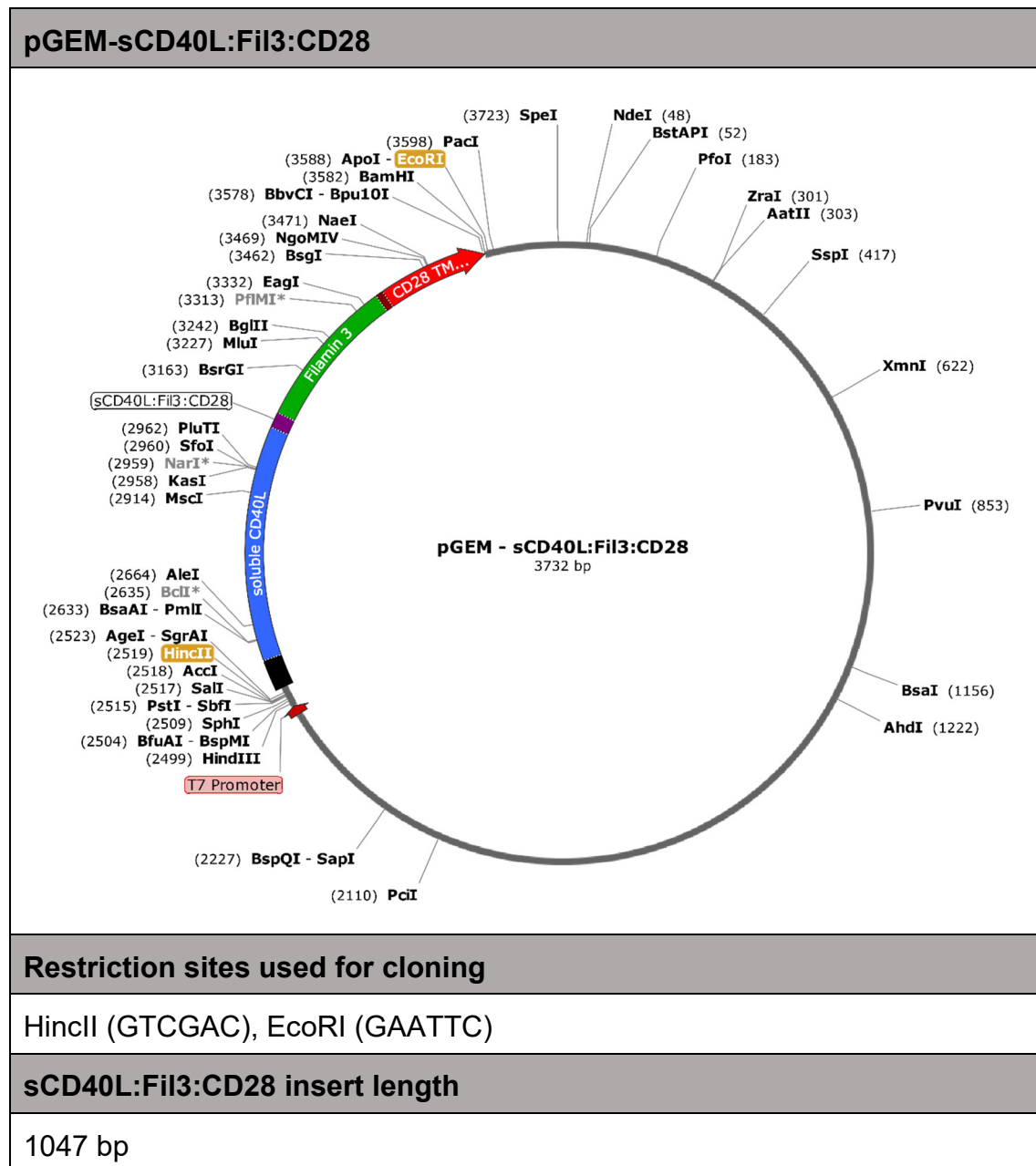


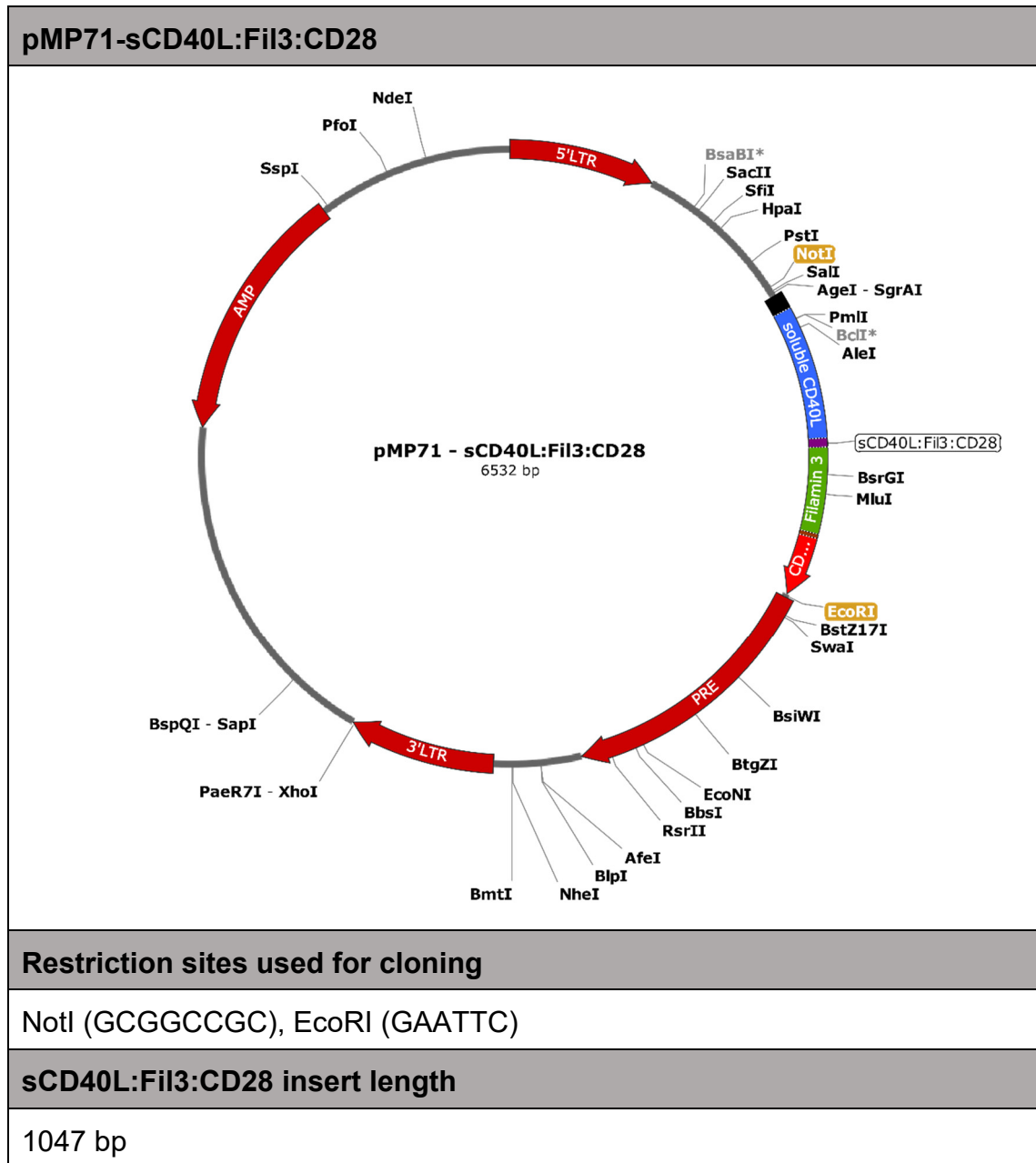


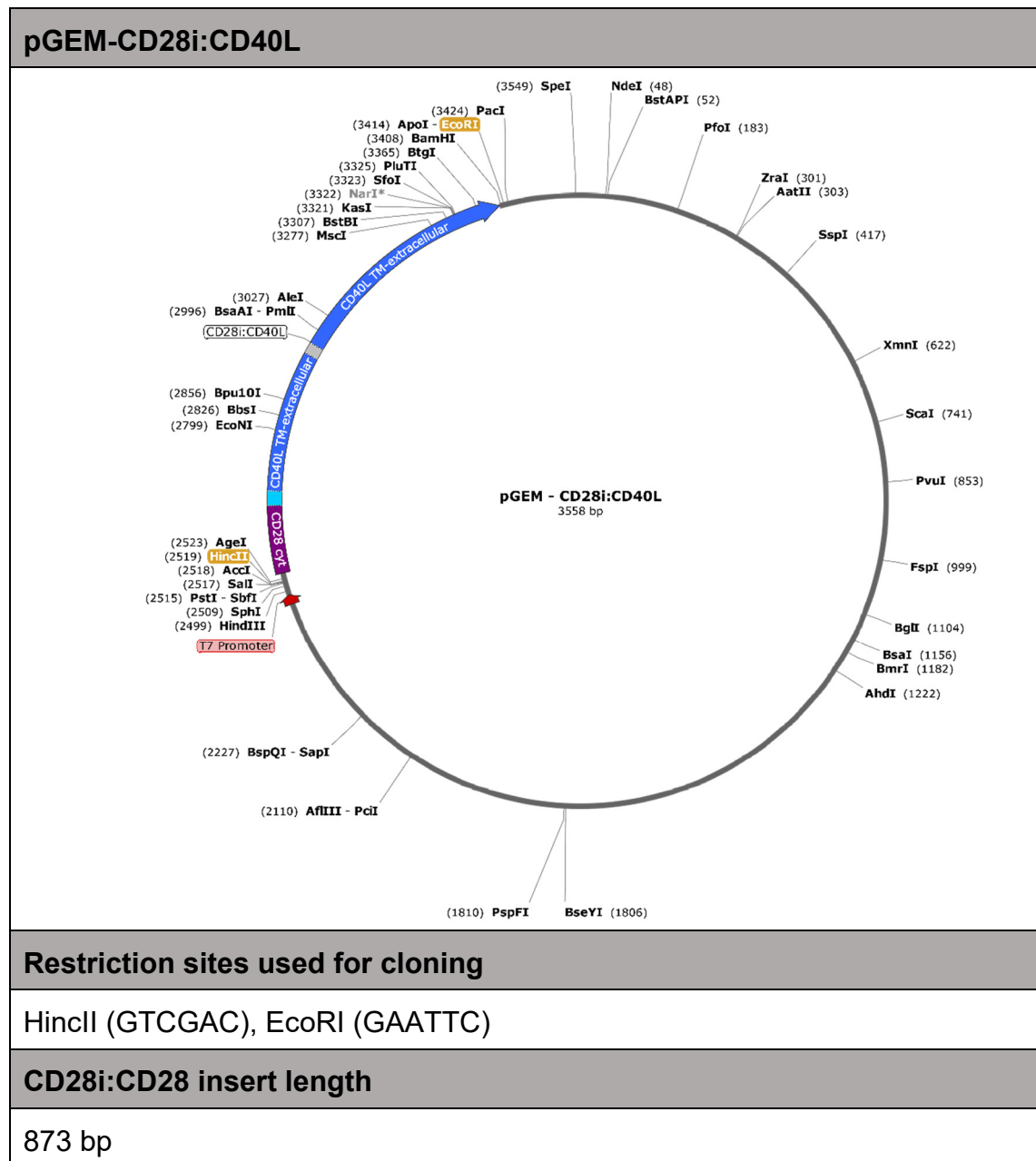


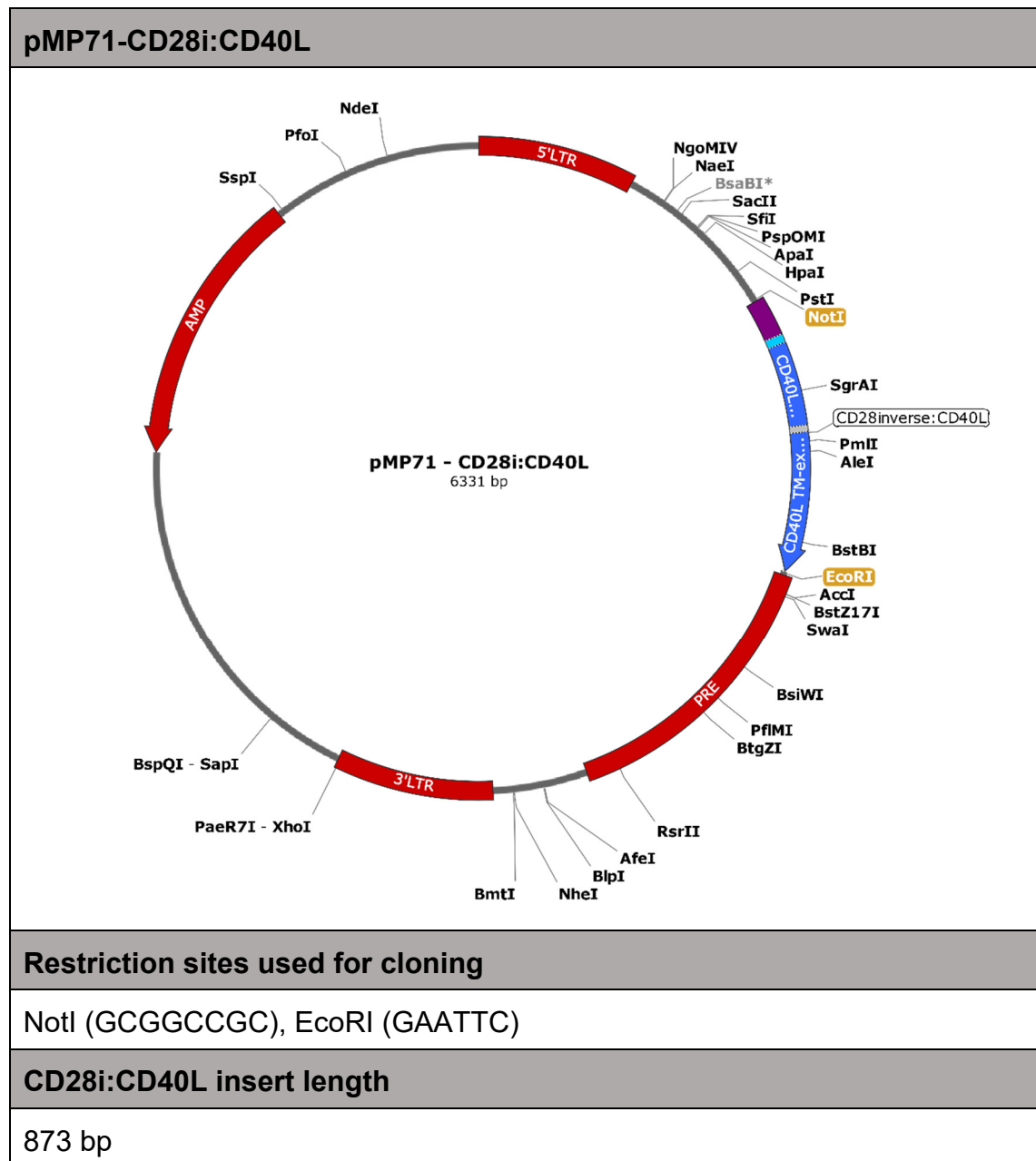












3.5.2 Primers

For cloning into the pGEM-vector		
CONSTRUCTS	SEQUENCE 5' → 3'	COMPANY
nCD40L	<i>Forward</i> ATAGTGTGCATGATCGAAACATACAACCAAAC	Metabion, Planegg, GERMANY
	<i>Reverse</i> ATAGAATTCTCAGAGTTTGAGTAGCCAAAGGACG	
CD40L:IgGfC:CD28	<i>Forward</i> ATAGTCGACACCGGTGCCACC	Metabion, Planegg, GERMANY
	<i>Reverse</i> ATAGAATTCCGGATCCTCAGCTTC	
CD40L:Fil3:CD28	<i>Forward</i> ATAGTCGACACCGGTGCCACC	Metabion, Planegg, GERMANY
	<i>Reverse</i> ATAGAATTCCGGATCCTCAGCTTC	
CD40L:CD28i	<i>Forward</i> ATAGTCGACACCGGTGCCACC	Metabion, Planegg, GERMANY
	<i>Reverse</i> ATAGAATTCCGGATCCTCAGAGCT	
For cloning into the pMP71-vector		
CONSTRUCTS	SEQUENCE 5' → 3'	COMPANY
nCD40L	<i>Forward</i> ATAGCGGCCGCGCCGCCATGATCGAAACATACA ACCAAAC	Metabion, Planegg, GERMANY
	<i>Reverse</i> ATAGAATTCTCAGAGTTTGAGTAGCCAAAGGACG	
CD40L:IgGfC:CD28	<i>Forward</i> ATAGCGGCCGCGCCGCCATGCAGATTCCTCAGG C	Metabion, Planegg, GERMANY
	<i>Reverse</i> ATAGAATTCCGGATCCTCAGCTTC	
CD40L:Fil3:CD28	<i>Forward</i> ATAGCGGCCGCGCCGCCATGCAGATTCCTCAGG C	Metabion, Planegg, GERMANY
	<i>Reverse</i> ATAGAATTCCGGATCCTCAGCTTC	
CD40L:CD28i	<i>Forward</i> ATAGCGGCCGCATGCGGAGCAAGAGAAGCAGAC	Metabion, Planegg, GERMANY
	<i>Reverse</i> ATAGAATTCCGGATCCTCAGAGCT	

For qRT-PCR		
CONSTRUCTS	SEQUENCE	COMPANY
nCD40L	5' primer ACCAAACCTTCTCCCCGATCT	Metabion, Planegg, GERMANY
	3' primer TCAGCTGTTTCCCATTTTCC	
CD40L:IgG:CD28	5' primer CCTTGTGGCCAGCAGTCTAT	Metabion, Planegg, GERMANY
	3' primer GATCATCAGGGTGTCTTGG	
CD40L:Fil3:CD28	5' primer CCTTGTGGCCAGCAGTCTAT	Metabion, Planegg, GERMANY
	3' primer CCTTGAAGTCGGCTGTCTCT	
CD40L:CD28i	5' primer AAGCACTACCAGCCTTACGC	Metabion, Planegg, GERMANY
	3' primer CGAACTGGCTCTTGATTTCC	

3.5.3 Restriction enzymes


For cloning into the pGEM-vector			
ENZYME	BUFFER	RECOGNITION SITES 5' → 3'	COMPANY
Hinc II	CutSmart	GTCGAC	New England Biolabs Frankfurt am Main GERMANY
EcoRI - high fidelity	CutSmart	GAATTC	New England Biolabs Frankfurt am Main GERMANY
For cloning into the pMP71-vector			
ENZYME	BUFFER	RECOGNITION SITES 5' → 3'	COMPANY
NotI - high fidelity	CutSmart	GCGGCCGC	New England Biolabs Frankfurt am Main GERMANY
EcoRI - high fidelity	CutSmart	GAATTC	New England Biolabs Frankfurt am Main GERMANY
General cloning enzymes			
ENZYME	BUFFER	RECOGNITION SITES 5' → 3'	COMPANY
Linearization of pGEM plasmids SpeI - high fidelity	CutSmart	ACTAGT	New England Biolabs Frankfurt am Main GERMANY
Ligation of inserts and vectors T4 Ligase	T4 Ligase Buffer	Not applicable	New England Biolabs Frankfurt am Main GERMANY

3.6 Chimeric protein sequences

Native CD40 ligand (nCD40L) not codon optimized

5' → 3'

ATGATCGAAACATACAACCAAACCTTCTCCCCGATCTGCGGCCACTGGACTGCCCA
TCAGCATGAAAATTTTTATGTATTTACTTACTGTTTTTCTTATCACCCAGATGATTGG
GTCAGCACTTTTTGCTGTGTATCTTCATAGAAGGTTGGACAAGATAGAAGATGAAA
GGAATCTTCATGAAGATTTTGTATTCATGAAAACGATACAGAGATGCAACACAGGA
GAAAGATCCTTATCCTTACTGAACTGTGAGGAGATTAAGCCAGTTTGAAGGCTT
TGTGAAGGATATAATGTTAAACAAAGAGGAGACGAAGAAAGAAAACAGCTTTGAAA
TGCAAAAAGGTGATCAGAATCCTCAAATTGCGGCACATGTCATAAGTGAGGCCAG
CAGTAAAACAACATCTGTGTTACAGTGGGCTGAAAAGGATACTACACCATGAGCA
ACAACTTGGTAACCCTGGAAAATGGGAAACAGCTGACCGTTAAAAGACAAGGACT
CTATTATATCTATGCCCAAGTCACCTTCTGTTCCAATCGGGAAGCTTCGAGTCAAG
CTCCATTTATAGCCAGCCTCTGCCTAAAGTCCCCCGGTAGATTCGAGAGAATCTTA
CTCAGAGCTGCAAATACCCACAGTTCCGCCAAACCTTGCGGGCAACAATCCATTC
ACTTGGGAGGAGTATTTGAATTGCAACCAGGTGCTTCGGTGTTTGTCAATGTGACT
GATCCAAGCCAAGTGAGCCATGGCACTGGCTTCACGTCCTTTGGCTTACTCAAAC
TC TGA






 Native CD40L protein sequence

 – start codon

 – stop codon

sCD40L:IgGFc:CD28**5' → 3' (codon-optimized sequence)**


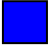
ATGCAGATTCCTCAGGCCCTTGGCCTGTCGTGTGGGCTGTGCTCCAGCT
 GGGATGGCGG**ATGCAGAAGGGCGACCAGAACCCTCAGATTGCCGCCAC**
GTGATCAGCGAGGCCAGCAGCAAGACCACCAGCGTGCTCCAGTGGGCCG
AGAAGGGCTACTACCCATGAGCAACAACCTCGTGACCCTGGAAAACGGC
AAGCAGCTGACCGTGAAGCGGCAGGGCCTGTACTACATCTACGCCCAAG
TGACCTTCTGCTCCAACAGAGAGGCCAGCTCCAGGCCCCCTTTATCGCC
AGCCTGTGCCTGAAGTCCCCCGGCAGATTCGAGAGAATCCTGCTGAGAG
CCGCCAACACCCACAGCAGCGCCAAGCCTTGTGGCCAGCAGTCTATCCA
CCTGGGCGGCCTGTTTGAAGTCCAGCCTGGCGCCTCCGTGTTTCGTGAAC
GTGACCGATCCTAGCCAGGTGTCCACGGCACCGGCTTACCAGCTTTG
GCCTGCTGAAACTGGGCGGAGGCGGATCTGGCGGAGGGGGAGATGAGC
CTAAGAGCTGCGACAAGACCCACACCTGTCCCCCTTGTCCTGCCCTCCA
GTGGCTGGCCCTAGCGTGTTTCTGTTCCCCCAAAGCCCAAGGACACCC
TGATGATCGCCCGGACCCCTGAAGTGACCTGCGTGGTGGTGGATGTGTC
TCACGAGGACCCAGAAGTGAAGTTCAATTGGTACGTGGACGGCGTGGAA
GTGCACAACGCCAAGACCAAGCCCAGAGAGGAACAGTACAACAGCACCT
ACCGGGTGGTGTCCGTGCTGACAGTGCTGCACCAGGACTGGCTGAACGG
CAAAGAGTACAAGTGCAAGGTGTCCAACAAAGCCCTGCCTGCCCCCATCG
AGAAAACCATCAGCAAAGCCAAGGGACAGCCCCGCGAGCCCCAGGTGTA
CACACTGCCTCCAAGCAGGGACGAGCTGACCAAGAATCAGGTGTCACTG
ACCTGTCTCGTGAAGGGCTTCTACCCCTCCGATATCGCCGTGGAATGGGA
GAGCAACGGCCAGCCCGAGAACAACACTACAAGACCACTCCCCCGTGCTG
GACAGCGACGGCTCATTCTTCTGTACAGCAAACCTGACCGTGGACAAGAG
CCGGTGGCAGCAGGGCAACGTGTTTCAGCTGCTCCGTGATGCACGAGGCC
CTGCACAACCACTACACCCAGAAAAGCCTGTCCCTGAGCCCCGGCAAGG
GCCCCAGCAAGCCCTTTTGGGTGCTGGTGGTTCGTGGGCGGAGTGCTGGC
CTGTTACAGCCTGCTCGTGACCGTGGCCTTCATCATCTTTTGGGTGCGCA
GCAAGCGGAGCCGGCTGCTGCACTCCGACTACATGAACATGACCCCCAG
ACGGCCTGGCCCCACCAGAAAGCACTACCAGCCTTACGCCCTCCAGA
GACTTCGCCGCCTACAGAAGCTGA



- | | | | |
|---|---|---|-----------------------------|
|  | Signal peptide |  | IgG1Fc Hinge-CH2-CH3 region |
|  | Soluble CD40L extracellular domain |  | Gly/Ser linker |
|  | CD28 <u>short extracellular fragment</u> , transmembrane domain (TM) and cytoplasmic domain | | |


ATG – start codon**TGA** – stop codon

sCD40L:Fil3:CD28**5' → 3' (codon-optimized sequence)**

ATGCAGATTCCTCAGGCCCTTGGCCTGTCGTGTGGGCTGTGCTCCAGCT
 GGGATGGCGG**ATGCAGAAGGGCGACCAGAACCCTCAGATTGCCGCCAC**
GTGATCAGCGAGGCCAGCAGCAAGACCACCAGCGTGCTCCAGTGGGCCG
AGAAGGGCTACTACACCATGAGCAACAACCTCGTGACCCTGGAAAACGGC
AAGCAGCTGACCGTGAAGCGGCAGGGCCTGTACTACATCTACGCCAAGT
GACCTTCTGCTCCAACAGAGAGGCCAGCTCCCAGGCCCCCTTTATCGCCA
GCCTGTGCCTGAAGTCCCCGGCAGATTTCGAGAGAATCCTGCTGAGAGCC
GCCAACACCCACAGCAGCGCCAAGCCTTGTGGCCAGCAGTCTATCCACCT
GGGCGGCGTGTTTGAAGTCCAGCCTGGCGCCTCCGTGTTTCGTGAACGTG
ACCGATCCTAGCCAGGTGTCCCACGGCACCGGCTTCACCAGCTTTGGCCT
GCTGAAACTGGGCGGAGGCGGATCTGGCGGAGGGGGAGATGGACAGGC
CTGCAATCCTAGCGCCTGTAGAGCCGTGGGCAGAGGCCCTCCAGCCTAAG
GGCGTCAGAGTGAAAGAGACAGCCGACTTCAAGGTGTACACAAAGGGCG
CTGGCAGCGGCGAGCTGAAAGTGACAGTGAAGGGCCCCAAGGGCGAGGA
ACGCGTGAAGCAGAAAGATCTGGGCGACGGCGTGTACGGCTTCGAGTACT
ACCCTATGGTGCCCGGCACCTACATCGTGACCATCACCTGGGGCGGACAG
AACATCGGCCGCAGCCCCTTGAAGTGAAAGTGGGCCCCAGCAAGCCCTT****
CTGGGTGCTGGTGGTTCGTGGGCGGAGTGCTGGCCTGTTACAGCCTGCTC
GTGACCGTGGCCTTCATCATCTTTTGGGTGCGCAGCAAGCGGAGCCGGCT
GCTGCACAGCGACTACATGAACATGACCCCAGACGGCCTGGCCCCACCA
GAAAGCACTACCAGCCTTACGCCCTCCAGAGACTTCGCCGCCTACAGA
AGCTGA

 Signal peptide
 Soluble CD40L
 extracellular
 domain

 Gly/Ser linker
 Filamin immunoglobulin-
 like internal homologous
 repeat 3

 CD28 short extracellular
fragment, TM and cyto-
 plasmic domain

ATG – start codon

TGA – stop codon

CD28i:CD40L**5' → 3' (codon-optimized sequence)**

ATCCGGAGCAAGAGAAGCAGACTGCTGCACAGCGACTACATGAACATGAC
 CCCCAGACGGCCTGGCCCCACCAGAAAGCACTACCAGCCTTACGCCCT
 CCCAGAGACTTCGCCGCCTACAGATCTGCCACCGGCCTGCCATCAGCAT
GAAGATCTTTATGTACCTGCTGACCGTGTTCTGATCACCCAGATGATCGG
 CAGCGCCCTGTTGCGCGTGTACCTGCACAGACGGCTGGACAAGATCGAG
 GACGAGCGGAACCTGCACGAGGACTTCGTGTTTCATGAAGACCATCCAGC
 GGTGCAACACCGGCGAGAGAAGCCTGAGCCTGCTGAACTGCGAGGAAAT
 CAAGAGCCAGTTCGAGGGCTTCGTGAAGGACATCATGCTGAACAAAGAGG
 AACTAAGAAAGAAAACAGCTTCGAGATGCAGAAGGGCGACCAGAACCCC
 CAGATTGCCGCCACGTGATCAGCGAGGCCAGCAGCAAGACCACCTCCG
 TGCTCCAGTGGGCCGAGAAGGGCTACTACCCATGAGCAACAACCTCGTG
 ACCCTGGAAAACGGCAAGCAGCTGACAGTGAAGCGGCAGGGCCTGTACT
 ACATCTACGCCCAAGTGACCTTCTGCTCCAACAGAGAGGCCAGCTCCCAG
 GCCCCTTTATCGCCAGCCTGTGCCTGAAGTCCCCCGGCAGATTCGAGAG
 AATCCTGCTGAGAGCCGCCAACACCCACAGCAGCGCCAAGCCTTGTGGC
 CAGCAGTCTATCCACCTGGGCGGCGTGTTCGAACTCCAGCCTGGCGCCT
 CCGTGTTTCGTGAACGTGACCGATCCTAGCCAGGTGTCCCACGGCACCGG
 CTTACCAGCTTCGGACTGCTGAAGCTCTGA

■ Inverted CD28 cytoplasmic domain

■ CD40L short cytoplasmic fragment,
transmembrane and extracellular
domain

ATC – start codon

TGA – stop codon

3.7 Antibodies

3.7.1 Antibodies for cell culture

SPECIFICITY	SPECIES/ ISOTYPE	CLONE	COMPANY	CONCENTRATION
CD3	Mouse IgG2a	OKT3	In house production	5 µg/ml (T cell activation)
CD28	Mouse IgG1	CD28.2	BD	1 µg/ml (T cell activation)
CD40 functional grade	Mouse IgG1	HB14	Miltenyi	1:11 (blocking experiments)

3.7.2 Antibodies for flow cytometry

SPECIFICITY	FLUOROCROME	SPECIES/ ISOTYPE	CLONE	COMPANY	CONCENTRATION
CD40L	PE	Mouse IgG1	89-76	BD Bioscience	2 µl / 10 ⁶ cells
CD40	APC/PE	Mouse IgG1	HB14	Miltenyi	1:11
PD-1	APC	Mouse IgG1	MIH4	eBioscience	1:25
PD-L1 (CD274)	BV421	Mouse IgG1	MIH1	BD Bioscience	5 µl / 10 ⁶ cells
CD3	PE-Cy7	Mouse IgG1	SK7	Biolegend	1:20
CD3	PerCP- Cy5.5	Mouse IgG1k	SK7	eBioscience	1:10
CD3	Alexa fluor A700	Mouse IgG1k	UCHT1	Biolegend	1:25

CD3	V500	Mouse IgG1	UCHT1	BD Bioscience	5 µl / 10 ⁶ cells
CD4	APC-eFluor 780	Mouse IgG1k	RPA-T4	eBioscience	1:25
CD8	V500	IgG1	RPA-T8	BD Bioscience	1:8
TCR	Pacific Blue	Armenian hamster IgG	H57-59	Biologend	1 µl / 10 ⁶ cells
HLA-A2	PE/APC	IgG2b	BB7.2	BD Bioscience	2 µl / 10 ⁶ cells
Tyrosinase	Unconjugated	Rabbit	Polyclonal	NSJ Bioreagent/ Biomol	1:20
Secondary antibody	Alexa Fluor A488	Goat-anti rabbit	-	Invitrogen	1:100
CD45	PE-Cy7	Mouse IgG1	HI30	Biologend	1:25
CD19	Alexa fluor A700	Mouse IgG1	HIB19	BD Bioscience	2 µl / 10 ⁶ cells
CD86	FITC	Mouse IgG1k	2331 (Fun-1)	BD Bioscience	3 µl / 10 ⁶ cells
CD83	PE	Mouse IgG2b	HB15a	Immunotech	5 µl / 10 ⁶ cells
Fas	PE-Cy7	Mouse IgG1	DX2	Biologend	5 µl / 10 ⁶ cells
CD14	Pacific Blue	Mouse IgG2a	M5E2	Biologend	3 µl / 10 ⁶ cells
CD56	APC	Mouse IgG1	N901 (NKH-1)	Beckmann Coulter	4 µl / 10 ⁶ cells
HLA-DR	APC-Cy7	Mouse IgG2a	L243	BD Bioscience	5 µl per test

CD80	PE-Cy7	Mouse IgG1	2D10	Biolegend	2 μ l/ 10^6 cells
CCR7	Pacific Blue	Mouse IgG2a	G043H7	Biolegend	2 μ l/ 10^6 cells
PD-L1	PerCP-Cy5.5	Mouse IgG2b	29E.2A3	Biolegend	2 μ l/ 10^6 cells
Ki67	Alexa Fluor A700	Mouse IgG1	Ki-67	Biolegend	5 μ l/ 10^6 cells
Granzyme B	PE-Texas Red	Mouse IgG1	GB11	Thermo Fisher Scientific	1:8
p-AKT (S473)	Pacific Blue	Mouse IgG1	M89-61	BD Biosciences	1:10
p-RPS6	PE	Mouse IgG1	N5-676	BD Biosciences	1:8
p-mTOR (S2448)	Alexa Fluor 647	Mouse IgG1	O21-404	BD Biosciences	1:10

3.7.3 Staining combinations

Aim of the combination	Surface markers	Intracellular markers
TCR staining after transduction	7AAD live/dead staining (PerCP) CD3 PE-Cy7 CD4 APC-Cy7 CD8 V500 TCR Pacific Blue	
CD40L and PD-L1 surface expression after CCP transduction	7AAD live/dead staining (PerCP) CD45 PE-Cy7 CD4 APC-Cy7 CD8 V500 PD-1 APC or CD40L PE TCR Pacific Blue	
CD40 Blocking co-culture assays	LIVE/DEAD™ Fixable Blue Dead Cell Stain (indo-1 violet) CD45 PE-Cy7 CD4 APC-Cy7 CD8 V500 CD40L PE	
B cell activation assay	7AAD live/dead staining (PerCP) CD19 Alexa Fluor® A700 CD83 PE CD86 FITC Fas PE-Cy7	
B cell purity check	7AAD live/dead staining (PerCP) CD19 Alexa Fluor® A700 CD3 V500 CD14 Pacific Blue CD56 APC	
DC maturation assay	LIVE/DEAD™ Fixable Blue Dead Cell Stain (indo-1 violet) CD3 Alexa Fluor® A700 CD80 PE-Cy7 CD83 PE CCR7 Pacific Blue HLA-DR APC-Cy7 PD-L1 PerCP-Cy5.5	
CD28 signaling assay	LIVE/DEAD™ Fixable Blue Dead Cell Stain (indo-1 violet) CD45 PE-Cy7 CD3 PerCP-Cy5.5	p-AKT Pacific Blue p-mTOR Alexa Fluor® 647 p-RPS6 PE

NSG xenograft mouse model	LIVE/DEAD™ Fixable Blue Dead Cell Stain (indo-1 violet) CD45 PE-Cy7 CD4 APC-Cy7 CD8 V500 PD-1 APC PD-L1 Pacific Blue CFDA-SE FITC	Ki67 Alexa Fluor® A700
Matrigel plug assay	LIVE/DEAD™ Fixable Blue Dead Cell Stain (indo-1 violet) CD45 PE-Cy7 Deep Red APC CFDA-SE FITC PKH26 PE PD-L1 Pacific Blue	

3.7.4 Antibodies for western blot

SPECIFICITY	SPECIES	ISOTYPE	COMPANY	CONCENTRATION
Monoclonal CD40L/CD154 (C-term)	Rabbit anti-human	IgG	Novus Biologicals	1:2000
Polyclonal CD28 (C-term)	Rabbit anti-human	IgG	GeneTex	1:1000
Monoclonal GAPDH loading control	Mouse anti-human	IgG	Acris antibodies	1:5000
Anti-mouse IgG HRP-linked	Horse anti-mouse	IgG	Cell Signaling Technology	1:1000
Anti-rabbit IgG HRP-linked	Goat anti-rabbit	IgG	Cell Signaling Technology	1:1000

3.8 Primary cells and cell lines

CELL LINE	CHARACTERISTICS	CULTURE MEDIUM	SOURCE
HEK GaLV	Retroviral packaging cell line expressing gag, pol and env genes	HEK medium	Kindly provided by Wolfgang Uckert, Max Delbrück Center Berlin, Germany
HEK293 A2	Natural endogenous expression of HLA-A2	RPMI 4' medium	Kindly provided by Matthias Leisegang, Max Delbrück Center Berlin, Germany
HEK/Tyr	Transduced to express tyrosinase	RPMI 4' medium	Kindly provided by Matthias Leisegang, Max Delbrück Center Berlin, Germany
HEK/Tyr/PD-L1	Transduced to express tyrosinase and PD-L1	RPMI 4' medium	Kindly provided by Matthias Leisegang, Max Delbrück Center Berlin, Germany
HEK/Tyr/CD40	Transduced to express tyrosinase and CD40	RPMI 4' medium	Kindly provided by Anna Mendler, Helmholtz Zentrum München Germany
SK-Mel23	Melanoma cell line	RPMI 4' medium	Monica C. Panelli, NIH, Bethesda, USA
RCC26	Renal cell carcinoma cell line	RCC medium	In-house generated from tumor tissue of patient-26
RCC53	Renal cell carcinoma cell line	RCC medium	In-house generated from tumor tissue of patient-53
PBLs expressing TCR-53	Transduced to express specific RCC TCR-53 (Frozen aliquots)	TCM	In house generated by Matthias Leisegang and Adriana Turqueti-Neves

3.9 Blood samples

Properly trained personnel from the Helmholtz center was in charge of the blood collection from healthy donors after their consent. The procedure was approved by the local Ethics Committee.

3.10 Mice

In agreement with the local authorities, animal experiments were performed according to legal regulations. NOD-scid ILRgamma^{null} mice, also referred to as NSG mice, express two mutations that lead to a severe combined immune deficiency (*scid*) as well as to the absence of the allele corresponding to the IL2 receptor common gamma chain (*IL2rg^{null}*). The *Scid* mutation affects the DNA repair complex protein *Prkdc*, which in turn produces a B and T cell deficiency in the mice. The *IL2rg^{null}* mutation interferes with cytokine signaling via several receptors, which leads to a functionally deficient NK cell population. These characteristics allow these mice to be humanized by the engraftment of different human cell lines including peripheral blood mononuclear cells (PBMC), making it a suitable model for the research postulated in this work regarding functionality of CCPs in the context of ACT. The mice used in this thesis were supplied by Charles River Laboratories.

4. Methods

This thesis is embedded in the larger research topic of the group of E. Nößner. A previous doctoral thesis was performed by R. Schlenker, which is available on the webpage of the LMU (69). Therefore, overlaps in Material and Methods exist. Parts of the original work of this thesis, including the adoptive T cell transfer in human xenograft NSG mice, contributed to the publication by R. Schlenker with L. Olguin Contreras as second author (70).

4.1 Density gradient centrifugation for isolation of peripheral blood mononuclear cells (PBMC)

Blood was collected from healthy donors by venous puncture using syringes containing 10 IU heparin-sodium/ml. Blood was diluted 1:2 with PBS and aliquots of 35 ml were transferred into 50 ml falcon tubes that contained 15 ml Ficoll. The blood was pipetted along the tube wall onto the ficoll layer very carefully not to mix with the ficoll. The tubes were centrifuged at 840 g for 20 minutes without using the centrifuge brake. After centrifugation, an interphase between the plasma and the Ficoll is formed while the red blood cells precipitated to the bottom. The interphase containing the PBMCs was carefully collected and transferred to a fresh tube. After 1:2 dilution with PBS, the cell suspension was centrifuged at 758 g for 12 minutes, this time with activated break. After this washing step, supernatant was discarded and cell pellet was resuspended in TCM. The cells were counted and were then ready to be used for the experiments. Leftover cells were frozen.

4.2 Cell counting, cryopreservation and thawing

For cell counting, cells were harvested using the individually suitable procedure. Once the cell suspension was prepared and knowing the final volume of the suspension, cell numbers were calculated by using the Neubauer counting chambers. An aliquot of cell suspension was taken and diluted 1:2 with trypan blue containing 3% acetic acid (for erythrocyte lysis). Trypan blue helps discriminate viable cells from dead cells (the damaged membranes allows trypan blue to enter dead cells). Live cells within the 4 quadrants of the chamber were counted, and calculation of the total number was done using the formula below:

$$\text{Cells per ml} = \frac{\text{Total cell number}}{4 \text{ (total of quadrants)}} \times \text{dilution factor} \times 10\,000 \text{ (chamber factor)}$$

For cryopreservation, freezing vials were prepared and pre-cooled on ice. The cell suspension was centrifuged at 400 g for 10 minutes, supernatant was discarded and the cell pellet was resuspended in ice cold freezing medium (volume depended on the amount of cells per vial to freeze in 1 ml). Cell suspension was then aliquoted into the freezing vials (1 ml/vial) and stored in Mr. Frosty containers at -80°C for up to three weeks. For long time storage, vials were transferred to liquid nitrogen tanks.

For experiments, freezing vials were thawed quickly using a water bath at 37°C. Cell suspension was transferred to a tube containing 2 ml prewarmed FBS and centrifuged at 400 g for 5 minutes. Supernatant was discarded and pellet was resuspended in the corresponding cell medium. Cells were then counted and adjusted to be used in the experiments.

4.3 Cultivation of human cell lines

All experiments involving cell culture were performed using properly sterilized material to avoid contamination with yeast, bacteria or fungi. The work and manipulation of all media, buffers and biological material was done inside a laminar flow work bench.

In vitro cultivation of human derived cell lines was performed using the media listed in section 3.4 and differently sized culture flasks were used (T25-, T75- or T175 cm²).

The HEK GaLV cell line used for production of viral particles, which were later used in transduction experiments, was grown in HEK medium until confluency was reached by visualization in the inverted microscope (Zeiss). This cell line had low adherence to plastic and cells could be detached by pipetting up and down thoroughly. Thereafter, cells were resuspended to a homogeneous suspension and passaged 1:8 in fresh medium every 3-4 days.

HEK/Tyr, HEK/Tyr/PD-L1 and HEK/Tyr/CD40L (human kidney epithelial derived cells) and human melanoma cell line SK-Mel 23 were grown in RPMI 4' medium until confluency was reached. Their adherence to plastic was stronger, for which an enzymatic process was needed for detachment. Medium in the flask was

discarded and 1-2 ml of Trypsin-EDTA were added to the cell monolayer (making sure that the cell monolayer was evenly covered), incubated for 5 minutes at RT or 37°C until detachment, which was confirmed by microscope visualization. The enzymatic reaction was stopped by adding 9 ml of serum supplemented medium (RPMI 4'). Cells were resuspended by gently pipetting up and down. This process will be referred to trypsinization. Above mentioned cells were passaged 1:10 every 3 days. The renal cell carcinoma cell lines RCC26 and RCC53 were grown in RCC medium and passaged 1:3 by trypsinization every 3-4 days.

4.4 Transient transfection of human T cells and HEK293 cell line using *ivt*-RNA

4.4.1 *In vitro* transcribed RNA (*ivt*-RNA) generation

The transcription plasmids (pGEM) containing the sequences corresponding to the different CCPs must be linearized for a proper transcription process. Linearization was performed using 80 units of the SpeI-HF enzyme mixed with 40 µg of each pGEM vector using the suitable enzyme CutSmart buffer and bringing the samples to a final volume of 100 µl using nuclease-free water. The mixture was incubated for 16 hours at 37°C. To stop the digestion, 4 mM EDTA, 48 mM sodium acetate and 67% ethanol were added to the digestion samples, mixed well and chilled at -20°C for at least 15 minutes. Then, DNA was pelleted by centrifuging at 4°C for 15 minutes at 17000 g. Supernatant was discarded and pellet resuspended in nuclease-free water at a concentration of 0.5-1 µg/µl.

A sample of 3 µg of each linearized plasmid was used for *ivt*-RNA production by using the mMMESSAGE mMACHINE kit (Ambion) following the manufacturer's instructions. Once the *ivt*-RNA production was ready, the samples were purified using the RNeasy Mini Kit (Quiagen) according to the manufacturer's instructions. The *ivt*-RNA recovered after the last elution step was harvested in a 1.5 ml Eppendorf tube in a final volume of 40 µl nuclease-free water. The concentration of the sample was determined using the NanoDrop spectrophotometer, and, as a quality control, the sample was also run on a 1% agarose gel prepared with 1x TAE in DEPC water containing ethidium bromide. The sample should focus in a neat band on the gel and the size should correspond to the base pair number of the corresponding CCP sequence. This

can be determined by comparing to the RNA ladder that was run simultaneously on the gel.

4.4.2 Electroporation of cells with *ivt*-RNA

For electroporation of *ivt*-RNA into HEK or T cells, cells were harvested and counted according to the corresponding protocols. Final resuspension was done in Opti-MEM medium that was kept on ice for the assay. *ivt*-RNA samples were thawed on ice.

24 well tissue culture treated plates with 1 ml per well TCM + 50 U/ml IL-2 (RPMI 4' medium for HEK cells) were prewarmed in the incubator before starting the experiment. Cells were aliquoted ($2 \times 10^6/200\mu\text{l}$) into precooled 0.4 mm electroporation cuvettes. Each cuvette was placed individually in the electroporator (BIO-RAD) and was electrically pulsed according to the following conditions:

	Protocol	Voltage (V)	Time
HEK cells	Time constant	400 V	8 ms
PBMCs	Time constant	900 V	2.3 ms

After the pulse, the cuvette was taken from the electroporator and the cells were gently transferred to the corresponding prewarmed well plate containing medium. The cuvette was rinsed three more times, each time with 200 μl medium. All cell suspensions were combined. Plates containing electroporated cells were transferred to the incubator for an incubation period of 3-4 hours, after which cells were harvested and prepared for flow cytometry analysis.

4.5 Retroviral transduction of Human T cells

The transduction of human T cells followed the protocol established by M. Leisegang, MDC, Berlin (71), with some modification as detailed in the thesis of R. Schlenker (69). Briefly, the protocol of human T cell transduction consisted of a 13 day period, days marked with a – symbol (i.e. Day -4) correspond to preparation days before the 2nd and final transduction hit, which marks day 0.

Day -4

- HEK GaLV cells were seeded in the late afternoon at a 1.5×10^6 concentration into a 100 mm Petri dish using a final volume of 10 ml RPMI 4' medium.
- Plates used to activate the PBMCs were prepared by coating 24-well plates with OKT-3 antibody (5 $\mu\text{g/ml}$) and anti-CD28 antibody (1 $\mu\text{g/ml}$) in a final volume of 500 μl PBS. Plates were sealed with parafilm and stored at 4°C overnight.

Day -3

- Plasmids corresponding to the different transgenes (TCRs or CCPs) were thawed on ice.
- Transfection reagent was prepared by mixing 30 μl of TransIT[®]-LT1 with 470 μl of DMEM medium in a 1.5 ml Eppendorf tube for 5 minutes at room temperature (RT).
- 12.5 μg of each plasmid was mixed with the previously prepared transfection reagent, gently mixed by snapping the tube with the finger and incubated for 15 minutes at RT.
- After the incubation time, the mix was added dropwise to the Petri dish containing the HEK GaLV cells. The petri dish was then swirled gently to allow the transfection mix to distribute homogeneously.
- PBS on the activation plates prepared the day before was replaced with 2% BSA and incubated for 30 minutes at RT. After washing one time to remove the BSA, the well was rinsed with PBS.
- PBMCs used for the transduction were freshly isolated on this day or thawed from a previously prepared aliquot. Cells were resuspended in TCM containing 100 U/ml IL-2 and distributed in a concentration of 1×10^6 cells per well to the activated plate.

Day -2

- Plates to be used for viral particle coating are prepared using non-tissue culture treated 24 well plates by adding 10 $\mu\text{g/ml}$ RetroNectin in 500 μl final volume of PBS. Plates were sealed with parafilm and stored at 4°C until used the next day.

Day -1

- PBS on the RetroNectin coated plates was replaced with 2% BSA, incubated for 30 minutes at RT and then washed one time by removing the BSA solution and rinsing the well with PBS.
- Medium on the Petri dishes containing the HEK GaLV cells was harvested into 50 ml falcon tubes and centrifuged at 200 g for 10 minutes at 32°C
- After centrifugation, the supernatant was gently decanted into a fresh tube and, using this supernatant, aliquots of 1 ml/well were distributed into the RetroNectin coated plates.
- RetroNectin plates were sealed and then centrifuged for 90 minutes at 3200 g at 32°C. The plates needed for the second transduction hit were also prepared at this point. After the centrifugal inoculation (spinoculation), the plates were stored at 4°C until their use.
- PBMCs that were cultured on the activation plate for 3 days, were harvested and counted. 0.5×10^6 cells were transferred to the corresponding wells of the RetroNectin plate coated with viral particles in TCM containing 100 U/ml IL-2. PBMCs cultured in supernatant that didn't contain viral particles were used as MOCK controls (1st transduction hit).

Day 0

- Each well from the 1st transduction hit coated plates was splitted 1:4 into the previously prepared plate for the 2nd hit of transduction plus 750 µl TCM containing 100 U/ml IL-2.

Day 3

- Cells from the 2nd hit transduction plate were harvested and centrifuged at 1500 rpm for 5 minutes. Supernatant was carefully discarded into the appropriated waste container for S2 biosafety and pellet was washed once again with PBS.
- PBS was discarded and cells were resuspended in fresh TCM containing 100 U/ml IL-2 and distributed at a concentration of 1.5×10^6 cell/ml in T75 cm² culture flasks.
- 0.3×10^6 cells were harvested and prepared for flow cytometry analysis to determine transduction efficacy.

Day 6

- Cells were splitted according to cell density into new flasks with fresh TCM supplemented with 100 U/ml IL-2.
- 0.3×10^6 cells were harvested and prepared for flow cytometry analysis to determine transgene expression.

Day 10

- 0.3×10^6 cells were harvested and prepared for flow cytometry analysis to determine transgene expression.

Day 12

- 1×10^6 cells were harvested and transferred to a 24-well tissue culture treated plate with fresh TCM containing 100 U/ml IL-2.
- 0.3×10^6 cells were harvested and prepared for flow cytometry analysis.
- The rest of the cells were frozen as $15\text{-}20 \times 10^6$ cells aliquots per freezing vial.

Day 13

- Cells kept in the 24-well plate were harvested and counted.
- 0.3×10^6 cells were prepared for flow cytometry analysis.

4.6 Protein detection (Western Blot)

T cells transduced with the different CD40L:CD28 CCPs were assessed for protein presence by western blot. Therefore, samples of 1.5×10^6 cells were harvested at each time point of the transduction kinetic (3, 6, 10, 12 and 13 days), counted and adjusted. The cell pellet was washed using ice cold PBS, then resuspended in ice cold NP-40 lysis buffer containing protease inhibitors (1 ml per 10^7 cells). Samples were incubated at 4°C under constant agitation for 30 minutes. After incubation, cells were centrifuged at 4°C for 5 minutes at 12000 rpm, supernatants were then transferred to a precooled 1.5 ml Eppendorf tube and cell pellet was discarded.

Protein concentration was determined using the microBCA™ protein assay kit according to the manufacturer instructions. After protein determination, samples were stored at -20°C for later use until all time points were collected.

For western blot (WB) assay, lysates were thawed on ice, samples were prepared by adjusting 30 µg of total protein from the lysates in 27 µl of buffer. 10 µl of loading buffer were added to the samples before loading the gel for a total volume of 37 µl of sample per well. Samples were heated for 5 minutes at 95°C for protein denaturalization, and afterwards samples were loaded into the gel (precasted gels from Invitrogen) together with the molecular weight ladder.

The gel was placed on the WB chamber (Invitrogen) that was filled with running buffer and the chamber was connected to the power bank to let it run at 100 Volts for 30 minutes, then at 200 Volts for another 45-60 minutes. The gel run was performed at 4°C in a cool room.

After the run, the gel was carefully taken out of the casting and soaked in transfer buffer to equilibrate it. Meanwhile the PVDF membrane was prepared for the gel transfer. Transfer of the proteins was performed using the XCell II™ blot module, this time the chamber was filled with transfer buffer and the run was performed at 30 Volts for 60 minutes at 4°C.

After the run, the membrane was taken out of the blot module and rinsed with washing buffer. The membrane then was blocked using 5% non-fat milk blocking reagent by incubating it at 4°C under constant gentle agitation. After blocking, membrane was rinsed twice with washing buffer without letting the membrane dry.

The membrane was then incubated with the diluted primary antibodies against either CD40L, CD28 or GAPDH (loading control). For CD40L antibody, a 1:2000 dilution was used, for CD28 antibody a 1:1000 dilution and for GAPDH antibody a 1:5000 dilution was used. All antibodies were diluted in 5% non-fat milk reagent. For membrane incubation, full covering of the membrane with the antibody dilution has to be assured and for each antibody an independent membrane was used derived from the same initial samples. Incubation with the primary antibody was performed at 4°C overnight with constant gentle agitation and protecting the incubation container with plastic or a hard lid.

After incubation with primary antibody, the membrane was rinsed twice with washing buffer, and then washed 5 times with washing buffer by incubating 5 minutes on a rocking table at room temperature (RT).

For secondary antibody incubation, HRP labeled antibodies were used according to the species specificity of the primary antibody (anti-mouse or anti-rabbit) see section 3.7.4. Secondary antibodies were also diluted in blocking reagent at a 1:1000 dilution. Membrane was then incubated for 1 hour at RT under gentle agitation.

After incubation with the secondary antibody, the membrane was rinsed twice with washing buffer, and then washed 5 times with washing buffer by incubating 5 minutes on a rocking table at RT.

Development of the membrane was performed using the chemiluminescent Amersham ECL prime western blot detection reagent according to the manufacturer instructions.

Final X-ray film exposure and development was performed in a dark room using an Automatic X-ray film processor from AGFA.

4.7 Molecular biology methods

4.7.1 Cloning CCP sequences into vectors for retroviral transduction and *in vitro* transcription

Nucleotide sequences from the designed chimeric co-stimulatory proteins were codon optimized and ordered using the Geneart project manager from Life technologies. At arrival, vectors containing the corresponding sequences were dissolved according to the manufacturer's instructions and used for further cloning into the pGEM transcription vector and pMP71 transduction vector.

Geneart plasmids were used to transform MACH1 *E. coli* bacteria through a heat shock protocol in which 1 μ l of plasmid was incubated with the bacteria suspension for 30 minutes on ice. Immediately thereafter incubation at 42°C for 30 seconds followed causing DNA uptake as a consequence of cell membrane disruption due to the sudden temperature change. After heat shock, bacteria suspension was placed on ice for 2 more minutes to ensure successful DNA uptake. A volume of 350 μ l of SOC medium provided with the competent MACH1 bacteria was added to the suspension and incubated at 37°C under gentle

agitation for one hour. After this incubation, in which bacteria was allowed to recover from the heat shock, 20 μ l of the suspension were spread using a sterile L-shaped glass Pasteur pipette on prewarmed petri dishes containing agar medium supplemented with 100 μ g/ml ampicillin as selection antibiotic and incubated overnight at 37°C.

The next day, colonies of transformed bacteria, that grew nicely isolated on the agar plate, were selected and transferred with the help of a 100 μ l pipette tip to a tube containing 4 ml of LB medium also containing ampicillin. Tubes were incubated afterwards under constant 200 rpm agitation at 37°C overnight. After incubation, a 200 μ l sample from the highly dense bacteria culture was transferred to an upscaled volume of ampicillin supplemented LB medium (300 ml) and placed again in the incubator under the same incubation conditions.

Once a high volume of bacteria suspension was reached, isolation of plasmidic DNA was performed using the Jetstar preparation kit according to the manufacturer's instructions. The final pellet containing the isolated plasmids was resuspended using nuclease-free water. Purity and concentration values were determined using the NanoDrop spectrophotometer and aliquots of each sample were sent for sequencing to Eurofins MWG.

Accuracy of plasmid sequences were corroborated by aligning the original sequence provided by Genart with the sequencing results from Eurofins. When sequence corresponded positively to the original, I proceeded to clone the chimeric co-stimulatory protein sequences into the vectors for transcription (pGEM) and transduction (pMP71). For this process, protein sequences had to be amplified by PCR, mixing the purified plasmid DNA (5-9 μ g) with the corresponding primers (see section 3.5.2), 5% DMSO and 1x PCR master mix, a final volume of 100 μ l was completed adding nuclease-free water.

The program used to amplify the sequences was set as follow:

No. of Cycles	Step	Temperature	Duration
1	Denaturation	94°C	5 minutes
35	Denaturation	94°C	5 minutes
	Annealing	62°C	30 seconds
	Polymerization	72°C	2 minutes
1	Final extension	72°C	5 minutes
	Hold	4°C	Infinite

The apparent molecular weight of the reaction products was determined by running the samples alongside a 1kb DNA reference ladder on a 1% agarose gel prepared with 1x TAE buffer containing ethidium bromide. Gel was run for 45 minutes at 130 V. Bands detected on the gel corresponding to the right size of the amplified sequence were purified using the Quiagen extraction kit according to the manufacturer's instructions.

DNA was finally resuspended after purification in 90 µl of nuclease-free water and placed on ice for immediate ligation with the corresponding vectors.

Amplified purified sequences as well as the pGEM and pMP71 vectors were digested in preparation for ligation using the corresponding enzymes listed in section 3.5.3. After thawing on ice, a 10 µg aliquot of each vector was taken and was mixed 1:10 with CutSmart buffer. For pGEM vector, restriction cutting was performed using EcoRI-HF and HincII enzymes, while for the pMP71 the used enzymes were EcoRI-HF and NotI-HF (60 units of each enzyme was used per sample). The final volume was adjusted to 106 µl. The digestion process consisted of a one hour incubation time at 37°C, after which time samples were run in a 1% agarose gel containing ethidium bromide for 45 minutes at 130 V to determine the size of the fragments produced after the plasmid digestion. The biggest fragment corresponded to the vector backbone needed for the ligation. Thus, this fragment was cut out of the gel and purified following the same steps as for the Genart plasmids (see above). Amplified PCR sequences went through the same enzymatic digestion process. At the end, bands corresponding to the

size of the CCP sequences were purified from the gel using the MinElute reaction Cleanup kit (Quiagen) according to the manufacturer's instructions.

For the final ligation, purified vectors and PCR products were mixed (7 μ l of vector + 1 μ l PCR product) together with 400 units of T4 ligase using T4 ligase buffer (1:10). Ligation samples were incubated for 4-5 hours at 16°C. After this incubation time, MACH1 bacteria were transformed with 1 μ l of the ligation sample, followed by plasmid purification as described above for the Genearth plasmids.

4.7.2 RNA isolation and quantitative reverse transcription PCR (qRT-PCR)

Cells used for qPCR analysis were washed one time with PBS and the pellet was resuspended with 200 μ l of TRI reagent[®] followed by vortexing. After incubation for 10 minutes at room temperature, samples were stored at -20°C until RNA isolation.

4.7.3 RNA isolation

Samples for RNA isolation were thawed on ice, then 20 μ l of Linear Acrylamide was added to each of the samples and homogenized by thorough vortexing. Next, 40 μ l of 1-Bromo-3-chloropropane (1/5 Vol) was added, vortexed for 15 seconds and incubated for 10 minutes at RT. After incubation, samples were centrifuged at 12000 g for 12 minutes at 4 °C to achieve phase separation. Then, the upper transparent phase (containing RNA) was carefully transferred to a new Eppendorf tube and placed on ice. For RNA precipitation, 120 μ l isopropanol (2-Propanol) was added to the samples, mixed by pipetting up and down then vortexed, followed by a 10 minutes of incubation on ice. After a centrifugation step at 12000 g for 12 minutes at 4°C, the RNA pellet was visible and the supernatant was discarded. 75% ethanol was added to the pellet (500 μ l/tube) to wash the RNA by slowly mixing it with ethanol until the pellet was detached from the surface of the tube. The sample was shortly vortexed and centrifuged at 12000g for 8 minutes at 4°C. The supernatant was then discarded For RNA solubilization, the tube was left open for 3 minutes at RT to evaporate the remaining ethanol (pellet should not be dried out completely). 20 μ l H₂O (PCR grade) was added to the RNA pellet and mixed. Samples were then shortly centrifuged and incubated for 10 minutes at 55°C to dissolve secondary structures. Following a short vortexing,

the OD values were determined using the NanoDrop® ND-1000 Spectrophotometer.

4.7.4 cDNA synthesis

For the cDNA synthesis, AffinityScript qPCR cDNA Synthesis Kit was used according to manufacturer's instructions, using previously isolated RNA and the reagents provided in the kit, as follows:

Mix
10 µl master mix
2 µl oligo dT
1 µl Affinity Script (RT)
Σ 13 µl
+ RNA
+ RNase Free Water
Σ 20 µl end volume

The amount of RNA used for cDNA synthesis was 1 µg in total, the cDNA run was performed on a Thermocycler TGradient 48 using the following program:

cDNA synthesis program (26 minutes duration)		
Annealing	25°C	5 minutes
Reverse Transcription	42°C	15 minutes
MMLV – Denaturation	96°C	5 minutes
Cooling	4°C	

Short term storage of samples was at -20°C until the qRT-PCR was performed.

4.7.5 qRT-PCR analysis

qRT-PCR assay was performed using the LightCycler® - FastStart DNA Master-PLUS Kit (Roche) according to the manufacturer's instruction using the primers listed in section 3.5.2.

Mix
2 µl – 5' primer (5 pmol/µl)
2 µl – 3' primer (5 pmol/µl)
10 µl - Reaction Mix SYBR Green
4 µl - H ₂ O (PCR grade)
2 µl - cDNA sample
Σ = 20 µl end volume

Samples were run on LightCycler® 96 using the following program:

Preincubation – 1 Cycle	
Description	Acquisition mode
95°C for 600 seconds	None
Amplification – 38 Cycles	
Description	Acquisition mode
95°C for 10 seconds	None
60°C for 25 seconds	None
72°C for 10 seconds	Single
Melting – 1 Cycle	
Description	Acquisition mode
95°C for 10 seconds	None
65°C for 60 seconds	None
97°C for 1 second	Continuous (slope 0.1°C/second)

As the reference gene, amplification of 18S rRNA was used. The data was analyzed using LightCycler® 96 SW 1.1 program.

Normalized fold expression was calculated using the formula: $2^{\Delta\Delta Ct}$, where ΔCt represents Cq value of 18S reduced by Cq value of the specific probe.

4.8 Functional assays

4.8.1 Activation of antigen-specific T cells

For artificial stimulation that mimics TCR specific activation, antigen-specific T cells transduced with the different CD40L:CD28 CCPs were thawed and seeded in a culture plate that had been coated with anti-CD3 and anti-CD28 antibodies. 24-well non-tissue culture treated plates were coated with a PBS solution containing OKT-3 antibody (5 µg/ml) and anti-CD28 (1 µg/ml). The plate was stored at 4°C overnight. On the day of the activation, the PBS solution was removed from the plate and the wells were rinsed once with PBS. The wells were then filled with 500 µl of 2% BSA and incubated at RT for 30 minutes. After incubation time, the BSA solution was removed from the wells, each well was rinsed one more time with PBS and finally 1×10^6 T cells were added in 1 ml TCM supplemented with 100 U/ml IL-2 per well and cultured for 3 days. After the 3-day activation, cells were removed from the antibody coated plate and continued to be cultured without anti-CD3/CD28 antibodies. For the 6-day restimulation approach, cells activated using the antibody coated plate were splitted 1:4 on day 3 and transferred to a tissue culture treated plate for 3 extra days. On day 6, cells were harvested and prepared for flow cytometry analysis and used in further functional assays.

4.8.2 Co-culture set up for analysis of T cell function

Transduced T cells or PBMCs were thawed or harvested, cells were resuspended in the appropriate medium, counted and adjusted.

Target cells, selected according to the experiment requirements, were harvested by trypsinization (HEK/Tyr, HEK/Tyr/CD40, HEK/Tyr/PD-L1, SK-Mel23, RCC26 and RCC53). Cells were washed once with PBS, resuspended in TCM, counted and adjusted.

Co-cultures were performed in a 1:5 or 1:10 ratio of T cells to target cells (as indicated for each experiment) and supernatants were harvested after 16, 24 or 48 hours and used fresh for ELISA assay or stored at -20°C until use. Effector cells and target cells cultured alone were used as reference controls.

4.8.3 B cell activation assay

T cells transduced with the CCPs were thawed and reactivated using anti-CD3 plus anti-CD28 antibody-coated 24-well plates (1×10^6 cells per well) and TCM supplemented with 100 U/ml IL-2 for 3 days. Thereafter, the cells were collected and transferred to a new plate without antibodies using fresh medium plus 100 U/ml IL-2 for 3 additional days to allow downregulation of endogenous CD40L expression on Mock T cells. Fresh PBMCs cells were isolated from 150 ml peripheral blood from HLA-A2 positive healthy donors. From this PBMC fraction, fresh B cells were isolated using a CD19 magnetic (negative isolation) Naïve B Cell Isolation Kit II, human (Miltenyi) according to the manufacturer's instruction. 0.15×10^6 naïve B cells were co-cultured at a 1:1 ratio per triplicate on a 96-well u-bottom plate with the previously prepared T cells expressing the CD40L:CD28 CCPs overnight at 37°C and 5% CO₂. Naïve B cells that didn't receive any stimulation were used as negative control. Two positive controls were included in the assay, B cells activated using a soluble CD40L reagent (Enzo) (sCD40L and enhancer 1:10 dilution 2 µl of each per well), and B cells activated using HEK cells that stably expressed CD40L (kindly provided by Kathrin Gärtner, Helmholtz Zentrum München). Cells were harvested from triplicate wells after incubation time and analyzed by flow cytometry for B cell specific surface activation markers CD83, CD86 and Fas.

4.8.4 DC maturation assay

To determine if the T cells transduced with the CD40L:CD28 CCPs can stimulate the maturation of DCs through CD40 ligation, a co-culture stimulation assay was performed. Therefore, iDCs were generated *in vitro* using an 8-day protocol and the Jonuleit maturation cocktail for maturation (72). Monocytes were derived from freshly isolated PBMC by plastic adherence. Hence, PBMC were isolated from a healthy HLA-A2-positive donor as previously described (see section 4.1). Subsequently, 75×10^6 PBMC were resuspended in 15 ml of DC medium and transferred into a 75 cm² Nunclon® Δ surface cell culture flask. After 25 minutes of incubation at 37°C, the flask was gently shaken and incubated for additional 25 minutes at 37°C. Non-adherent cells were carefully washed away by two washing steps using 15 ml of fresh DC medium. These non-adherent cells represented the 'PBL fraction'. Adherent monocytes were kept in culture overnight adding 15

ml of DC medium into the flask. In order to mature monocytes into DCs, 100 ng/ml GM-CSF and 20 ng/ml IL-4 were added to the cells on the following day as well as after three days (day 3). At this point day 7 of the maturation process, immature DCs (iDCs) were harvested to co-culture them with the T cells expressing the different CD40L:CD28 CCPs on a 1:1 (0.1×10^6 cells per triplicate) ratio in 96-well U-bottom plates in a final volume of 200 μ l TCM. iDCs that were not further stimulated as well as iDCs stimulated with mock T cells were used as a negative control, iDCs stimulated with the Jonuleit maturation cocktail (20 ng/ml IL-4, 100 ng/ml GM-CSF, 15 ng/ml IL-6, 10 ng/ml IL-1 β , 20 ng/ml TNF α and 1 μ g/ml PGE₂) on day 7 were used as positive controls. All conditions were harvest on day 8 and prepared for flow cytometry analysis.

4.8.5 Enzyme-linked-immunosorbent assays (ELISA)

Supernatant samples collected from the co-culture assays were analyzed using a “sandwich” ELISA for the detection of the secreted cytokines IL-2 and IFN- γ . This ELISA method consists of a plate coated with a specific antibody that recognizes the antigen (IL-2 or IFN- γ) to immobilize the cytokines present in the supernatant to the plate. A second specific biotin-labeled antibody recognizing a different epitope of the cytokine is added, which will bind to the previously immobilized cytokine. Finally, avidin conjugated to peroxidase is added; this binds the biotin-labeled secondary antibody converting the substrate into a colored product. Optical density of the different samples reflecting the different cytokine concentrations of the sample or standard was detected at 562 nm using an ELISA reader sunshine. The cytokine concentration was calculated by the Tecan software according to a titration of the cytokine standard.

All samples were analyzed in triplicates. The human IFN- γ and IL-2 ELISA kits were purchased from BD Bioscience and used according to the manufacturer’s instructions.

4.8.6 Chromium release assay

For the cell-mediated lysis assay (CML), targets were labeled with radioactive ⁵¹Chromium. When recognized by T cells carrying the antigen-specific TCR, the ⁵¹Chromium is released and the amount of released chromium is detected in the

harvested supernatant. The amount of detected radioactive chromium can be used to calculate the T cell-induced cell death.

Target cells were harvested, counted and adjusted. Then, 1×10^6 cells in 100 μ l FBS were labeled with 50 μ Ci 51 Chromium for 1 hour at 37°C followed by two washing steps with CML medium. Effector cells that express the antigen-specific TCR with or without the co-expression of the different CCPs were thawed according to section 4.2 and resuspended in CML medium. Effectors were plated at titrated cell numbers according to T cell to target cell ratios from 20:1 to 1.25:1 in a 96 well plate. Targets cells were added at a concentration of 2000 cells per well in 50 μ l. The final volume of the co-culture was 100 μ l and the plate was incubated for 4 hours at 37°C. For determining the maximum 51 Chromium release, 50 μ l of the target cell suspension was pipetted directly to the Luma plate. The spontaneous release was calculated from supernatants of target cells cultured without effectors. Each co-culture was set up in triplicates

After the coculture time, a 50 μ l aliquot from each co-culture was transferred to the filter plate (Luma) and dried overnight. The dried Luma plate was then placed into a TopCount machine that detects the gamma radiation in each well according to the released 51 Chromium. Specific cell lysis was then calculated by applying the following formula:

$$\% \text{ cell lysis} = \frac{\text{measured } ^{51}\text{Cr-release} - \text{spontaneous } ^{51}\text{Cr-release}}{(\text{max. } ^{51}\text{Cr-release}/2) - \text{spontaneous } ^{51}\text{Cr-release}} \times 100$$

4.9 Flow cytometry

4.9.1 FACS analysis principle

Fluorescence-activated cell sorting (FACS) constitutes a flow cytometry technique which uses highly specific antibodies directed against several different markers present on the cell. These antibodies are labeled with different fluorescence conjugates. By making a cell suspension of these labeled cells pass through a laser beam in a single cell fashion, it is possible to detect the way each cell interacts with the light. Data concerning the volume of the cell or forward scatter (FSC), cell internal complexity or side scatter (SSC), and specific fluorescence signals can be collected and analyzed. These characteristics provide a

diversity of parameters which can be used to functionally characterize different cell populations present within a biological sample.

The LSRII flow cytometer (BD) was used to acquire all samples analyzed in this thesis using the FlowJo software.

4.9.2 Cell surface and intracellular markers FACS staining

All cells used for flow cytometry staining were harvested according to their corresponding cell culture conditions mentioned in section 4.3.

After cells were collected, counted and adjusted, an aliquot of $0.2-0.5 \times 10^6$ was taken and transferred to FACS tubes. All samples were washed with 500 μ l FACS buffer by centrifuging the tubes at 400 g for 5 minutes at RT (all washing steps were the same unless other conditions are stated). After washing, supernatant was removed from the tubes but 50 μ l were left behind. Cell pellet was resuspended in the residual volume by vortexing. The antibodies corresponding to the specific markers (section 3.7.3) were added to the cell suspension, 7-AAD or Fixable blue live dead discriminating reagent was also included for each staining followed by a short vortexing step. Samples were incubated for 30 minutes on ice and in the dark. After incubation, all samples were washed using 500 μ l FACS buffer, resuspended in 200 μ l of buffer and finally acquired on the LSRII and analyzed using the FlowJo software.

In case of intracellular marker staining, surface markers were stained first, then cells were fixed by incubation in 500 μ l 1% paraformaldehyde for 20 minutes and washed with FACS buffer. Then, cells were permeabilized using 0.1% saponin and incubated for 30 minutes on ice in the dark. Another washing step was performed, followed by incubation with 0.35% saponin for 30 minutes. After another centrifugation, the supernatant was removed from the tubes leaving a 50 μ l residual volume, in which the cells were resuspended by vortexing. At this point, antibodies for intracellular markers were added at the corresponding concentrations and incubated for 30 minutes on ice in the dark. In case a secondary antibody was needed for intracellular staining, the washing with the two different saponin concentrations was performed again before the secondary antibody was added. After the final antibody incubation, cells were washed one more time with saponin 0.1% and once again with FACS buffer. Cells were finally resuspended

in 200 µl of buffer, acquired on the LSRII Cytometer and analyzed using the FlowJo software.

4.9.3 Flow cytometry staining of phosphorylated signaling proteins

Cells used for this staining were prepared as follows: T cells transduced to express the Tyrosinase-specific TCR-T58 plus CD40L:CD28 CCPs were thawed and activated for 6 days using anti-CD3 and anti-CD28 antibody coated plates (see section 4.8.1) to upregulate the surface expression of the CD40L:CD28 CCPs.

On the day of the signaling assay (day 6), T cells were harvested and washed with PBS, then incubated for 4 hours in RPMI 4' medium without additional IL-2 to reduce constitutive background activation signals. After the 4-hour incubation time, T cells were harvested, washed with PBS, counted and resuspended in RPMI 4' medium. Washing steps were performed using the indicated buffers, cells were centrifuged and supernatant was discarded leaving always a 50 µl residual volume in the tubes.

0.4×10^6 T cells will be used for the co-culture assay, shortly before the activation co-culture, T cells were washed with 500 µl PBS/EDTA (2 mM), and fixable Blue reagent for viability was added followed by a short vortex mixture. Cell suspensions were incubated at RT in the dark for 10 minutes and then washed with 500 µl FACS-buffer.

HEK293/Tyr/CD40 were used to stimulate the T cells through the TCR-Tyr/HLA-A2 interaction and to trigger the CCPs through CD40. HEK293/Tyr/CD40 were harvested and incubated at a 1:2 ratio with the previously prepared CD40L:CD28 CCP-transduced T cells in 1 ml FACS tubes at a final volume of 100 µl RPMI 4' medium for 30 minutes at 37°C and 5% CO₂, unstimulated T cells were kept in culture as a negative control. Detection of phosphorylated proteins was performed using the commercial buffer set (BD Phosflow™).

After the co-culture incubation time, cells were immediately fixated using 200 µl of Cytifix Fixation Buffer (BD) followed by 15 minutes incubation at 37°C. After incubation, cells were centrifuged at 380 g for 8 minutes at RT and supernatant was discarded. For permeabilization, 500 µl of ice cold Phosflow Perm Buffer III were added and incubated for 30 minutes. Cells were centrifuged again at 380 g for 8 minutes at RT, supernatants were discarded and surface markers antibodies

were added together with the antibodies for the phosphorylated intracellular proteins. Following a 30 minute incubation time, cells were washed by centrifuging at 380 g for 8 minutes at RT with 500 μ l of FACS-buffer. Cells were finally resuspended in 200 μ l of buffer, acquired on the LSRII cytometer and analyzed using the FlowJo software.

4.10 Mouse experiments

Local authorities approved all animal experiments in accordance with the corresponding legal regulations. The xenograft model performed in this thesis was included in the publication by R. Schlenker et al. (70).

4.10.1 Human melanoma xenograft NSG model

Human melanoma tumor cell line SK-Mel23 was grown following the corresponding cell culture conditions (see section 4.3). The xenograft was established by injecting 5×10^6 SK-Mel23 cells subcutaneously (s.c.) into the left flank of 7-11 weeks old NSG mice. Tumor growth was monitored daily by the personnel of the animal facility. The starting point of adoptive T cell therapy was when the tumor achieved a size of 800 mm^3 , this was determined using a caliper. At this point, frozen T cells that were transduced to express the tyrosinase antigen specific TCR D115 with and without the PD-1:CD28-CCP were thawed, counted and labelled with CFDA-SE tracking reagent according to the manufacturer's instruction. Afterwards, labelled T cells (6×10^6 in 100 μ l PBS) were injected intratumorally (i.t.). The tumor dimension was measured using a caliper at 4 hours, 1, 2, 4, 6 and 10 days after i.t. injection of the T cells. The tumor volume was calculated using the following formula:

$$volume = (length \times width^2) \times 0.52$$

After being measured live using the caliper, tumors were resected at the 4 hour, 1, 2, 4, 6 and 10 days after i.t. injection, weighed and prepared for analysis of the infiltrated T cell population. The mechanical and enzymatic process to obtain the tumor cell suspension is described in section 4.10.3.

4.10.2 Matriplug assay

The Matriplug assay was developed to assess the specific killing capacity of CCP-transduced T cells in a 3D microenvironment created by a Matrigel matrix. The Matrigel plug containing the cell mixture (see below) was locally injected in the flank of the mice. This allowed me to evaluate the T cell effector function in an *in vivo* system without the need of growing a tumor. For this assay, two different HLA-A2 positive cell lines were used, one comprising the human melanoma SK-Mel23 cell line positive for the tyrosinase antigen and the other one being the HEK293 cell line which does not express tyrosinase.

Each cell line was labeled with a different cell tracking dye to be able to assess specific effects on each population. SK-Mel23 were labeled with a 1.5 μM concentration of Deep Red dye while HEK293 cells were labeled with a 1.5 μM concentration of CFDA-SE cell tracker. Furthermore, both cell lines were also labeled with a 2 μM concentration of the PKH26 dye. Each labeling procedure was done according to the manufacturer's instructions. The cell-type specific labeling allowed subsequent distinguishing of the cell types once the Matrigel plug was harvested from the mice. A mixture of both cell lines (2×10^6 each) was combined with 4×10^6 transduced T cells (1:1 final ratio) in a final volume of 150 μl PBS. - This cell mixture was then gently mixed with 200 μl Matrigel on ice so that the Matrigel stayed liquid. Final aliquots (350 μl total) were taken up into insulin syringes on ice and injected s.c. into NSG mice. Cytokine support was given by injecting mice with 300 units of IL-15 intraperitoneally (i.p.). Plugs were recovered after 2 days and dissolved at 37°C for 30-60 minutes using the Corning Dispase according to the manufacturer's instruction. Dispase yields a single cell suspension more gently and effectively than other proteolytic enzymes, it doesn't damage cells nor cleave cell surface proteins. After single cell suspension was obtained, the cells were washed with PBS and prepared for flow cytometry analysis. Cells were gated on PKH26⁺/CD45⁻ cells and from this population, percentages were determined for HEK293 cell labeled with CFSE and SK-Mel23 cells labeled with Deep Red dye. Using this data, the specific killing was calculated using the following formula:

$$\% \text{ specific killing} = \left[1 - \left(\text{sample} \frac{\% \text{ SK-Mel23}}{\% \text{ HEK 293}} \right) / \left(\text{ctrl} \frac{\% \text{ SK-Mel23}}{\% \text{ HEK 293}} \right) \right] \times 100$$

whereby ctrl is a cell mixture without T cells and sample is a cell mixture with T cells (SK-Mel23 is the T cell target and HEK293 is the non-target).

4.10.3 Preparation of cell suspensions from NSG mice melanoma xenografts

All tumors were measured using a caliper before sacrificing the mice. After tumor resection from NSG mice, tumors were collected in empty 50 ml falcon tubes, weighed and immediately submerged in 5 ml RPMI 4' medium and processed within the next hour. The tumor processing was performed inside a laminar flow work bench and all material was properly sterilized. Each tumor was transferred to a glass 100 mm petri dish and thoroughly sliced into small fractions using a scalpel and scissors. The finely disrupted tumor tissue was pipetted back into a fresh 50 ml tube using a 25 ml plastic pipette and the dish was rinsed twice using 5 ml HBSS buffer with Ca and Mg. The volume was completed to 20 ml using the same buffer. Samples were then centrifuged at 472 g for 2 minutes at RT. All supernatants were transferred individually to a fresh 50 ml falcon tube and kept on ice while the cell pellets were resuspended using digestion buffer at a concentration of 1 ml buffer per ml of pellet. The pellet suspension was incubated on a roller mixer for 30 minutes at 36°C. After incubation, samples were centrifuged again at 472 g this time for 5 minutes at RT, supernatants were individually collected in fresh 50 ml falcon tubes and kept on ice while the pellet was washed with HBSS without Ca and Mg by centrifuging at 472 g for 2 minutes. Supernatants were again individually transferred to a fresh 50 ml falcon tube and kept on ice, while the pellet was resuspended in HBSS without Ca and Mg supplemented with 5 mM EDTA at a concentration of 6 ml buffer per ml of tissue pellet and incubated for 5 minutes on a rocking table for 5 minutes at RT. Samples were centrifuged as described before, supernatants collected and kept on ice. The pellet was this time passed through a 40 µm filter with the help of a 10 ml syringe plunger and flow through was collected in a fresh 50 ml falcon tube. The filter was finally rinsed two times using HBSS containing Ca and Mg.

All the supernatants that were collected and kept on ice during the whole tumor tissue processing were centrifuged at RT for 10 minutes at 472 g, supernatants were discarded and all cell pellets were pooled in fresh ice cold PBS, counted

and prepared for flow cytometry analysis according to the corresponding staining combination (see section 3.7.3).

4.11 Statistical analyses

Statistical analysis of the results was performed using the software Graph Pad Prism setting the significance level to 0.05.

Sidak's multiple comparisons test was used to compare selected pairs of means following one-way ANOVA.

5. Results

5.1 CD40L:CD28 CCP design

According to the topological classification of transmembrane proteins, the CD28 protein and the CD40L (also known as CD154) protein belong to the type 1 and type 2 groups, respectively (**73**). Type 1 membrane proteins are present within the membrane with their N-terminal domain facing the endoplasmic reticulum (ER) lumen during synthesis. Therefore, once they are expressed on the cell membrane, the N-terminus is located in the extracellular domain, and the C-terminus on the cytoplasmic domain. On the other hand, type 2 membrane proteins are anchored with a signal-anchor sequence, being targeted to the ER lumen with its C-terminal domain during synthesis. Once transported to the cell membrane, the C-terminus will be located in the extracellular domain and the N-terminus on the cytoplasmic domain.

Having different membrane orientation, creating a chimeric protein that combines domains of CD40L and CD28, represents a structural and functional challenge (Fig. 5A).

Considering these features, three different constructs were designed for the CD40L:CD28 chimeric protein (see Fig. 5B, 5C). Two of them possess a type 1 membrane protein structure in which the C-terminal part of the soluble CD40L fragment (AA 113-261) was linked to the transmembrane (TM) plus cytoplasmic domain of CD28. Both domains are connected through a Glycine/Serine linker that provides flexibility and allows mobility of the connected functional domains (**8**), and a specific spacer for expression improvement. The first construct, CD40L:IgGFc:CD28, used the IgG1Fc domain as a spacer to provide the protein with a better membrane stability thanks to its dimerization property, which was observed during its previous use in the design of chimeric antigen receptors (CAR) for antigen-specific T cell engineering (**74**). Thanks to the expert insights of structural biologist Grzegorz M. Popowicz from the institute of Structural Biology of the Helmholtz Zentrum München, the second construct, CD40L:Fil3:CD28, exchanged the IgG1Fc spacer for the third Ig-like repetition corresponding to the Filamin protein. This is a protein sequence that adopts an immunoglobulin-like fold without dimerization properties (**75**). The reason to opt for this variation comes from the concern of linking a primarily trimeric molecule like CD40L with

a dimeric region like the IgG1Fc spacer. This potential oligomerization might result in the formation of clusters in the membrane that might interfere with the proper protein function. Finally, the third construct, CD40L:CD28i adopted a type 2 transmembrane protein structure (like the native CD40L) by linking the CD40L extracellular and transmembrane domain with the inverted intracellular domain (AA 180-220) of CD28 (CD28i). This particular construct was based on the NKG2D chimeric protein design, which linked the type 2 protein NKG2D with the type 1 protein CD3 zeta (**76**).

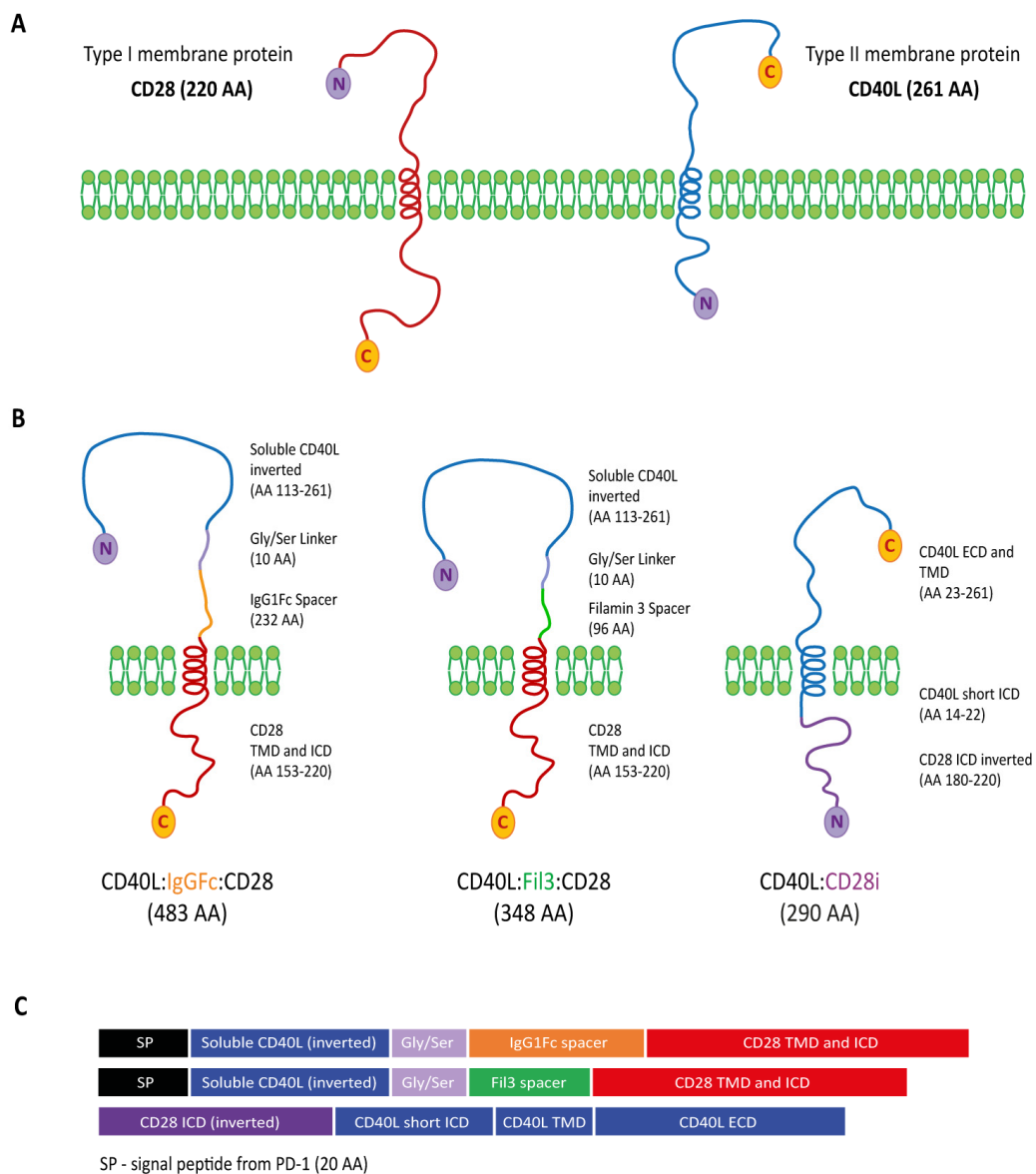


Figure 5. Design of CD40L:CD28 chimeric co-stimulatory proteins (CCPs).

A) CD28 and CD40L are depicted according to their classification as type 1 and type 2 membrane proteins, respectively. C-terminal amino acid (C) and N-terminal amino acid (N) mark the membrane orientation. B) Schematic representation of the three different approaches for the structure of the CCPs with different membrane orientation, AA length and origin of protein fragments are specified on the right side of each molecule, name and total AA length is specified below each CCP. C) Domain representation of the CCPs including the signal peptide (SP) region from the PD-1 protein for type 1 membrane protein approaches.

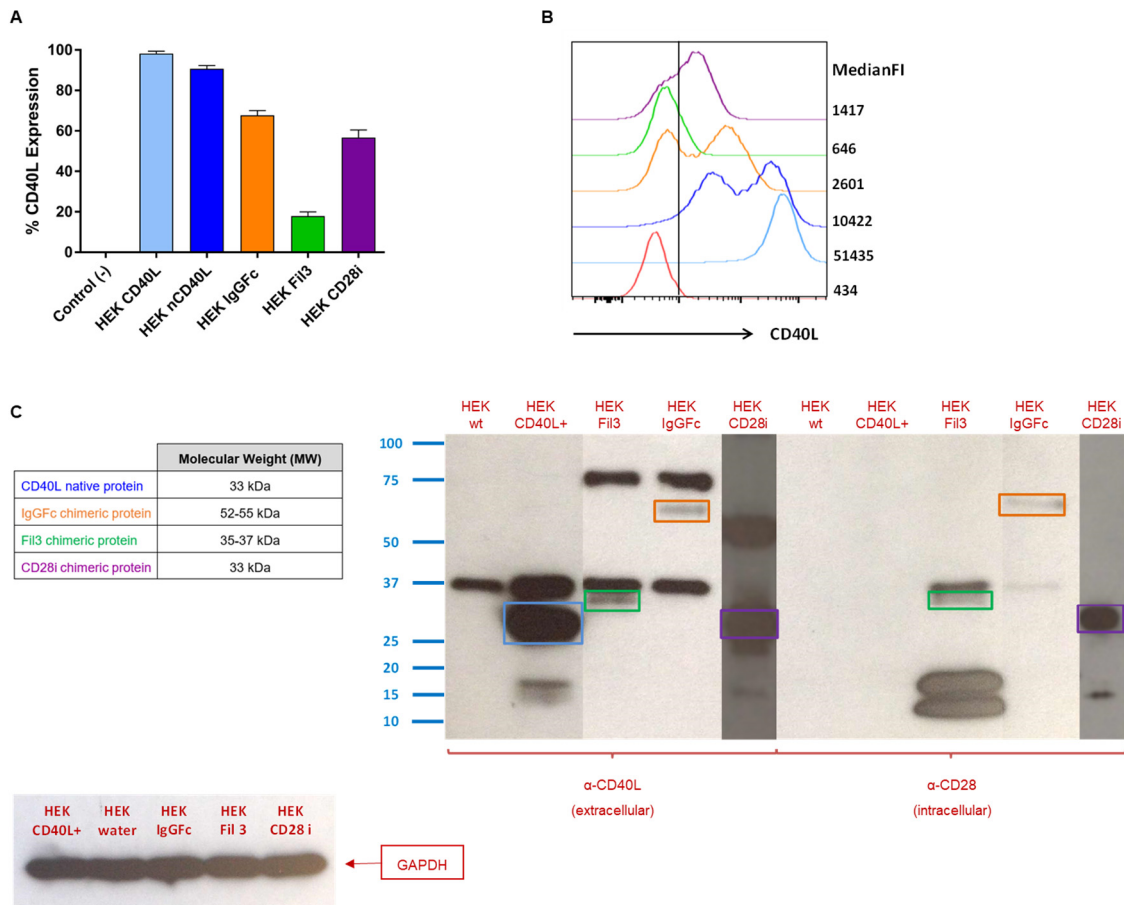
5.2 Surface expression capability of the CD40L:CD28 CCPs

To determine whether the constructs can be successfully expressed on the cell membrane, HEK293T cells were electroporated with *ivt*-RNA coding for the corresponding CCPs. Four hours after electroporation, HEK293T cells were analyzed for CD40L surface expression using an anti-CD40L antibody, which recognizes the extracellular domain of the CD40L protein. Alive, single, CD40L⁺ cells were analyzed and CCP surface presence was assessed. HEK293T cells electroporated with water were used as a negative control. HEK293T cells modified to stably express CD40L using the plasmid pcDNA3.1 (kindly provided by Kathrin Gärtner from Dr. Reinhard Zeidler's group at Helmholtz Zentrum Munich), and HEK293T cells electroporated with *ivt*-RNA for the unmodified native CD40L (nCD40L) protein, were used as a positive controls. The intensity of CCP expression was deduced from the median fluorescence intensity (medianFI). HEK293T cells stably expressing the native CD40L showed the highest percentage of expression and intensity as expected for the positive control. 4 hours after electroporation, the nCD40L protein was most efficiently expressed in terms of both percentage of positive cells and the medianFI. IgGFc and CD28i chimeric proteins followed as the second and third best surface-expressed proteins, in terms of percentages as well as intensity, respectively. Last, the Fil3 CCP was expressed on significantly less cells and with lower intensity compared with the nCD40L, IgGFc and CD28i (Fig. 6A, 6B).

To corroborate the presence of the chimeric proteins in the cells western blot was performed. One million cells from each condition were lysed 4 hours after electroporation, and the lysates were analyzed for protein expression using antibodies that bind specifically to the extracellular domain of CD40L and to the intracellular domain of CD28, respectively.

Since not all CCPs can be differentiated from the nCD40L by their molecular weight, using only a CD40L antibody for western blot analysis (Novus Biologicals) was not enough to clearly distinguish all three CCPs. For this reason, an antibody directed against the C-terminal region of CD28 (GeneTex) was also used to analyze the same lysates. This way, as depicted in figure 6C, nCD40L protein can only be detected using the anti-CD40L western blot antibody but not with the anti-CD28 antibody. On the other side, since the IgGFc, Fil3 and CD28i chimeric proteins share the extracellular domain of CD40L and the intracellular domain of

CD28, all were detected by both antibodies. Both antibodies identified bands at the same molecular weight according to the respective chimeric protein (nCD40L/33kDa, IgGFc/52-55kDa, Fil3/35-37kDa and CD28i/33kDa). This way the expression and structural conformation of the proteins was confirmed. GAPDH antibody (Acris Antibodies) was used as loading control for all lysates.



To assess if the differences in surface expression seen after electroporation was due to the transient expression from *ivt*-RNA, the pMP71 vector containing the different CCPs sequences was used for transduction of T cells. Since transduction leads to integration of transferred DNA, this process should result in stable expression of the transduced sequences. T cells were stained with anti-CD40L antibody to detect the CCP surface expression on different time points after transduction (3 days, 6 days, 10 days and 13 days). As depicted in figure 7, the expression profile of the different chimeric proteins 3 days after transduction correlated to those observed after electroporation, the Fil3 construct still being significantly less expressed. Furthermore, the expression kinetic over time showed that, regardless the retroviral transduction, expression of all transduced proteins decreased over time, with the IgGFc being the most stable one, while the nCD40L, Fil3 and CD28i expression decayed dramatically by day 13 after transduction.

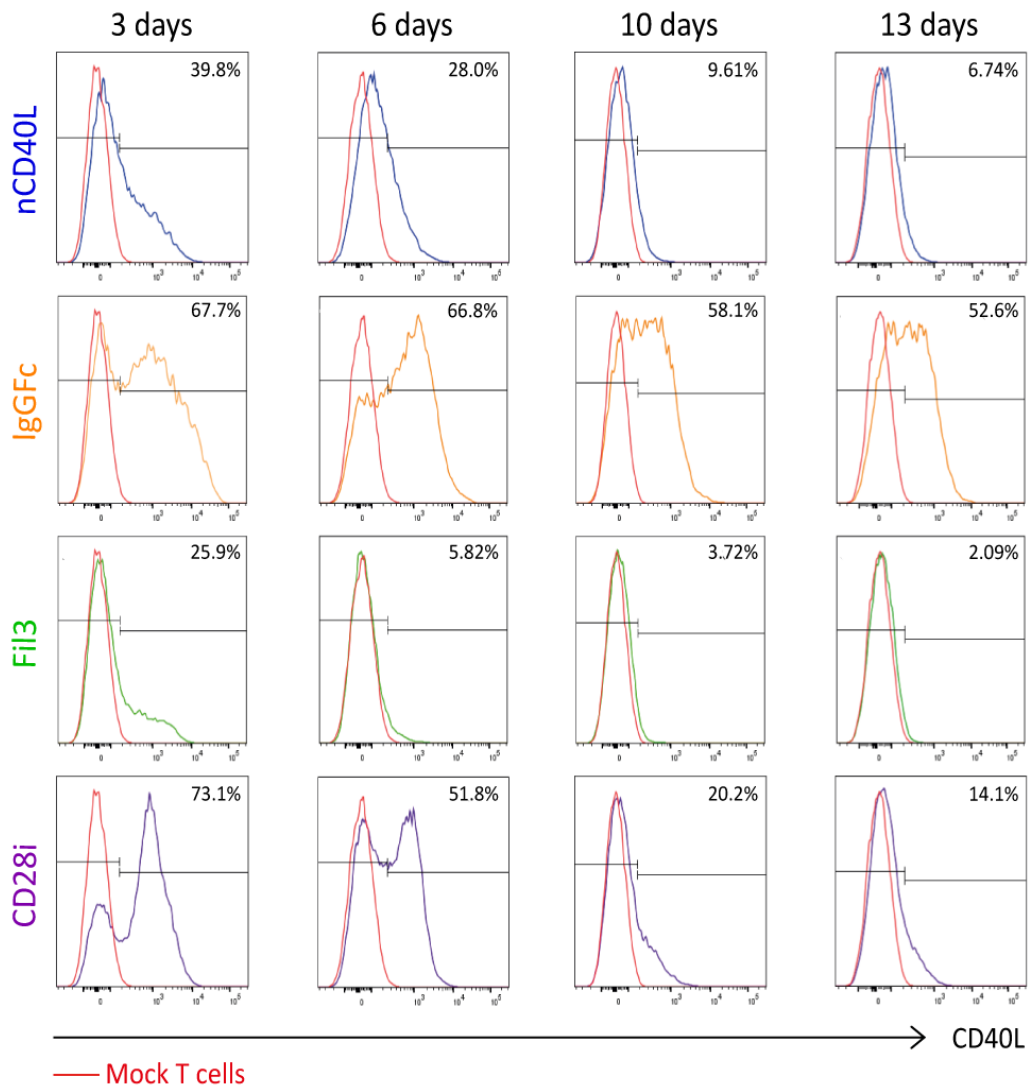


Figure 7. CCP surface expression kinetic in PBLs after retroviral transduction.

Human PBMCs were activated using anti-CD3 plus anti-CD28 antibodies and 100 U/ml IL-2 for 2 days. Thereafter, cells were collected and transduced with the chimeric proteins and expanded for 13 days. CD40L expression was measured by flow cytometry at 3, 6, 10 and 13 days after transduction. Percentage of CD40L positive cells within gated live, single, CD3⁺ population are shown in the histograms. Mock-transduced PBMCs were used as negative control (red line), cells transduced with the native CD40L (nCD40L) protein were used as expression reference and are depicted in blue, CD40L:IgGFc:CD28 CCP is depicted in orange, CD40L:Fil3:CD28 CCP is depicted in green and CD40L:CD28i CCP is depicted in purple. Shown is one representative experiment of at least 5 repeats.

5.3 Culture conditions influence surface expression of the CD40L:CD28 CCPs

In order to determine the impact of the culture conditions on the expression kinetic, retroviral transduction was performed again as described in figure 8A. The aim was to improve the cell expansion conditions by splitting the cells early to control cell density, renewing medium (IL-2 addition) and exchanging the culture flask every third day. The previously mentioned downregulation of the transduced constructs over time was still evident. Additionally, an upregulation of the CD40L surface expression was evident at those time points that followed the medium and culture flask exchange as depicted in figure 8B, by the increase of CD40L positive cells (blue) when superimposed to the CD40L negative cells (red). Given the fact that every medium exchange also includes IL-2 addition, the upregulation seemed to be linked to the culture condition and stimulation status of the transduced cells. Moreover, the observation that the expression kinetic of the CCPs was similar to the native CD40L suggests that the CD40L extracellular domain incorporated in the CCP transfers the tightly regulated expression kinetic of the native CD40L protein, which is known to wane within 16-24 hours after stimulation. The natural kinetic is presumed to minimize bystander activation of CD40 positive cells (**77**).

In figure 8C a line graph depicts the surface expression kinetic of the CD40L:CCPs upon changes in culture conditions on day 6 and day 12. With mock transduced T cells and within them the CD4 T cells, which are known to express CD40L upon activation (**46**) an internal reference is provided to observe the kinetic of the endogenous CD40L expression in comparison to the kinetics of the CCPs.

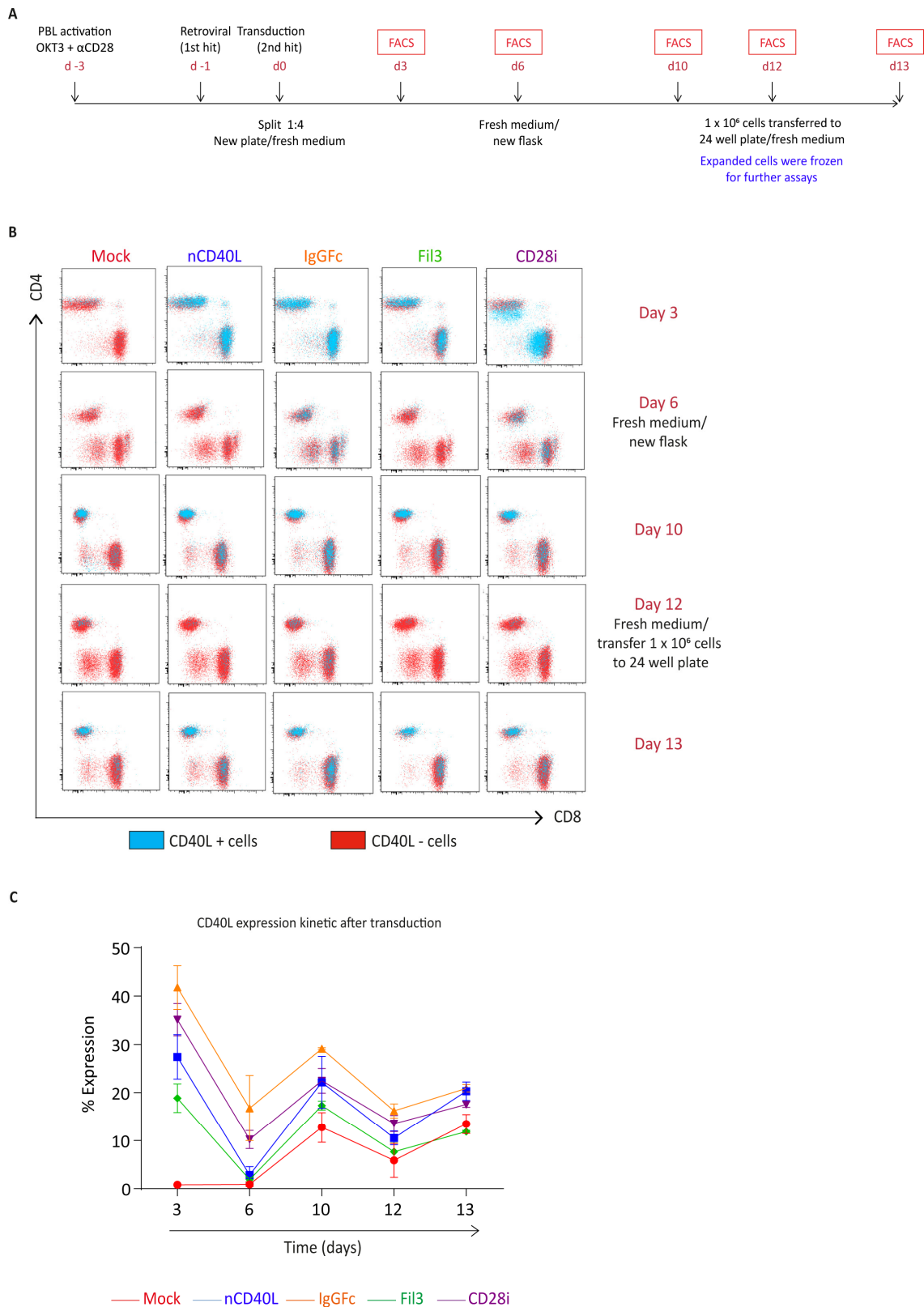


Figure 8. CCP expression kinetic in PBLs after retroviral transduction is modulated by medium replacement.

Human PBMCs were activated using anti-CD3 plus anti-CD28 antibodies and 100 U/ml IL-2 for 2 days. Thereafter cells were collected and transduced with the native CD40L sequence or the chimeric constructs and expanded for 12 days. Cells got transferred to a new flask or plate with fresh medium with 100 U/ml IL-2 on day 6 and 12. A) Timeline describing the transduction steps

for Human PBMCs, CCP expression kinetic diagram and medium replacement conditions. Starting point at day -3 using anti-CD3 (OKT-3) plus anti-CD28 antibodies and 100 U/ml IL-2 for 2 days. Cells were transferred to a new flask or plate with fresh medium with 100 U/ml IL-2 on day 6 and 12. B) CD40L surface expression was measured by flow cytometry at day 3, 6, 10, 12 and 13 after transduction. The CD4 and CD8 cells within the live, single, CD3⁺ population are depicted in the dot plots and the CD40L positive (blue dots) and CD40L negative (red dots) are graphically superimposed. Mock transduced PBMCs were used as negative control and cells transduced with the native CD40L (nCD40L) protein were used as positive reference. C) Percentage of expression at the different time points after transduction are depicted in the graphic. Summary of two independent experiments. Mock transduced cells (red line) and cells transduced to express the native CD40L (blue line) were used as reference. Cells transduced with CD40L:IgGFc:CD28 are depicted in orange, those with CD40L:Fil3:CD28 CCP are depicted in green and T cells with CD40L:CD28i CCP are depicted in purple.

Once observing the loss of CCP from the cell surface, it was assessed if the loss of surface detection was a result of protein internalization, lack of transport to the surface or loss of transcription. For this, the mRNA level was analyzed by qPCR in parallel to measuring surface expression by flow cytometry and total protein presence by Western blot during the same kinetic period as before.

As depicted in figure 9, when analyzing the CD8 T cell population at each given time point, loss and reappearance of the CCPs (IgGFc and CD28i) was observed. The initial downregulation of the surface protein followed the loss of total protein (western blot) and the loss of mRNA level. For the IgGFc CCP, the surface expression levels stabilized with time, while transcripts and total protein decreased and then increased again. The CD28i CCP, on the other side, presented a different pattern in which the surface expression followed the mRNA and total protein levels. This data combined suggest that the loss of protein from the cell surface was likely a result of weaning transcription, and not due to protein internalization or poor transport to the cell surface. Differences in expression patterns between the CD40L:IgGFc and the CD40L:CD28i CCPs might be explained by their structural difference due to the different engineering approaches, creating the CD40L:IgGFc in a type 1 membrane protein orientation and the CD40L:CD28i in a type 2 orientation.

The mock control CD8 cells showed, as expected, low levels of surface expression, mRNA and total protein since CD40L is reported not to be typically expressed on effector CD8 T cells (**78**). Using this as a reference, it can be concluded that the detected CD40L expression on the CD8 T cells transduced with the IgGFc and CD28i constructs corresponds to the transduced chimeric co-stimulatory protein and not to an endogenously expressed CD40L protein.

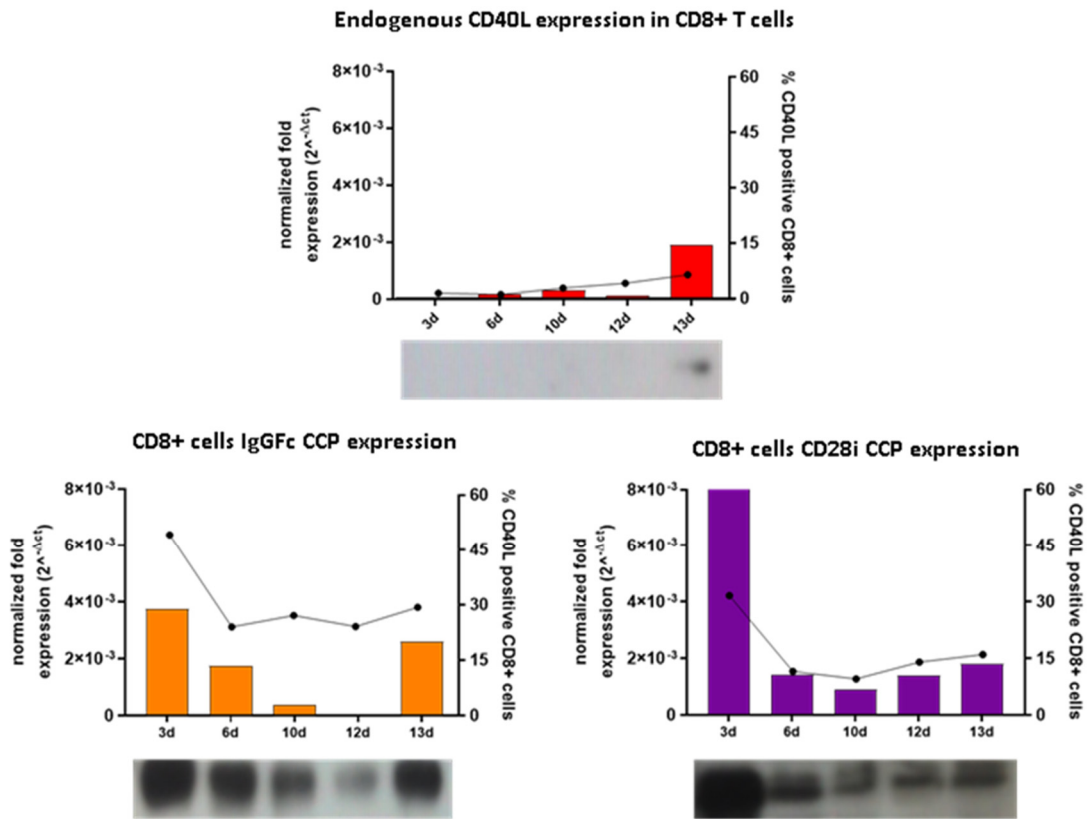


Figure 9. CCP expression kinetic on mRNA and surface protein level and whole protein detection by western blot.

Human PBMCs were activated using anti-CD3 plus anti-CD28 antibodies and 100 U/ml IL-2 for 2 days. Thereafter, cells were collected and transduced with the native CD40L and CCP constructs and expanded during a period of 13 days. Samples were enriched for CD8 T cells before retroviral transduction using magnetic beads and were then analyzed for CD40L surface protein by flow cytometry, whole protein expression by western blot and RNA level by qPCR at day 3, 6, 10 and 13 after transduction. Primers were designed to specifically detect the chimeric constructs. Normalized mRNA fold expression is depicted by the colored bars. The percentage of cells positive for CD40L on the cell surface was measured by flow cytometry and is depicted by the line diagram, colors correspond to the different chimeric proteins. Below the graphs are the western blots with bands corresponding to the molecular weights of the respective proteins. Representative results for the Mock transduced T cells and the two higher expressed CCPs are shown.

Having noticed that culture conditions had some effect on the surface expression of the CCPs, it was speculated whether T cell activation could also play an important role.

To test this hypothesis, CCP-transduced T cells, which had been frozen on day 12 when CCP expression was only slightly present for the IgGFc construct, were thawed. CD40L staining was performed and surface expression of the CCPs was analyzed directly after thawing (day 0 status) (Fig. 10A). Then, 1 million of each transduced T cell type (mock, nCD40L, CD40L:IgGFc, CD40L:Fil3 and CD40L:CD28i) were *in vitro* activated using 24 well plates coated with anti-CD3 and anti-CD28 antibodies and fresh medium with IL-2.

On day 3, cells were transferred to a non-antibody coated 24 well plate and cultured with fresh medium for another 3 days. The CCP surface expression was monitored on day 0, 3 and 6 (Fig. 10B).

Results showed that transduced T cells had upregulated the expression of the CD40L CCPs upon *in vitro* activation on day 3. Once the T cells were transferred to a new plate without antibody stimulation, the expression started to decline again, with considerable expression on day 6 seen for CD40L:IgGFc only (Fig. 10C, D). This kinetic allowed the CCPs to be expressed on the cell surface on day 6 with variable percentage of expression depending on each construct. At the same time point the endogenous CD40L expression was no longer detectable, as evidenced by the absence of staining of CD4 mock T cells on day 6. Therefore, CD4 mock transduced T cells was used as a negative control in further assays that assessed the CCPs functionality.

Based on this results, it must be concluded that some regulatory mechanism is activated in order to upregulate the expression of the CCPs upon CD3/CD28 stimulation.

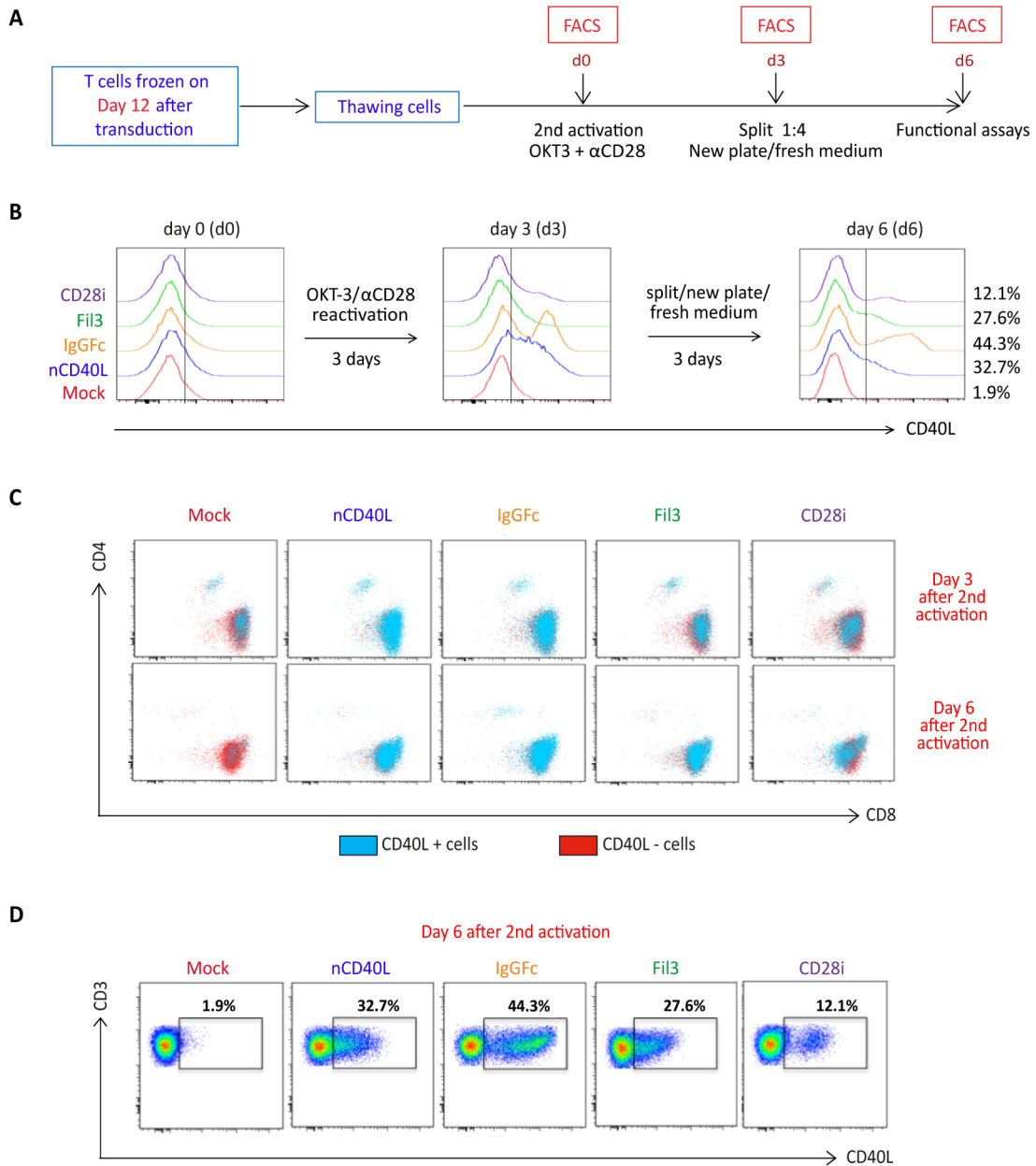


Figure 10. CCP surface expression is upregulated upon T cell activation.

A) Timeline depicting re-activation of human PBMCs, which were frozen on day 12 after CCPs transduction. Cells were thawed and reactivated using anti-CD3 plus anti-CD28 antibodies and 100 U/ml IL-2 for 3 days. Thereafter, cells were collected and transferred to a new plate without antibodies in fresh medium plus 100 U/ml IL-2 for 3 additional days to allow downregulation of endogenous CD40L expression on Mock T cells. B) Histograms showing CD40L surface expression by flow cytometry after thawing and every third day after reactivation. C) CD40L positive CD4 and CD8 cells within the live, single, CD3⁺ population are shown in the dot plots as the overlaid blue population and the CD40L negative cells are shown in red. Mock transduced PBMCs were used as negative control and cells transduced with the native CD40L (nCD40L) protein are the reference against the CCPs. D) Percentage of live, single, CD3 positive cells are shown in dot plots measured 6 days after reactivation of CCP-transduced T cells.

5.4 Downregulation of CD40L:CD28 CCPs by CD40 ligation.

It is well established that CD40L expression on CD4 T cells undergoes a rapid downregulation upon contact with its receptor CD40, which can be expressed on APCs like B cells and dendritic cells, as well as endothelial cells and a variety of tumor cells (**79,80**).

After observing that the CD40L-CCPs exhibit similar expression kinetic as the endogenous CD40L protein, and that upregulation is possible with CD3/CD28 activation, it was tested whether antigen-specific activation through MHC-TCR interaction can also induce CCP upregulation and whether interaction of the CD40L-CCP with its CD40 receptor expressed by target cells can cause its downregulation (Fig. 11A, 11B).

Target cells used in the following experiment were SK-Mel23, which is a melanoma cell lines that expresses Tyrosinase antigen in the context of MHC-class I HLA-A2 and the CD40 receptor. HEK293 cells stably transduced to express Tyrosinase antigen and the CD40 receptor were also used, named HEK293/Tyr/CD40 cells (Fig. 11E). To determine the influence of CD40 on the CD40L:CD28 CCP expression level after specific activation of the T cell through Tyr/HLA-A2 ligands, SK-Mel23 cell lines were treated with a CD40 blocking antibody before co-culturing them with the antigen-specific T cells. In the system, where HEK293/Tyr/CD40 cells were used for stimulation, control cells were HEK293/Tyr cells that were not co-transduced with CD40. The antigen-specific T cells in both systems were T cells that expressed the tyrosinase specific, HLA-A2 restricted TCR-T58 after retroviral transduction (**81**). The TCR-T58 T cells co-expressed the different CD40L:CD28 CCPs or without CCPs to be used as mock controls. TCR-T58 T cells with or without CCP were frozen on day 12, at the time point where the CD40L:CD28 CCPs had the lowest surface expression. They were thawed and immediately co-cultured with either SK-Mel23 or HEK293/Tyr/CD40 or HEK293/Tyr target cells. CD40L expression on the TCR-T58 effector T cells was measured before setting up the co-culture (0 hours) and at 16, 24 and 48 hours of co-culture.

Results showed that upregulation of the CCPs on the T cell surface was achieved in co-culture with HEK293/Tyr that express the Tyr/HLA-A2 target antigen complex (Figure 11C, left graph). The strongest induction was seen on TCR-T58 T cells that expressed the native CD40L (blue line) and the CD40L:IgGFc:CD28

(orange line). Less upregulation was seen for the CD40L:CD28i CCP, and very low induction was seen for the CD40L:Fil3:CD28 CCP (green line), which was at the level of TCR-T58 T cells that were not transduced with any CCP (mock, red line). Thus, it was observed that the upregulation of each CD40L-CCP followed the same pattern as the one previously observed with the CD3/CD28 unspecific activation, with CD40L:IgGFc CCP being the one that reached highest surface expression and CD40L:Fil3:CD28 reaching the lowest. Maximal upregulation was achieved at 16 hours of co-culture, reaching a sustained expression until the 48h time point. When HEK293/Tyr/CD40 cells were used as targets, upregulation of CD40L:28 CCPs was only seen for CD40L:IgGFc:CD28 until 24 h of co-culture. At 48 h of co-culture, marginal induction of nCD40L and CD40L:Fil3:CD28 and CD40L:CD28i was observed (Figure 11C right graph). Using the SK-Mel23 cells as target in the co-culture, a pattern similar to that of HEK293/Tyr/CD40 was seen (Figure 11D left graph). Since SK-Mel23 expresses CD40 endogenously, it was hypothesized that the CD40 expression on the target cell might disturb CD40L-CCP surface expression. To test this, SK-Mel23 were pre-treated with anti-CD40 blocking antibody before setting up the co-culture. Using SK-Mel23 cells with “masked” CD40 surface expression, strong induction of all CD40L-CCPs was observed (Figure 11D, right graph). This result allows the interpretation that T cell stimulation through physiologic TCR-peptide/MHC interaction indeed induces CD40L:CD28 CCP surface expression as does the experimental CD3/CD28 stimulation. Moreover, the dynamics of surface expression is modulated by CD40 expressed on the target cells, which causes downregulation of the CD40L:CD28 CCPs as well as the native CD40L from the T cell surface.

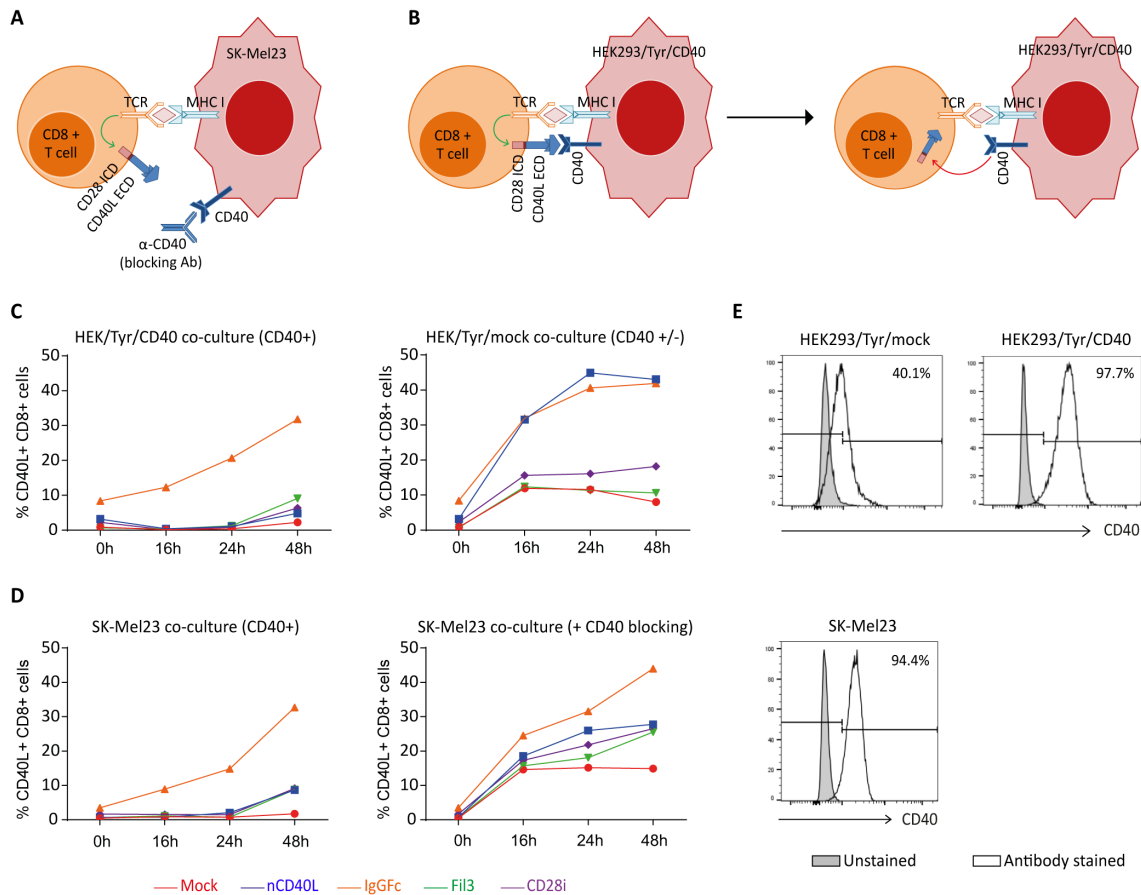


Figure 11. CD40L:CD28 CCP expression kinetic on T cells after T cells recognizing peptide/MHC ligands in the presence or absence of CD40 receptor.

Human T cells transduced with the tyrosinase-specific TCR-T58 and CD40L:CD28 CCPs were frozen on day 12 after CD40L:CD28 CCPs transduction. After thawing, the TCR-T58 T cells with or without CD40L:CD28 CCP were used in co-cultures at a T cell to target cell ratio of 1:10 with tyrosinase-transduced target cells HEK293/Tyr/mock cells that had very low to no endogenous CD40 expression or were transduced to strongly express CD40, HEK293/Tyr/CD40, or with the melanoma cell line SK-Mel23 that endogenously expresses CD40. A, B) Schematic diagram of the co-culture assay. Briefly, by blocking the CD40 receptor, antigen-specific activation produced by the TCR/MHC interaction will allow the re-expression of the CCPs on the cell surface (A). If CD40/CD40L interaction is not blocked re-expression would still happen, but a downregulation of the CCPs will be produced immediately upon interaction with CD40, rendering surface expression detection impossible (B). C) depicts the CD40L:CD28 CCP expression on TCR-T58 T cells after indicated times of co-culture with either HEK293/Tyr or HEK293/Tyr/CD40 cells; or D) in co-culture with SK-Mel23 cells or with SK-Mel23 that had been pre-treated with anti-CD40 antibody in a 1:11 concentration (clone HB14 pure functional grade - Miltenyi) before setting the co-culture to block the endogenous CD40. The percentage of TCR-T58 T cells with CD40L:28 surface expression was analyzed by flow cytometry. Mock transduced TCR-T58 T cells (red line) and TCR-T58 T cells transduced to express the native CD40L (blue line) were used as reference. TCR-T58 T cells transduced with CD40L:IgGFc:CD28 are depicted in orange, those with CD40L:Fil3:CD28 CCP are depicted in green and T cells with CD40L:CD28i CCP are depicted in purple. E) Histograms of CD40 expression on target cells, whereby the line histogram depicts the specific staining for CD40 and the grey filled histogram is the isotype control. Staining was done with an anti-CD40 PE labeled antibody (clone H-10, Santa Cruz Biotechnology).

5.5 Biological functionality of CD40L and CD28 domains in the CD40L:CD28 CCPs

5.5.1 Biological activity of the extracellular CD40L domain

After having determined that the composite proteins can be expressed on the cell surface, assessing if the different domains were functionally incorporated into the chimeric CD40L:CD28 CCPs was the next step.

To test the biologic activity of the CD40L extracellular domain, a B cell stimulation assay was established. It is well described that B cells express the CD40 receptor. Upon interaction with the CD40 ligand (CD40L) B cells undergo activation which can be detected by measuring key surface activation markers on the B cells like CD86, Fas and CD83 (Fig. 12A). Upregulation of the three markers, CD83, CD86 and Fas, are linked to the CD40/CD40L interaction. CD86 and Fas expression might also be influenced by TCR/MHC interaction that occurs between T cells and B cells when latter serve as antigen presenting cells. CD83 has been reported to be induced on B cells via CD40 engagement independent of TCR/MHC binding (82).

In our system, the Tyrosinase-specific TCR-T58 T cells were used transduced with the CD40L:CD28 CCPs and B cells were isolated from blood of healthy donors. No tyrosinase was present in the system so that B cell activation through antigen was excluded. T cells without and with CD40L:CD28 CCPs were thawed and reactivated using CD3/CD28 antibody-coated 24 well plate for 6 days (Fig. 12B) to re-induce CCP expression. T cells were harvested for co-culture on day 6 when CD40L:CD28 CCP levels were still detectable, but the mock controls were CD40L negative (red histograms), indicating endogenous CD40L that would conceal effects of the CD40L:CD28 CCPs was no longer expressed (Fig. 12B). T cells were co-cultured with freshly isolated B cells overnight (12 h) in a 1:1 ratio followed by analysis of surface activation markers on the B cell population by flow cytometry (Fig. 12C). It was observed that CD83, CD86 as well as Fas were induced on B cells that were co-cultured with T cells expressing the CD40L:CD28 CCPs or the native CD40L compared the co-culture with mock T cells that did not express any CD40L construct or control B cells without T cell co-culture (control). Gradual levels of activation marker expression on B cells was observed depending on the variant of CD40L:CD28 CCP expressed by the T cells with highest

expression of activation markers achieved with T cells expressing CD40L:IgGFc:CD28, followed by native CD40L, CD40L:CD28i and lowest CD40L:Fil3:CD28. As reference, two different positive controls were included to stimulate the B cell population: one control setting used a commercial soluble CD40L agonist combined with an enhancer to promote CD40L trimerization and hence B cell activation, the other control was a co-culture with the HEK293 cells that stably expressed high levels of CD40L. Using the sCD40L/enhancer agonist achieved induction of activation markers on B cells similar to the T cell culture with CD40L:CD28 CCP engineered T cells. Highest levels of B cell activation were achieved with the HEK293/CD40 cells.

These results show that maturation of B cells can be achieved by the effect of the interaction between T cells expressing CD40L:CD28 CCPs and the CD40 receptor expressed on the surface of B cells, providing proof of concept that the CD40L extracellular domain within the CCPs is capable of exerting biologic activity.

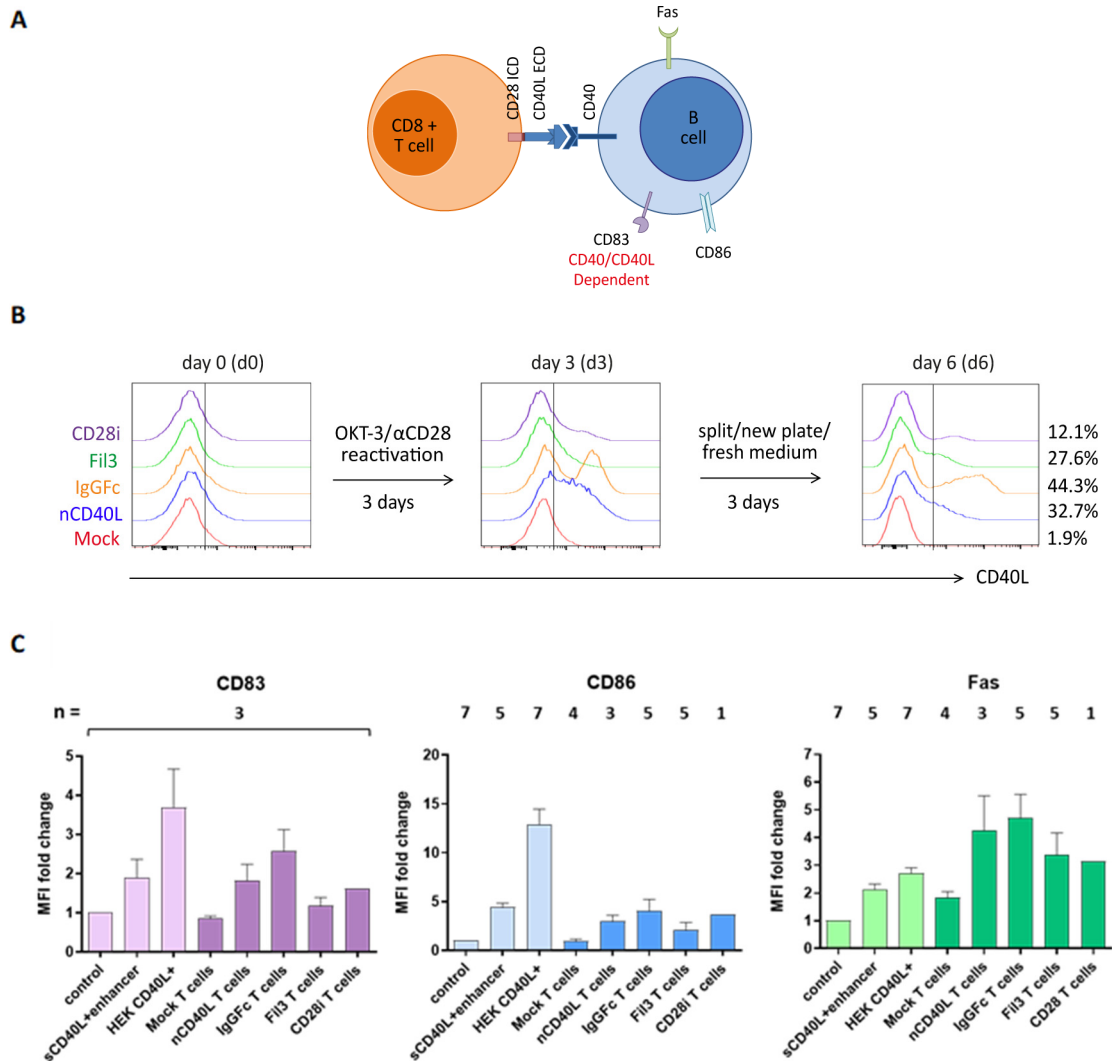


Figure 12. Assessing the biologic activity of the extracellular CD40L domain within the chimeric CCPs using a naïve B cell stimulation assay.

T cells transduced with the CCPs were frozen on day 12 after CCPs transduction. They were thawed and reactivated using anti-CD3 plus anti-CD28 antibody-coated 24well plates and 100 U/ml IL-2 for 3 days. Thereafter, the cells were collected and transferred to a new plate without antibodies using fresh medium plus 100 U/ml IL-2 for 3 additional days to allow downregulation of endogenous CD40L expression on Mock T cells. Fresh B cells were isolated from 300 ml peripheral blood using a CD19 magnetic negative isolation kit (Miltenyi). Naïve B cells were co-cultured at a 1:1 ratio with anti-CD3/CD28-activated T cells expressing the CD40L:CD28 CCPs overnight at 37°C and 5% CO₂. Then, cells were harvested and analyzed by flow cytometry for B cell specific surface activation markers CD83, CD86 and Fas. Three control conditions were included: i) a negative control consisting of naïve B cells without T cells (unstimulated control), ii) a positive control using naïve B cells stimulated with a soluble enhanced trimeric CD40L (Enzo Life Science), and iii) naïve B cells co-cultured with CD40L-expressing HEK293 cells. A) Schematic diagram of the stimulation assay. B) Histograms depicting the CD40L:CD28 CCP expression on the transduced T cells after thawing and anti-CD3/CD28 reactivation and culture for 6 days. C) Graphs depicting the mean fluorescence intensity (MFI) of CD83 (purple), CD86 (blue) and Fas (green) on the surface of B cells after overnight co-culture with the corresponding stimulation conditions. Controls are the first three bars distinguished by light colors, respectively. Bars are the mean values of indicated number of independent experiments. The error bars are the standard deviation of the corresponding number of experiments n.

In a next step, experiments were performed to test the hypothesis outlined in figure 4, whether T cells expressing CD40L:CD28 CCPs can activate antigen presenting cells. The binding of CD40L extracellular domain to CD40 on antigen-presenting cells (APCs), such as B cells, dendritic cells (DCs), and monocytes, should lead to their maturation and activation (Fig. 13A). In case of DCs, this should license them to secrete pro-inflammatory cytokines that support CD4⁺ T cells responses and CD8⁺ cytotoxic T cell priming (**83**).

Dendritic cells were generated *in vitro* following a 7 day protocol (**72**). Tyrosinase-specific TCR-T58 T cells transduced with the CD40L:CD28 CCPs were thawed and reactivated using anti-CD3/CD28 antibody coated 24 well plate for 6 days (see figure 10).

On day 6, when CD40L levels for the cells transduced with the nCD40L and chimeric CD40L:CD28 proteins were still detectable, but the mock control T cells were negative for CD40L (avoiding effect of endogenous CD40L expression levels) (Fig.13B), T cells were harvested and co-cultured with the *in vitro* generated immature dendritic cells (iDCs) overnight (12 h) in a 1:1 ratio.

iDCs without T cell co-cultures served as a negative control, while DCs matured with an specific cytokine cocktail (Jonuleit) were used as a positive control.

After the co-culture, 5 characteristic activation markers (CD80, HLA-DR, PD-L1, CCR7 and CD83) were evaluated on the surface of the DCs.

As depicted in figure 10B, the nCD40L and chimeric CD40L:CD28 proteins were nicely detected on the T cells when starting the co-culture with gradual expression levels as typically observed for each variant of CCP. Also, the CD40L level of mock transduced T cells was below detection limit, which was a prerequisite to avoid that endogenous CD40L might conceal effects of the CD40L:CD28 CCPs. In figure 13C, the expression of DC maturation markers after each culture condition is depicted as the mean fluorescence intensity. For CD83, CCR7 and PD-L1, the expression levels were highest after co-culture with T cells expressing the CD40L:IgGFc:CD28 closely followed by the levels observed on mDC. T cells expressing CD40L:Fil3:CD28 or CD40L:CD28i still induced levels above those achieved with Mock T cells or T cells with native CD40L or iDCs that were not stimulated at all. For HLA-DR and CD80 markers, no significant difference was seen for any of the culture conditions.

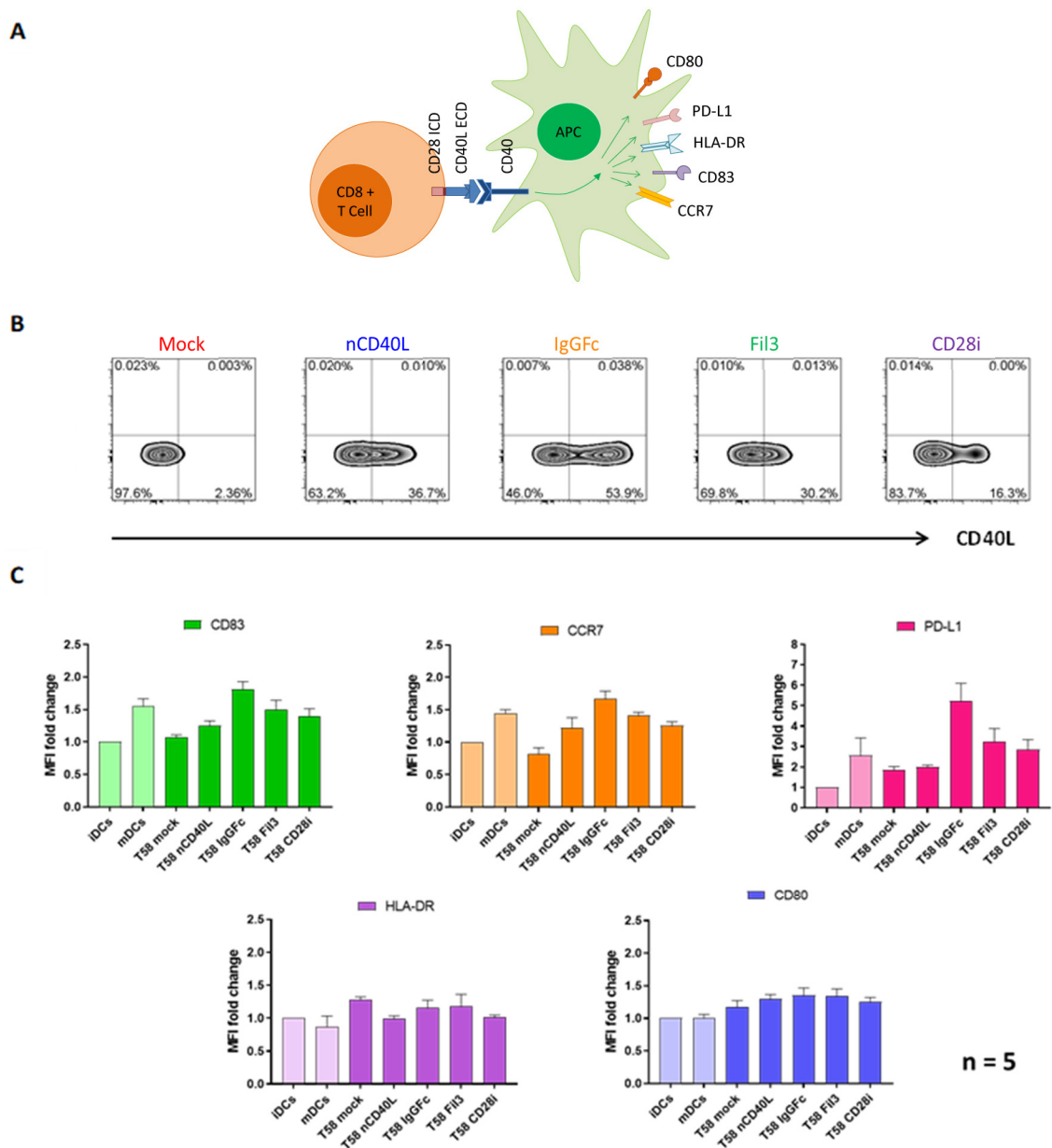


Figure 13. T cells expressing the CD40L:CD28 CCPs can activate dendritic cells through CD40/CD40L interaction.

T cells transduced to express CD40L:CD28 CCPs were frozen on day 12 after CCP transduction. They were thawed and reactivated using anti-CD3 plus anti-CD28 antibody coated 24 well plates and 100 U/ml IL-2 for 3 days. Thereafter, T cells were collected and transferred to a new plate without antibodies in fresh medium plus 100 U/ml IL-2 for 3 additional days to allow downregulation of endogenous CD40L expression on Mock T cells. Immature dendritic cells (iDCs) were generated from CD14⁺ monocytes isolated from PBMCs using the plastic adherence technique by culturing them in medium supplemented with 20 ng/ml IL-4 and 100 ng/ml GM-CSF on day 0 and day 3. On day 7, the iDCs were harvested and incubated at a 1:1 ratio with the CD40L-CCP-transduced T cells overnight at 37°C and 5% CO₂. The next day, cells were harvested and analyzed by flow cytometry for surface expression of specific DC maturation markers. Two control conditions were used as reference: i) negative control consisting of iDCs that didn't receive any maturation stimuli, ii) a positive maturation control, consisting of iDCs incubated on day 7 with a cytokine maturation cocktail consisting of 20 ng/ml IL-4, 100 ng/ml GM-CSF, 15 ng/ml IL-6, 10 ng/ml IL-1 β , 20 ng/ml TNF α and 1 μ g/ml PGE₂. A) Schematic drawing of the DC maturation assay.

B) Density plots depicting the CD40L:CD28 CCP expression on the transduced T cells after thawing and activation for 3 days plus 3 additional days of culture. C) Graphs depicting the CD83 (green), CCR7 (orange), PD-L1 (dark pink), HLA-DR (light pink) and CD80 (purple) surface expression on DCs after overnight co-culture with the corresponding stimulation. Controls correspond to the first two bars distinguished by light colors, respectively. Bars are the mean values of the median fluorescence intensity of respective marker from 5 independent experiments. Error bars show the standard deviation.

5.5.2 Biological activity of the intracellular CD28 signaling domain

After addressing the biologic activity of the CD40L extracellular domain of the different CD40L:CD28 CCPs, it was determined whether the CD28 intracellular domain was capable to deliver a proper co-stimulation signal to the T cells that were transduced with the different formats of the CD40L:CD28 CCPs.

CD28 co-stimulation, acting through phosphatidylinositol 3'-kinase (PI3K) and phosphorylation of AKT, is required for T cells to increase their glycolytic rate in response to activation. CD28 co-stimulation also extends the viability of T cells by preventing apoptotic cell death linked to the TCR signaling (**84**).

The protein Kinase B, also known as AKT, affects downstream signaling interactions leading to improved cytokine secretion via NF- κ B activation. Among these interactions is the mammalian target of rapamycin (mTOR) molecule, which in turn becomes a key player for metabolism regulation, influencing cell proliferation and growth as well as T cell memory generation (**85**). A downstream product of mTOR activation is the ribosomal protein S6 (RPS6), which influences T cell response by stimulating IFN- γ secretion and other T cell effector molecules.

The functionality of the CD28 intracellular domain of our CD40L:CD28 CCPs to activate the CD28 signaling cascade was determined by analyzing the phosphorylation of AKT, mTOR and RPS6 in CCP-transduced antigen-specific T cells after co-culturing them with antigen positive and CD40 positive target cells.

T cells with the tyrosinase-specific TCR-T58 and transduced with the different CD40L:CD28 CCPs, as well as mock transduced T cells as controls (all T cells frozen on day 12 after activation, corresponding to the lowest CD40L surface expression) were thawed and reactivated with the described 6 day schedule (see description on Fig. 10). CCP expression levels on the T cell surface are depicted in figure 14A. For stimulation, the HEK293/Tyr/CD40 cells were used which can trigger the T58-TCR through HLA-A2/Tyr ligands and the CD40L:CD28 CCPs through CD40 expression. Before setting up the stimulation co-culture, T cells were deprived of IL-2 for 4 hours to reduce the level of constitutive AKT activation. After the IL-2 starving time, antigen-specific TCR-T58 T cells expressing the different CD40L:CD28 CCPs were co-cultured with HEK293/Tyr/CD40 target cells for 30 minutes, which was previously determined as the optimal time for AKT activation to reach its peak (**86,87**). After stimulation, cells were fixed, stained

and analyzed for the phosphorylation of the described CD28 signaling cascade proteins.

Results showed that phosphorylation of AKT protein increased after co-culturing the CCP-transduced T cells with antigen-specific CD40-positive target cells in comparison with the Mock T cells without CCP, the native CD40L-transduced T cells that does not contain the CD28 signaling domain and the unstimulated T cells (Fig. 14B, left graph). Same results were detected for the phosphorylation of the mTOR and RPS6 proteins (Fig. 14B), which is in line with the knowledge that phosphorylation of AKT provokes phosphorylation of mTOR, which in turn causes the phosphorylation of RPS6.

Induction of phosphorylation was strongest with T cells that expressed the CD40L:Fil3:CD28 or the CD40L:CD28i compared to T cells with the CD40L:IgGfc:CD28. The differences between the three CD40L:CD28 CCPs can be appreciated better when phosphorylation for the three different proteins is depicted using histogram graphs, where an increased MFI of phosphorylated AKT and mTOR relative to the unstimulated T cells was present only when the T cells expressed the CCPs (colored histogram), while the MFI in Mock and native CD40L expressing T cells was similar to unstimulated control (Fig. 14C). For the phosphorylation of RPS6, the picture was a bit different: The MFI of phosphorylated protein p-RPS6 was lower in stimulated T cells that expressed no CCP or the native CD40L protein compared with the unstimulated control, while phosphorylation was upregulated in stimulated T cells expressing the CD40L:Fil3:CD28 or the CD40L:CD28i CCP, reaching levels of the unstimulated T cells.

Finally, the correlation of phosphorylation of the CD28 downstream signaling proteins was depicted by plotting the p-AKT against p-mTOR and p-mTOR against p-RPS6. The percentages of double-positive populations, corresponding to T cells that had phosphorylated both the AKT plus mTOR or mTOR plus RPS6, was notably higher in T cells that were transduced with the CD40L:CD28 CCPs compared to Mock T cells without CCP or T cells transduced with the native CD40L that does not contain a CD28 signaling domain (Fig. 14D).

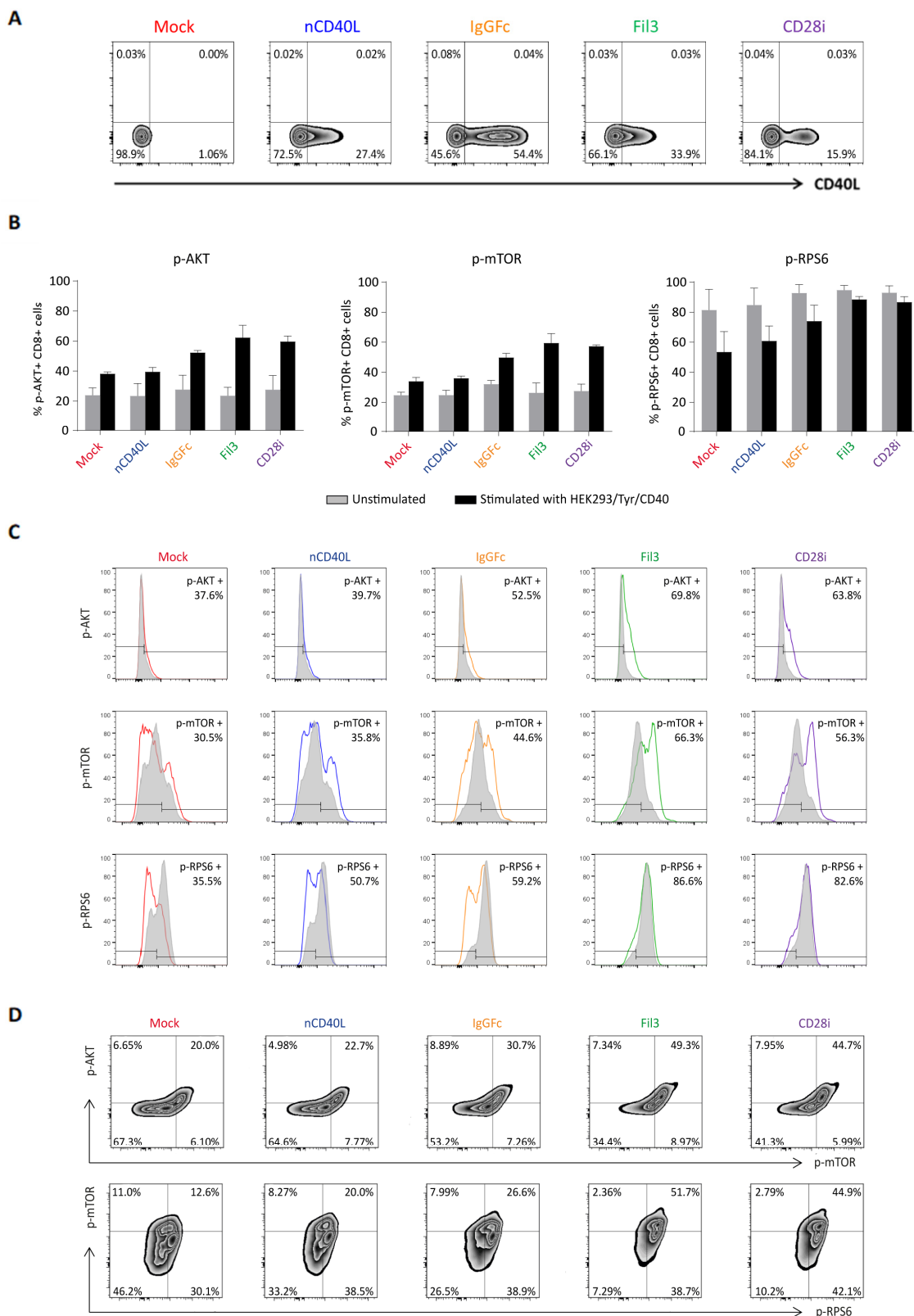


Figure 14. Interrogating the biological activity of the CD28 intracellular domain by measuring the phosphorylation of AKT, mTOR and RPS6.

T cells transduced to express the Tyrosinase-specific TCR-T58 plus CD40L:CD28 CCPs were frozen on day 12 after CCP transduction. They were thawed and reactivated using anti-CD3 plus anti-CD28 antibody-coated 24 well plates and 100 U/ml IL-2 for 3 days. Thereafter, T cells were collected and transferred to a new plate without antibodies in fresh medium plus 100 U/ml IL-2

for 3 additional days to allow downregulation of endogenous CD40L expression on Mock T cells. Before performing the CD28 signaling assay, T cells were deprived of IL-2 for 4 h to reduce constitutive AKT signaling. HEK293/Tyr/CD40 were used to stimulate the T cells through the TCR-Tyr/HLA-A2 and trigger the CCPs through CD40. HEK293/Tyr/CD40 were harvested and incubated at a 1:2 ratio with the CD40L:CD28 CCP-transduced T cells for 30 minutes at 37°C and 5% CO₂, unstimulated T cells were kept in culture as a negative control. After 30 minutes, cells were fixed, stained and analyzed by flow cytometry to detect phosphorylated proteins p-Akt, p-mTOR and p-RPS6 by flow cytometry using a commercial buffer set (BDPhosflow™). A) Density plots depicting the CD40L:CD28 CCP expression on the T cells at the starting point of the co-culture. B) Graphs corresponding to the percentage of phosphorylated intracellular proteins p-AKT, p-mTOR and p-RPS6 in T cells after 30 minutes co-culture, grey bars corresponding to the unstimulated controls and black bars corresponding to the T cells stimulated with the HEK293/Tyr/CD40 target cells. Bars are the mean values of the percentages of three independent experiments. The error bars are the standard deviation. C) Histograms depicting the fluorescence intensity of each phosphorylated protein in T cells expressing the different CCPs unstimulated (grey histogram) and after stimulation (colored histogram). D) Density plots showing the correlation between p-AKT with p-mTOR and p-mTOR with p-RPS6 in T cells expressing the different CCPs. Mock-transduced T cells (red) and T cells transduced to express the native CD40L (blue) were used as references. T cells transduced with CD40L:IgGfC:CD28 are depicted in orange, those with CD40L:Fil3:CD28 CCP are depicted in green and T cells with CD40L:CD28i CCP are depicted in purple. Unstimulated control is depicted in grey.

5.6 CD40L:CD28 CCPs improve T cell function

Functionality of both domains of the CD40L:CD28 CCPs was demonstrated in the previously described experiments. Knowing that human T cells engineered to express TCR- ζ and CD28 signaling domains into its cytoplasmic tail demonstrated enhanced cytokine secretion and antitumor efficacy (34), it was tested if the CD28 signaling provided by the CCPs was able to improve T cell effector function, namely cytokine secretion and cytotoxicity.

After a co-culture of tyrosinase antigen-specific TCR-T58 T cells transduced to express the different CD40L:CD28 CCPs with SK-Mel23 cells (tyrosinase positive and CD40 positive), IFN- γ and IL-2 secretion levels were higher compared to TCR-T58 mock T cells without CD40L:CD28 CCP (Fig. 15A, 15C). A similar IFN- γ secretion result was observed when renal cell carcinoma specific TCR-53 T cells transduced with CD40L:IgGFc:CD28 and CD40L:CD28i CCPs were co-cultured with CD40 positive RCC53 and RCC26 cell lines (Fig. 15B, 15C) Due to limited numbers of TCR-53 T cells the native CD40L and the CD40L:Fil3 CCP could not be tested (Fig. 15B).

Among the different CCP formats, the CD40L:IgGFc:CD28 (orange) had the lowest effect on cytokine secretion, while the CD40L:CD28i (purple) enhanced the cytokine secretion more strongly. This is of note, since it contrasts with the expression level of the CCPs on the T cells where the CD40L:IgGFc:CD28 had highest level and the CD40L:CD28i the lowest (see for example figure 14A).

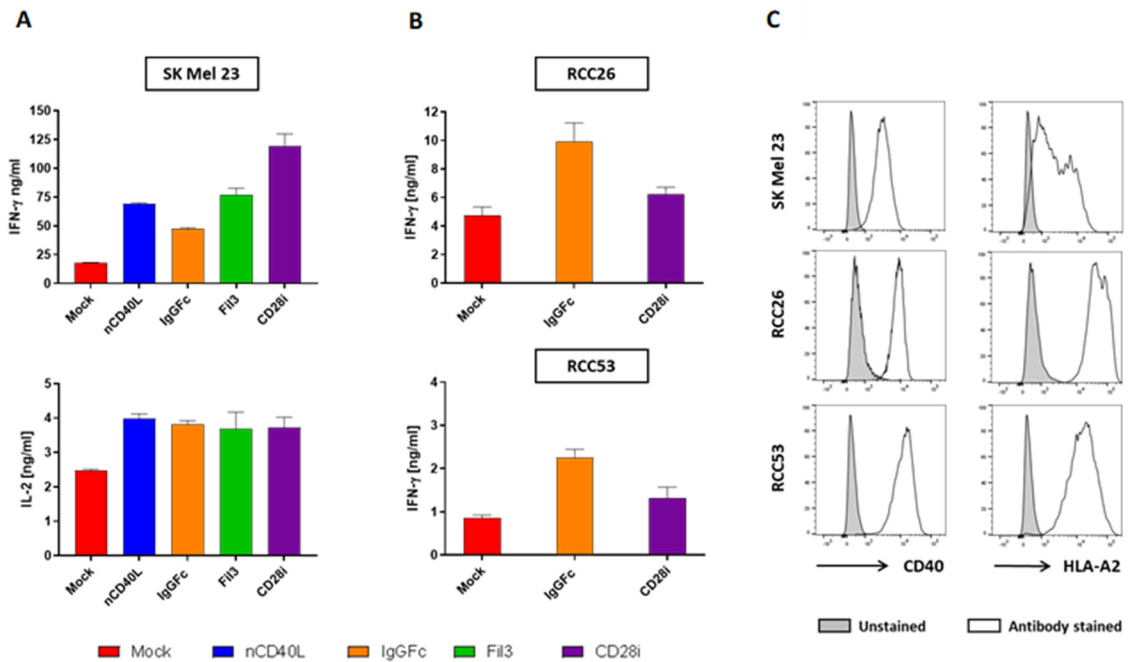


Figure 15. CD40L:CD28 proteins improve T cell cytokine secretion.

Human T cells transduced with the RCC-specific TCR-T53 or tyrosinase-specific TCR-T58 together with CD40L:CD28 CCPs were frozen on day 12 after CD40L:CD28 CCPs transduction. After thawing, the TCR-53 and TCR-T58 T cells without or with CD40L:CD28 CCP were used in co-cultures at a T cell to target cell ratio of 1:10 with tyrosinase-positive target cells SK-Mel23 for TCR-T58 T cells, and RCC26 and RCC53 renal cell carcinoma tumor cell lines for TCR-53 T cells. All target cells expressed CD40 endogenously (C). Supernatants were collected at 48 hours for the SK-Mel23 co-cultures and 24 hours for the RCC co-cultures. IFN- γ and IL-2 ELISA were performed. A) IFN- γ (top) and IL-2 (bottom) ELISA results for the co-cultures of TCR-T58 cells transduced with the different CD40L:CD28 CCPs and the tumor cell line SK-Mel23. B) IFN- γ ELISA results for the co-cultures of TCR-53 cells transduced with two different CD40L:CD28 CCPs and the tumor cell lines RCC26 (top) and RCC53 (bottom). Mock transduced TCR-T58 and TCR-53 T cells (red) and TCR-T58 T cells transduced to express the native CD40L (blue) were used as reference. Antigen-specific T cells transduced with CD40L:IgGfc:CD28 are depicted in orange, those with CD40L:Fil3:CD28 CCP are depicted in green and T cells with CD40L:CD28i CCP are depicted in purple. Shown are mean values of duplicates from one representative experiment. The error bars are the standard deviation. C) Histograms of CD40 and HLA-A2 expression on target cells, whereby the line histogram depicts the specific staining for CD40 and HLA-A2 and the grey filled histogram is the unstained control.

Beyond cytokine secretion, tumor cell death through effector T cells plays a major role in the antitumor response. Since the CD40L:CD28 CCPs showed indications of improved cytokine secretion and activation of key components of the CD28 signaling cascade such as AKT, mTOR and RPS6, specific lysis of target cells was analyzed. Tyrosinase-specific TCR-D115 transduced T cells with the different CD40L:CD28 CCPs were co-cultured with ^{51}Cr -labeled SK-Mel23 and HEK/Tyr/CD40 target cells at various effector to target cell ratios (Fig. 16A, 16B). It was observed that TCR-D115 expressing the CD40L:CD28 CCPs had higher lytic activity against both targets at all effector to target ratios compared to the mock control (red) and the native CD40L transduced T cells (blue line), which lacked the CD28 intracellular domain and is, thus, unable to transmit co-stimulatory signal.

As already noted for the cytokine secretion, the CD40L:IgGFc:CD28 (orange line) had the lowest effect among the different CCP formats, while the CD40L:Fil3:CD28 (green) and the CD40L:CD28i (purple) enhanced the lytic activity more strongly.

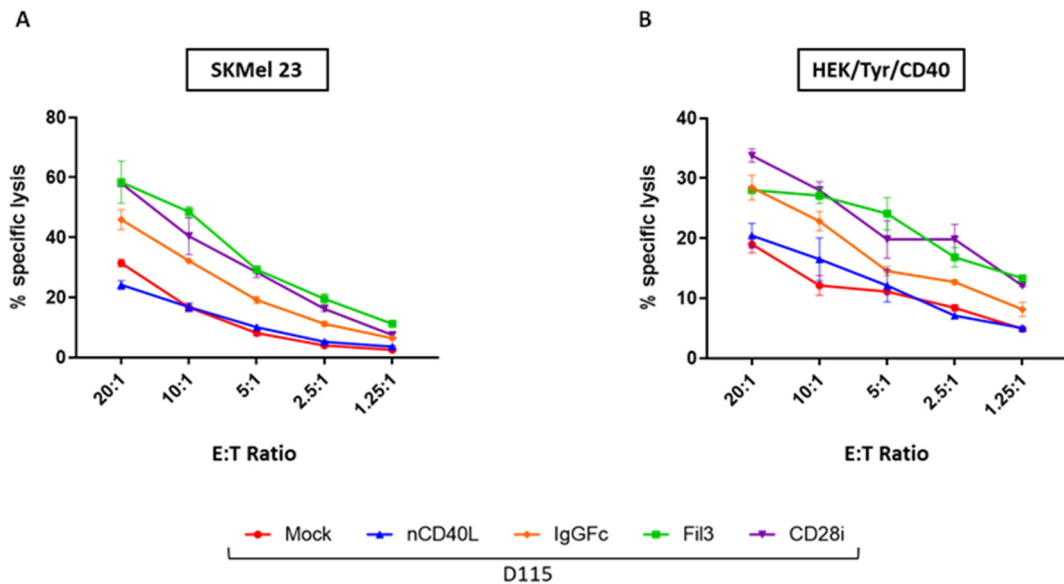


Figure 16. Effect of CD40L:CD28 CCPs on the cytolytic activity of antigen-specific T cells. Human T cells transduced with the tyrosinase-specific TCR-D115 were frozen on day 12 after CD40L:CD28 CCP transduction. Directly after thawing, TCR-D115 T cells with the different CD40L:CD28 CCPs were used in co-cultures at five different T cell to target cell ratio (E:T) against ^{51}Cr -labelled tyrosinase and CD40 positive target cells SK-Mel23 and HEK/Tyr/CD40. Target cell lysis was assessed by detecting released ^{51}Cr after 4 hour co-culture. A) SK-Mel23 co-culture. B) HEK/Tyr/CD40 co-culture. Mock transduced TCR-D115 T cells (red) and TCR-D115 transduced

to express the native CD40L (blue) were used as reference. Antigen-specific T cells transduced with CD40L:IgGFc:CD28 are depicted in orange, those with CD40L:Fil3:CD28 CCP are depicted in green and T cells with CD40L:CD28i CCP are depicted in purple. Shown are mean values of duplicates from one representative experiment. Shown are mean values of duplicates from one representative experiment. Error bars show the standard deviation.

The results depicted in figures 15 and 16, are one representative out of three experiments. They suggest a positive effect of the CD40L:CD28 CCPs on two central effector functions, cytokine secretion and cytotoxicity. These observations need to be further reaffirmed through more repetitions. Since the CD40L:CD28 CCP have a unique expression dynamic, which was not seen in other chimeric constructs such as the PD-1:CD28, different time frames might be necessary for the assays to reveal strongest effects. Short term assays, like ELISA for cytokine and ⁵¹Cr release for cytotoxicity analysis, might not be completely suitable to assess the benefit of the CCPs on the key effector functions of antigen-specific T cells.

5.7 *In vivo* performance of CCPs composed of PD-1 extracellular domain and intracellular signaling domain CD28 (PD-1:CD28 CCP)

The results of these experiments are part of the publication by R. Schlenker et al. (70). All the experiments corresponding to figure 6 in the publication (figure 17 of this thesis) and the interpretation of the results were done as part of this thesis. According to the Copyright criteria established by Cancer research, I am as an author of the publication authorized to use the figures and text of the publication without requiring the journal permission.

The adoptive T cell experiments using the mouse xenografts were part of this thesis and, thus, are presented here briefly. While the CD40L:CD28 CCPs were designed and characterized *in vitro*, another chimeric protein had been already functionally evaluated *in vitro* (Schlenker PhD) (69). This CCP consisted of the extracellular domain of PD-1 and the transmembrane domain plus intracellular signaling domain of CD28. The PD-1:CD28tm CCP should be triggered by tumor-expressed PD-L1 and deliver co-stimulation and, thus, functional support to the T cells. The functional performance of T cells expressing this PD-1:CD28tm CCP was assessed in an *in vivo* human melanoma xenograft mouse model. The mice

were immunocompromised NSG mice that are devoid of endogenous T and B cells as well as NK cells. For adoptive T cell transfer (ATT) experiments, mice carried established vascularized subcutaneous melanoma tumors formed by the SK-Mel23 melanoma cell line, which is HLA-A2 and tyrosinase positive (Fig. 17A). The two different T effector cells that were injected consisted of T cells expressing the TCR-D115 with and without (Mock) the presence of the PD-1:CD28-CCP (PD-1:28tm). Expression of PD-1 was tracked after i.t. injection according to the time points depicted in figure 17A.

It was observed that the TCR-D115/MOCK T cells stained positive for PD-1 on 1d, 2d and 4d after ATT. The PD-1 staining decreased thereafter, but never completely disappeared (Fig. 17B, 17C). This temporary expression of endogenous PD-1 is indicative of T-cell activation within the tumor microenvironment, as PD-1 has been described to be expressed on recently activated T cells (88). Activation lasted until day 4 after ATT. For TCR-D115/PD-1:28tm-transgenic T cells, a transient expression of endogenous PD-1 could not be distinguished from the transgenic PD-1:28tm expression. However, a temporary increase in median FI of PD-1 was observed with similar kinetics suggesting that here an activation of the T cells also occurred.

T cells were labeled with the CFSE reagent, which allowed to determine their proliferation by analyzing the dilution of this dye over time. It was observed that T cells containing the PD-1:28tm CCP lost the dye faster, indicating stronger proliferation in comparison to the Mock T cells (Fig. 17D, 17E). It was not possible in this model to assess tumor growth control through ATT since tumors were grown to large size to ensure that a challenging microenvironment had been established before T cells were injected. With tumor being already large at the time T cell injection, animal regulatory restrictions did not allow that the observation time was extended beyond day 7 after ATT, which would have been required to track a possible reduction in tumor size. Nevertheless, when the tumor volumes were compared within the 7 day time period, tumors that were injected with TCR-D115 cells carrying the CCP were smaller compared to the tumors injected with the Mock T cells without CCP (Fig. 17F). Moreover, tumors injected with TCR-D115/PD-1:28tm T cells had higher T cell numbers compared to tumors injected with TCR-D115/Mock T cells and TCR-D115/PD-1:28tm T cells had higher percentages of cells positive for the proliferation marker Ki-67 and lower frequencies

of cells expressing PD-L1 (Fig. 17G). PD-L1 on T cells has been described to inhibit T cell expansion and function (89). Therefore, lower PD-L1 positive cells and higher T cell numbers might underly the observed better tumor control in ATT with TCR-D115/PD-1:28tm-T cells.

To provide further evidence that TCR-D115/PD-1:28tm T cells are capable to perform better tumor control, a Matrigel matrix plug assay was performed. Here, T cell/tumor cell mixtures comprising of an antigen-positive (SK-Mel23) and an antigen-negative (HEK/PD-L1) tumor cell line at a 1:1 ratio were embedded in Matrigel and implanted s.c. in NSG mice. T cells were either TCR-D115/PD-1:28tm T cells or TCR-D115/Mock T cells. After 2 days, the matriplug was recovered and the ratio of antigen-positive and antigen-negative tumor cells was determined by flow cytometry. A shift away from the 1:1 ratio is indicative of unequal cell death. In the mixture containing the D115/PD-1:28tm T cells, antigen-positive SK-Mel23 were proportionally more lost compared to the culture with TCR-D115/mock T cells indicating a higher specific SK-Mel23 tumor cell killing through T cells expressing D115/PD-1:28tm than through TCR-D115/Mock T cells (Fig. 17H).

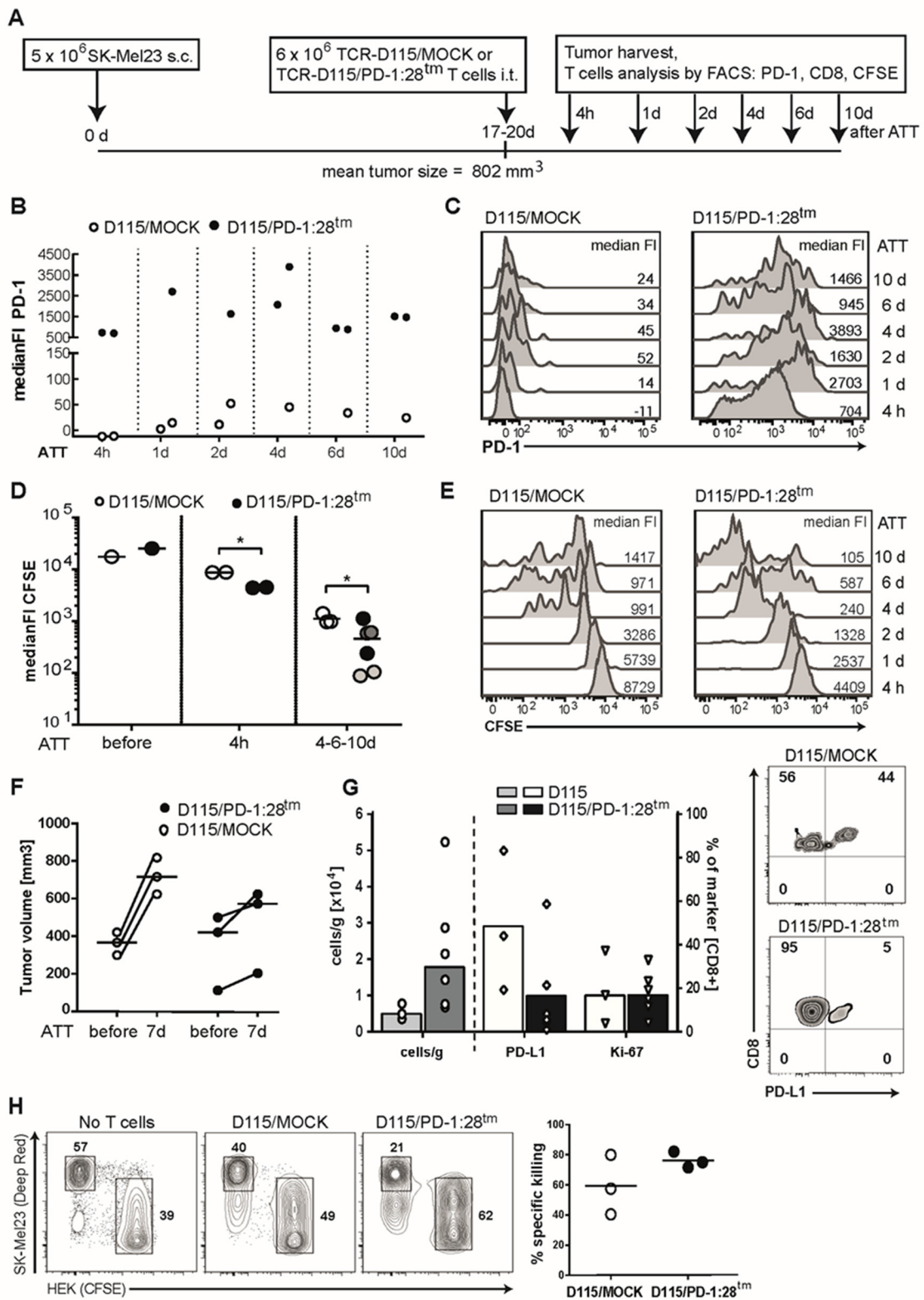


Figure 17. PD-1:28tm expression on T cells fosters intratumoral T cell proliferation in a human melanoma xenograft model.

A) Graphical description of the experiment timeline. Briefly, i.t. injection of SK-Mel23 tumor cells in NSG mice marked the beginning of the experiment. After 17-20 days average tumor size of 800 mm³ was achieved and effector T cells were injected i.t., resection of the tumors and FACS analysis of the isolated cell suspension took place at 4 hours, 1, 2, 4, 6 and 10 days after effector

cell injection. B) Kinetic of PD-1 surface expression on isolated TCR-D115 Mock effector cells and TCR-D115 cells expressing the PD-1:28tm CCP, and the corresponding histograms (C) depicting medianFI values through all the experimental time points. D) medianFI values CFSE dye dilution representing cell proliferation of the injected effector populations (Mock and PD-1:28tm cells). White circles represent TCR-D115 Mock T cells values on defined recovery time points, while light grey (10 day time point), dark grey (6 day time point) and black filled circles (4 day time point) represent those of the TCR-D115 T cells carrying the PD-1:28tm CCP. Sidak's multiple comparison test was performed and significance was set at a p value < 0.05. E) medianFI histograms showing CFSE intensity values of both injected T effector cell populations through the different T cell recovery time points. F) Graph representing tumor size variation before and 7 days after effector T cell injection where symbols representing an individual mouse are connected by a line. Calculated group median is represented by horizontal lines. G) Representative graph containing absolute cell count of T cells recovered at day 7 after effector cell injection (cells/g values defined on the left axis) and percentages of cell markers that define proliferation Ki-67 and the inhibitory surface protein PD-L1 (% values defined on the right axis). Each symbol on top of the bars represent an individual mouse, while the columns represent the median of the group. Representative dot plots of PD-L1 surface expression on CD8⁺ T cells isolated from the tumors. H) Matrigel plug assay representative dot plots of target and non-target distribution. Reference values correspond to Matrigel plug without T cells and Matrigel plugs containing TCR-D115 mock T cells and TCR-D115 T cells containing the PD-1:28tm CCP. Graph on the right shows the summarized data of the experiment, where each symbol corresponds to an individual mouse (group mean value is shown as a horizontal line).

6. Discussion

Adaptive immune response against tumors is mediated by T cells expressing TCRs that can recognize peptide antigens presented on the surface of tumor cells by the MHC molecules. The proper recognition process that will produce an appropriate T cell activation and function depends on two key signals, the TCR-MHC interaction, and the engagement of co-stimulatory molecules necessary for efficient T cell activation (**5,90**).

When the interaction of the TCR with the MHC molecule occurs in the absence of co-stimulation it is insufficient to fully activate the T cells, causing unresponsiveness to further antigenic stimulation (**91**). Thus, the two-signal model required for a full T cell activation remains to be a key component to carry out an efficient response against tumor cells.

Adoptive cell therapy (ACT) that uses isolated or engineered antigen-specific T cells, which later are transferred back to the patients, has achieved clinical benefits for treatment of various hematological malignancies and a few solid tumors. But poor functionality and lack of persistence of the transferred cells produce an often marginal efficacy of the therapy. Despite the expression of antigens by cancer cells that can be recognized by T cells, an immune mediated tumor elimination can fail based on multiple factors including poor or deficient T cell priming, lack of expression of positive co-stimulatory molecules and a tolerogenic tumor microenvironment rather than an immunostimulatory one (**92**).

Several studies have been aiming to manipulate co-stimulation signals, cytokine secretion and blocking inhibitory molecules (PD-1, CTLA-4) to overcome the negative regulation of the tumor microenvironment. By incorporating them into different modalities, an improvement of clinical responses is expected (**93**).

One resource that has evolved overcome the tolerance to tumors become the use of genetically modified T cells expressing highly specific TCRs or chimeric antigen receptors (CAR). CAR consist of antibody-based recognition domains linked to different signaling sequences. The use of CARs has been successful in hematological malignancies (**94**). However, their use is restricted by the limited number of specific surface expressed tumor antigens. On the other side, the use of highly specific TCRs, while not limited to surface antigens, is constrained by the MHC restriction and the tumor escape through impairments in antigen presentation, HLA expression and lack of co-stimulation signals (**28**). Nevertheless, the

genetic modification of T cells is not only focused on conferring new antigen reactivity by generating structural modifications of TCRs with improved specificity and enhanced affinity, but also includes genes that encode molecules involved in co-stimulation, the prevention of apoptosis, remodeling of tumor microenvironment, induction of proliferation, T cell homing and long-term persistence (**69**).

Unlike CARs, which carry the recognition and co-stimulatory domains in a single receptor (2nd and 3rd generation CARs), T cells modified to express TCRs still require independent triggering of a co-stimulatory signal. To achieve this, immunomodulatory chimeric proteins, where the extracellular domain from inhibitory molecules (PD-1, FAS, TIGIT or CD200R) is fused with the intracellular co-stimulatory signaling domain (CD28, 4-1BB, CD27 or ICOS), can be used as a TCR complement. Using such chimeric proteins (CCPs), enhanced T cell function can be achieved by helping surpassing the hurdles of the immunosuppressive tumor microenvironment (**35,37,38,95**).

In this thesis, I explored a novel CCP design that should not only provide the necessary co-stimulatory signals to the genetically engineered antigen-specific T cells, but that could work simultaneously on different axis within the tumor microenvironment, enhancing tumor targeting by providing means to overcome tumor escape mechanisms and T cell inhibitory signals. By combining the extracellular domain of the CD40L protein, also known as CD154, with the intracellular domain of the CD28 co-stimulatory receptor, a double strike approach against tumor was hypothesized consisting of boosting T cell activity against tumor cells and additionally attacking tumor stroma. The extracellular CD40L domain of the CCP is key to this double action approach since its receptor, CD40, is aberrantly expressed by many tumor cells, including RCC and melanoma, and is also expressed on tumor stroma, including antigen presenting cells, tumor-associated macrophages (**96**) and tumor endothelial cells. In the tumor milieu, T cells expressing the CD40L:CD28 CCP are expected to activate the respective CD28 co-stimulatory cascade when interacting with CD40⁺ tumor cells thereby enhancing the TCR activation cascade leading to stronger tumor cell killing and inducing expression of critical survival factors allowing longer persistence in the tumor milieu and, possibly, the development of memory. Triggering of CD40 on tumor vasculature could cause activation of the endothelium and increase expression of

adhesion molecules like E-selectin and VCAM-1, which in turn will promote a facilitated infiltration of antigen-specific T cells (64–66), whereas, triggering CD40 on macrophages might induce their activation allowing *de novo* priming of anti-tumor immune responses. The principles of designing this type of proteins are not yet clearly defined (97) and represent a challenge in terms of achieving surface expression and biological function. For that reason, three different protein structures were engineered and tested with the aim of elucidating the proposed mechanisms of action of a CD40L:CD28 CCP.

6.1 Chimeric protein design

The advent of genetic engineering that combines synthetic biology in the field of adoptive cell therapy has allowed reprogramming of cytotoxic T cells targeting tumor cells to improve T cell function through redesigning of systems that are already found in nature. That is why this work focused on three different structural approaches for developing a CD40L:CD28 CCP that is successfully expressed on the cell surface and has biological functionality to enhance tumor targeting.

The extracellular domain of CD40L was selected because its corresponding receptor CD40 is expressed on a plethora of different cell types, including B cells, macrophages, dendritic cells, endothelial cells and fibroblasts, as well as in several hematologic and non-hematologic malignancies, including B-cell acute lymphoblastic leukemia, chronic lymphocytic leukemia, non-Hodgkin lymphoma, Hodgkin lymphoma, nasopharyngeal carcinoma, osteosarcoma, Ewing sarcoma, renal cell carcinoma, melanoma, breast, ovarian and cervical carcinoma (59). Moreover, the CD40 receptor is known to convey signals that are able to regulate several cellular responses, from proliferation and differentiation to growth suppression and cell death (53). This wide expression fulfilled the criteria we were looking for to create a protein that is able to interact with different components of the tumor microenvironment besides tumor cells to enhance the overall tumoral response in a more complete way. For the intracellular domain, we decided to incorporate the CD28 signaling tail since its pathway has been shown to constitute the primary and strongest co-stimulatory signal to amplify T cell activation, including increased cytokine gene expression, stabilization of cytokine mRNA, augmentation of glucose uptake and utilization, promotion of T cell survival and maintenance of T cell responsiveness upon repetitive restimulations (98).

The challenge in the CCP design using the previously described domains has to do with the different orientations of the domain donor proteins on the cell surface. The topology of a cell membrane protein is crucial for its function (**99,100**), and, therefore, the two topologies of the domains had to be considered in the design of the CCP to ensure its functionality.

Most of the chimeric proteins that have been developed to date, use the domains of two membrane proteins that both belong to the type 1 group. This simplifies the fusion of both domains since the orientation has the same direction on the cell membrane. In the case of CD40L, which is a type 2 membrane protein, two approaches were selected and compared. For the first two approaches, spacers and linkers, which are commonly used in the CAR design in order to stabilize and give flexibility to the receptor, were included in the CD40L:CD28 design (**101**). The first design considered the knowledge that the CD40L protein can also exist as an active soluble product, generated by proteolytic cleavage at methionine 113 of the full length molecule by the metalloproteinases ADAM10 and ADAM17 (**102**). Hence, the amino acid sequence of the soluble CD40L (sCD40L) was linked to the transmembrane and intracellular domain of CD28 by using a glycine/serine linker (**103**) attached to the carboxyl terminal end of the sCD40L fragment, followed by a IgG1Fc spacer that was then attached to the amino terminal end of the 153 amino acid long fragment of CD28 encompassing the transmembrane and intracellular domain. Adding the IgG1Fc spacer, I was aiming on stability of the resulting chimeric protein. The use of this spacer results in dimerization and thereby increased surface expression (**74**). The IgG1Fc spacer was, furthermore, modified to avoid unintended cross-activation of Fcγ receptor-positive cells. Commonly used glycine/serine linkers vary from 2 to 31 amino acids. They are usually used to separate multiple domains within a single protein without interfering with the function of each domain and providing flexibility so that the linker does not impose any constraints on the conformation or interactions of the linked partners or with their corresponding receptors (**104**). The second CD40L:CD28 design followed the same rationale as the one using the Glycine/Serine linker and IgG1Fc spacer but addressed the concern of potential high surface polymerization that the IgG1Fc spacer might cause and that might also impact the protein functionality. Therefore, in the second design, the IgG1Fc spacer was replaced

by the third Ig-like repetition of the Filamin protein, which is a cytoskeleton structural protein. This fragment lacks polymerization domains, tends to be more flexible and is considerably shorter than the IgG1Fc spacer (**105**), conferring an interesting variation towards the construction of a functional CD40L:CD28 CCP.

Both approaches, the one using the IgG1Fc spacer and the one using the Filamin spacer, generated chimeric proteins with the structure of a type 1 membrane protein according to their membrane orientation, shown in figure 5. For successful intracellular trafficking and surface expression, a signal peptide is typically present for type 1 membrane proteins, which destines the nascent peptide for translocation into the endoplasmic reticulum and its insertion in the lumen. The presence and selection of the signal peptide sequence can have dramatic consequences on protein expression with reports of up to fourfold enhanced expression levels (**106**). Therefore, the CD40L:IgC1Fc:CD28 and CD40L:Fil3:CD28 chimeric protein sequences were complemented with the addition of a signal peptide sequence that belonged to the PD-1 protein, which had been successfully used for PD-1 chimeric proteins in our group (PhD thesis of R. Schlenker) (**69**).

For the third CD40L:CD28 design, a more straight forward approach was used. This time, the CD40L protein extracellular and transmembrane domains were kept in the orientation of the native CD40L protein. The protein fragment included 9 amino acids of the intracellular domain thought to be helpful for the protein stability. This protein fragment was directly linked to the intracellular domain of the CD28 co-stimulatory protein. Since the orientation of the CD28 protein is different from the one of CD40L, as previously mentioned, the CD28 intracellular domain corresponding to the amino acid 140 to 220 was linked to the CD40L protein through its carboxyl terminal end, resulting, consequently, in an inverted CD28 intracellular domain (CD28i). Although the CD28 intracellular domain had an inverted orientation, it kept the signaling interaction motifs needed to make it functional. The decision to keep it this way was the previous work reported by Zhang et al. in 2006 (**76**) where a chimeric NK receptor was reported that linked the type 2 protein NKG2D with the type 1 protein CD3 zeta chain. In this work, the intracellular orientation of CD3 zeta chain was reversed and still kept its functional capacity, suggesting that successful interaction with adaptor proteins is orientation independent.

The final structure of the third CCP CD40L:CD28i resembled a type 2 membrane protein and had a similar size to the endogenous CD40L protein. This approach offered a design that theoretically had less structural modifications and went more naturally along with the structure of the CD40L protein, suggesting that it can make the interaction with its receptor CD40 easier. It was considered that this could be a useful characteristic that might help to fulfill all functional effects that were foreseen for the CD40L:CD28 CCP.

6.2 Impact of chimeric protein design on protein expression

The designs for the CD40L:CD28 CCP with different structural variations that showed a clear impact on the expression. The results observed in the initial evaluation using *ivt*-RNA to produce a transient expression on the cell surface corresponded to the protein detection by western blot. Following the rationale behind each structural component as previously described, the endogenous native protein had the highest expression and was used as a reference for our other CCPs. The CCP that included the IgG1Fc spacer followed as the second best expressed CCP with a percentage of surface expression ranging between 15 to 20% less than the native CD40L. However, total protein detection was lower, which could be logical since the size of the CD40L:IgGFc:CD28 receptor is considerably bigger (52-55 kDa) compared to the native protein (33 kDa). The CCP of the CD28i approach ranged slightly behind the IgGFc CCP in terms of percentage of surface expression. Regarding total protein detection, it fell closer to the nCD40L protein consistent with being of similar size than the nCD40L (33 kDa). This indicated that the molecule size has an impact on surface expression in the context of a transient expression system. On last place ranged the construct containing the Filamin 3 repetition spacer, with less than 20% of surface expression after *ivt*-RNA transfection and a total protein detection closer to the one of the IgG1Fc construct. Although the size of the Fil3 protein (35-37 kDa) is closer to the one of the nCD40L protein, this was not reflected in the total protein detection and might point out a translation deficiency or membrane instability. It is important to remember that the Fil3 spacer lacks polymerization domains, which are usually associated with membrane stabilization. In addition, it was the first time that it was included in the backbone of a chimeric protein. Therefore, no other reports are available to judge whether the Fil3 spacer might be of benefit in a CCP design.

Expression of the three protein constructs was also detected on the surface of primary human T cells (i.e. PBLs, data not shown) with a similar expression pattern to that observed with the transiently transfected HEK cells.

A stable retroviral transduction system was used then to test if the expression patterns seen using the transient expression systems were not related to an unknown poor translation of the *ivt*-RNA, and to assess a long-term cell surface expression kinetic.

The expression profile that was evaluated 3 days after stable transduction of PBLs was highly comparable to that achieved with *ivt*-RNA transient transfection. The CD28i and the IgGFc constructs were the highest expressed ones, with the CD28i construct showing a more homogeneous staining intensity compared to the IgGFc construct. The nCD40L followed with 39% surface expression, and consistently with the *ivt*-RNA assay, the Fil3 construct was poorly expressed with a 25% surface presence with no homogeneous intensity. Analyzing the long-term expression over 13 days of culture, a surprising kinetic was observed. A loss of surface expression was detected for all constructs including the nCD40L protein, with almost undetectable surface expression of the Fil3 CCP after 6 days, loss of the nCD40L at day 10, of CD28i CCP at day 13, and the IgGFc construct remaining detectable with 52% expression by day 13.

From these results it has to be concluded that the retroviral transduction, which is known to lead to integration of transferred DNA into the cell's genome, a process that should result in stable expression of transduced sequences, did not achieve this in our experiment. It is known that in activated T cells CD40L is expressed within minutes, peaking within 6 hours, and then declining over the subsequent 12-24 hours (**46,59**). This is a known dynamic is acknowledged for the nCD40L protein, but it shouldn't be the case for the CCPs, since these lack the intracellular sequence of CD40L. This suggested that, for our constructs, a cell activation associated factor or a post-translational degradation (**60,107**) might be regulating their expression.

We tested the impact of the culture conditions on the expression of the CCPs, thinking that supplementary stimulation during *in vitro* culturing together with culture conditions regarding fresh nutrients and lower cell density could improve the long-term surface expression. An interesting information came from this evaluation, showing that culture conditions indeed influenced the CCP expression on T

cells. Over a time period of 13 days after PBL transduction, cells received fresh medium, density was adjusted by splitting the expanding cells and complementary IL-2 was given. Notably, when surface expression was evaluated on the time points that followed these manipulations, an increment in surface detection was seen. The level of surface expression was still lower than the starting levels, but notably higher to attribute a clear influence of culture conditions to CCP surface expression. When analyzing mRNA levels and total protein presence during this time kinetic, we observed that downregulation of surface protein followed the loss of total protein and that of mRNA levels. These results suggested that loss of surface expression is likely a result of weaning transcription rather than protein internalization or poor transport to the cell surface. Surface expression tended to stabilize with time at lower levels compared to the initial values, thus, a post-transcriptional regulation might play an important role in the overall expression, similar to what happens with the nCD40L protein (**108**). This type of regulation was not seen in previous work in our lab when using PD-1:CD28 CCPs (**70**).

6.3 CCP surface expression is upregulated upon activation

After observing that there was a correlation between culture conditions and the surface expression of the CD40L:CD28 CCPs, our logical next step was to assess if T cell activation could also influence the expression. Cells that were frozen after specific TCR and CCPs transduction, specifically at day 12 of the expansion kinetic when cells showed the lowest CCP surface expression. After freezing, cells were thawed and immediately activated using anti-CD3 and anti-CD28 antibody coated plates, representing an artificial activation context. To our surprise after three days of a standard culture time for this kind of activation, all CCPs were upregulated and strong surface detection was possible. For cells that were not transduced with any construct a slight upregulation of endogenous CD40L protein was detected, allowing to distinguish endogenous levels from CCP levels. After 3 days of activation culture, the cells were transferred to a plate without activation factors for another 3 days, and, again, downmodulation occurred, suggesting a clear influence of the cell activation status on CCP synthesis and surface expression. This was an unexpected event, since previous transduction of antigen-specific TCRs or PD-1:CD28-CCPs never showed these expression changes. While making it difficult to experimentally evaluate transduced T cell,

such expression kinetic with the upregulation following T cell stimulation might be advantageous if it would actually happen under *in vivo* circumstances, since then a beneficial co-stimulatory effect might occur timely coupled with the recognition of tumor cells through the TCR-MHC interaction providing help for improved T cell functionality for as long as the antitumoral response lasts. Furthermore, the downregulation after this specific boost could prevent any undesired over activation of the immune system.

We then tested if a specific activation signal produced by TCR-MHC activation was able to have the same effect as the anti-CD3/anti-CD28 artificial activation. When cells from the same batch were thawed and co-cultured with antigen-positive cells, upregulation was observed in the same way than it was for the anti-CD3/anti-CD28 activation setting. Furthermore, co-culture with target cells revealed another interesting characteristic of the regulation of CD40L:CD28 CCP expression, in that it was dependent on the presence of the CD40 receptor on the target cells. If the target cell expressed CD40, an upregulation of CD40L:CD28 CCP was barely detectable until later time points of co-culture and different expression levels of CD40 on target cells directly corresponded with the detection level of the CCPs on the T cells. Johnson-Léger et al. observed that endogenous CD40L expression on CD4 T cells exhibit a continuous cycle of downregulation and re-expression upon interaction with CD40 expressing B cells, with this being dependent on the presence of antigen. At the same time, the re-expression could be stabilized by provision of CD28 co-stimulation, which might become more pronounced with time (**77,108**).

The results observed in this dissertation indicate that T cells transduced with an antigen-specific TCR and a CD40L:CD28 CCP might follow a similar pattern as the one described for endogenous CD40L. When T cells become activated due to specific antigen recognition, the CCPs enter a cycle of rapid re-expression upon TCR stimulation and downregulation upon interaction with the CD40 receptor. The CD40L:CD28 CCP expression tended to stabilize with time, which related directly with antigen presence. Once the tumor cells were eradicated, the CCPs underwent downmodulation until T cells are again activated. The CCPs proposed in this work should still be able to interact with the tumor stroma and tumor resident APCs even when target cells do not express CD40, thus still being able to offer benefits that might support the overall antitumoral response.

6.4 CD40L:CD28 CCPs are biologically active

6.4.1 B cell activation assay

After having determined that the designed proteins can be expressed on the cell surface, and showed an activation dependent expression pattern, assessing if the different domains were functionally incorporated into the chimeric CD40L:CD28 CCPs was the next step.

The CD40 receptor is reported to be expressed on normal B cells and is capable to interact with CD40L expressing T cells. Triggering of CD40 on the surface of B cells induces proliferation and activation. Furthermore, ligation of CD40 can induce class switching and immunoglobulin synthesis suggesting a role of CD40 in the normal physiology of B cell activation (**109**). In our experiments, T cells expressing our CD40L:CD28 CCPs were able to interact with freshly isolated B cells causing upregulation of the activation markers CD83, CD86 and Fas on the B cell surface. Each construct achieved B cell activation to the same extent as cells expressing the nCD40L protein or as achieved by using a commercial kit with soluble trimerized CD40L. Slight differences between the different CCP formats were observed, whereby the IgGFc construct induced activation marker expression to a slightly higher extent than the other two constructs. This suggests that the difference in cell surface expression of the CCPs seems not to have great influence on the scope of functionality of the CD40L domain. Cells that didn't carry any CCP nor nCD40L protein, surface expression of the activation markers was very low. Thus, the extracellular domain of CD40L in our CCPs apparently was biologically functional.

6.4.2 DC maturation assay

In addition to influencing B cell physiology, several studies also reported that CD40 signaling induces changes in dendritic cells making them more effective antigen presenting cells. CD40 licenses DCs to mature and achieve the necessary characteristics to trigger an effective T cell activation and differentiation. Changes include the upregulation of MHC class II and co-stimulatory molecules CD80/CD86 and activation markers like CD83, CCR7 and PD-L1 (**110,111**). Our experiments clearly demonstrated effects of the CD40L:CD28 CCPs on the maturation and activation of immature DCs, with induced levels of CD83, CCR7 and PD-L1 after co-culture with T cells expressing the CD40L:IgGFc:CD28,

approximating intensities observed on DC matured with a standard cytokine cocktail. T cells expressing CD40L:Fil3:CD28 or CD40L:CD28i, despite low surface expression, still induced levels above those achieved with Mock T cells or T cells with native CD40L or iDCs that were not stimulated at all. This not only follows our proposed logic where tumor resident APCs can get the benefit of the stimulation through the CD40L:CD28 CCPs to rescue their activity in the tumor microenvironment (**60**), but also confirms the functionality of the CD40L extracellular domain.

6.4.3 CD28 signaling assay

After addressing the biologic activity of the CD40L extracellular domain (ECD) of the different CD40L:CD28 CCPs, it was determined whether the CD28 intracellular domain (ICD) was capable to deliver a proper co-stimulation signal to the T cells that were transduced with the different formats of the CD40L:CD28 CCPs. T cell co-stimulation plays a major role in the antitumoral response, since it is capable of boosting the activation signaling produced after TCR/MHC interaction. Acuto and Michel described the involvement of AKT signaling in prolonging T cell viability and preventing apoptotic death (**112**). In addition, AKT signaling activates downstream molecules like mTOR and RPS6 (**91,113**), which support proliferation and protein synthesis (**114**).

The results of this thesis showed that phosphorylation of AKT protein increased after co-culturing the CCP-transduced T cells with antigen-specific CD40-positive target cells in comparison with the T cells lacking the CCPs. Similar results were detected for the phosphorylation of the mTOR and RPS6 proteins, which is in line with the knowledge that phosphorylation of AKT provokes phosphorylation of mTOR, which in turn causes the phosphorylation of RPS6.

Notably, T cells expressing the CD40L:CD28i or CD40L:Fil3:CD28 showed a 10-15% better signaling performance compared with T cells expressing the CD40L:IgGFc:CD28 construct, although the CD40L:IgGFc:CD28 CCP showed strongest surface expression.

This might be caused by the structural differences between the different CCPs. By using different length linkers, interaction with the receptor on target cells might not be optimal when the immunological synapse occurs, not to mention that different linkers might have different efficacy in transferring the signal in between the extracellular domain and the intracellular domain of the CCPs. Nevertheless,

all three CCPs proved to be able to transfer the CD28 co-stimulatory signal upon CD40 engagement.

The results document that the CD28 signaling domain incorporated in the chimeric proteins is functionally active and can facilitated the CD28 signaling cascade upon CD40L triggering as it was predicted from the native CD28 protein. This provides support for the hypothesis as outlined in figure 4, which postulates that T cells engineered to express the chimeric CD40L:CD28 should receive co-stimulation when triggered through the extracellular CD40L domain of the chimeric protein.

6.4.4 Cytokine secretion and cytotoxicity

Provision of additional, non-MHC restricted signals by professional APCs, results in the T cell becoming fully activated leading to expansion and development of effector function (**91**). CD28 mediates an important co-stimulatory signaling pathway in T cells. This stimulation synergizes with TCR stimulation to induce the secretion of multiple cytokines including IL-2 and IFN- γ , which are fundamental for T cell proliferation and effector functions (**115,116**).

Results from this work demonstrated that T cells expressing the CD40L:CD28 CCPs have improved IFN- γ and IL-2 secretion upon antigen-specific recognition. Effects of CD28-triggered enhanced signaling was appreciated when using tyrosinase-specific TCR-transduced T cells equipped with CD40L:CD28 CCPs against cells expressing the cognate melanoma-associated antigen. Similar effects were observed when using T cells transduced with a TCR with shared renal cell carcinoma specificity (**117**) complemented with CD40L:CD28 CCPs.

The improved cytokine secretion was also complemented with enhanced cytotoxicity effects observed for tyrosinase-specific TCR transduced T cells expressing the three different variants of the CD40L:CD28 CCPs. Killing of cells expressing the tyrosinase antigen and the CD40 receptor was significantly better when the TCR-transduced T cells additionally expressed the CCPs compared to T cells expressing the nCD40L protein without CD28 signaling domain. Similar to the effect on cytokine secretion, the T cells expressing the CD40L:CD28i and CD40L:Fil3:CD28 constructs had stronger specific lysis compared to T cells with the CD40:IgGFc:CD28 construct despite reverse surface expression levels. This corresponded also to the observed stronger CD28 signaling activation performed in this work. Although the CD40L:IgGFc:CD28 construct was the most strongly

expressed one it was not the one with the higher biological performance regarding T cell activation. These results, moreover, corresponded with the results from the B cell activation and DC maturation assays, where varied surface expression levels were not translating to different activation levels. It appears that the CCP design represents a key factor affecting expression and biological activity. Extent of expression apparently does not necessary correlate with the functional quality. In the case of using the IgGFc spacer, being the longest one of the three CD40L:CD28 CCP presented in this dissertation, it might result in a suboptimal interaction with the CD40 receptor due to longer distance of the extracellular domain from the membrane surface. This has been shown to impact the signaling outcome in CAR designs (**118**). On the other hand, the CCP with the Fil3 spacer, the size of which is close to the one of nCD40L protein, had poor membrane stability, but apparently signaling and effector functions in T cells were well supported in this context. Finally, the construct containing the CD28i domain, also lacked membrane stability, but presented the best biological effects of the three CD40L:CD28 CCPs. The functional assays regarding cytokine secretion and cytotoxicity presented in this thesis can be considered as first evidence, however, they require repetitions. Further analysis must be performed to reach a better understanding and a final conclusion of how high the benefit from the expression of the CD40L:CD28 CCPs in antigen specific T cells really is. Nevertheless, results presented here project a positive outcome of this specific double strike co-stimulatory improvement approach.

6.5 *In vivo* studies and the role of CCPs for adoptive cell therapy

Design and characterization of the CD40L:CD28 CCPs was a challenging process due to the complexity of its expression kinetic and biological behavior when expressed on antigen-specific T cells. Therefore, while this characterization process was ongoing, it was of strong relevance for the group to find another means to assess the concept whether CCP engineered T cells can support antitumoral activity in a "hostile" tumor microenvironment. To this extent, a well characterized PD-1:CD28 CCP, generated by R. Schlenker (**69**), was tested in a human xenograft model. Here, an inhibitory micromilieu is established allowing to assess if the CCP engineering can help overcome the inhibitory conditions. The results of

this study are published in (70) and are only briefly discussed here. It was observed that PD-1:28tm-transduced TCR-D115 T cells proliferated more strongly within the tumor microenvironment appreciated by stronger CFSE dye dilution, higher amounts of CCP-expressing T cells present in the resected tumor compared with TCR-D115/Mock T cells lacking the CCP. Furthermore, high PD-L1 expression on TCR-D115 Mock T cells might explain the unresponsiveness of this T effector cells. As described by Butte et al. (89), PD-L1 on T cells can inhibit T cell expansion and function. TCR-D115 T cells expressing the PD-1:28tm also showed improved cytotoxicity. Cytotoxicity and improved cell proliferation constitute important features to achieve tumor size reduction (119–121). Tumors injected with TCR-D115 cells expressing the PD-1:28tm protein grew slower over 7 days than tumors injected with T cells expressing only the TCR-D115. Testing the PD-1:CD28 CCP in the *in vivo* melanoma xenograft model provides the basis for future experiments that need to be done to evaluate the functionality of the CD40L:CD28 CCPs in the context of an *in vivo* established tumor microenvironment. From the ACT experiments with engineered T cells was also learned that larger group sizes of mice and longer observation times are required to obtain more conclusive results in this type of xenograft animal experiments.

6.6 Outlook

Triggering a robust co-stimulation signaling during antigen-specific T cell responses in the context of ACT has been addressed by many studies identifying co-stimulatory signaling as a key point for overall antitumoral improvement. We applied and extended this concept by designing and implementing a novel CD40L:CD28 chimeric co-stimulatory protein that not only triggers T cell activation for improved effector function, but also provides an overall boost across different axis of the antitumoral response in the suppressed tumor microenvironment. The observed characteristics of the CD40L:CD28 CCPs include a dynamic expression kinetic dependent on specific T cell activation and receptor interaction that might activate the co-stimulatory signal and functional support timely when the T cells interacts with the tumor cell and for as long as the tumor cell is present. CD40L:CD28 CCPs were found to improve CD28 co-stimulatory signaling in T cells, they enhanced cytokine secretion as well as cytotoxic effects. Furthermore,

efficient activation of B cell as well as DC maturation and activation were executed. Future experiments need to address the proposed CD40 MHC independent cytotoxic effect on tumor cells and the modulation of the tumor endothelium to complement the produced data and to re-enforce the biological plasticity that these proteins might offer within the tumor microenvironment (**122**). Building on the precedent of our work with CCPs containing the PD-1 extracellular domain in an *in vivo* xenograft model, further analysis of the CD40L:CD28 CCPs within an established suppressive tumor microenvironment is of great importance to establish the proposed additive effects of this type of CCP. Given the complexity behind the design of the CD40L:CD28 proteins, modifications in the design might be of interest to explore in the future, like using different co-stimulatory tails, the use of different signal peptide sequences for surface directed trafficking, and the use of linkers that provide better membrane stability. Overall, the concept of complementing the different pathways that the CD40/CD40L interaction offers for immune system stimulation with the means for boosting T cell co-stimulation in a chimeric CD40L:CD28 design is a very promising approach to improve T cell functionality for adoptive T cell therapy.

References

1. Marshall JS, Warrington R, Watson W, Kim HL. An introduction to immunology and immunopathology. *Allergy, Asthma Clin Immunol* (2018) **14**:1–10. doi:10.1186/s13223-018-0278-1
2. Sharpe AH. Mechanisms of costimulation. *Immunol Rev* (2009) **229**:5–11. doi:10.1111/j.1600-065X.2009.00784.x
3. Vinay DS, Kwon BS. 4-1BB (CD137), an inducible costimulatory receptor, as a specific target for cancer therapy. *BMB Rep* (2014) **47**:122–129. doi:10.5483/BMBRep.2014.47.3.283
4. Abken H, Hombach A, Heuser C, Kronfeld K, Seliger B. Tuning tumor-specific T-cell activation: A matter of costimulation? *Trends Immunol* (2002) **23**:240–245. doi:10.1016/S1471-4906(02)02180-4
5. Nandi D, Pathak S, Verma T, Singh M, Chattopadhyay A, Thakur S, Raghavan A, Gokhroo A, Vijayamahantesh. *T cell costimulation, checkpoint inhibitors and anti-tumor therapy*. (2020). doi:10.1007/s12038-020-0020-2
6. Bugeon L, Dallman MJ. Costimulation of T cells. in *American Journal of Respiratory and Critical Care Medicine*, 164–168. doi:10.1164/ajrccm.162.supplement_3.15tac5
7. Barber A. Costimulation of Effector CD8+ T Cells: Which Receptor is Optimal for Immunotherapy? *MOJ Immunol* (2014) **1**:8–11. doi:10.15406/moji.2014.01.00011
8. Chen L, Flies DB. Molecular mechanisms of T cell co-stimulation and co-inhibition. *Nat Rev Immunol* (2013) **13**:227–242. doi:10.1038/nri3405
9. Zarour HM. Reversing T-cell dysfunction and exhaustion in cancer. *Clin Cancer Res* (2016) **22**:1856–1864. doi:10.1158/1078-0432.CCR-15-1849
10. Rosenberg SA, Restifo NP, Yang JC, Morgan RA, Dudley ME. Adoptive cell transfer: A clinical path to effective cancer immunotherapy. *Nat Rev Cancer* (2008) **8**:299–308. doi:10.1038/nrc2355
11. Rohaan MW, Wilgenhof S, Haanen JBAG. Adoptive cellular therapies: the current landscape. *Virchows Arch* (2019) **474**:449–461. doi:10.1007/s00428-018-2484-0
12. Bertram JS. The molecular biology of cancer. *Mol Aspects Med* (2001) **21**:167–223. doi:10.1016/s0098-2997(00)00007-8
13. Hanahan D, Weinberg RA. Hallmarks of cancer: The next generation. *Cell* (2011) **144**:646–674. doi:10.1016/j.cell.2011.02.013
14. Farkona S, Diamandis EP, Blasutig IM. Cancer immunotherapy: The beginning of the end of cancer? *BMC Med* (2016) **14**:1–18. doi:10.1186/s12916-016-0623-5

15. Zhao L, Cao YJ. Engineered T Cell Therapy for Cancer in the Clinic. *Front Immunol* (2019) **10**: doi:10.3389/fimmu.2019.02250
16. Rath JA, Arber C. Engineering Strategies to Enhance TCR-Based Adoptive T Cell Therapy. *Cells* (2020) **9**:1485. doi:10.3390/cells9061485
17. Chruściel E, Urban-Wójciuk Z, Arcimowicz Ł, Kurkowiak M, Kowalski J, Gliwiński M, Marjański T, Rzyman W, Biernat W, Dziadziuszko R, et al. Adoptive cell therapy—harnessing antigen-specific t cells to target solid tumours. *Cancers (Basel)* (2020) **12**:1–30. doi:10.3390/cancers12030683
18. Sadelain M, Brentjens R, Rivière I, Park J. CD19 CAR Therapy for Acute Lymphoblastic Leukemia. *Am Soc Clin Oncol Educ B* (2015)e360–e363. doi:10.14694/edbook_am.2015.35.e360
19. Fousek K, Ahmed N. The evolution of T-cell therapies for solid malignancies. *Clin Cancer Res* (2015) **21**:3384–3392. doi:10.1158/1078-0432.CCR-14-2675
20. Karpanen T, Olweus J. T-cell receptor gene therapy - ready to go viral? *Mol Oncol* (2015) **9**:2019–2042. doi:10.1016/j.molonc.2015.10.006
21. Yaguchi T, Sumimoto H, Kudo-Saito C, Tsukamoto N, Ueda R, Iwata-Kajihara T, Nishio H, Kawamura N, Kawakami Y. The mechanisms of cancer immunoescape and development of overcoming strategies. *Int J Hematol* (2011) **93**:294–300. doi:10.1007/s12185-011-0799-6
22. Quesnel B. Tumor dormancy and immunoescape. *APMIS* (2008) **116**:685–694. doi:10.1111/j.1600-0463.2008.01163.x
23. Dunn GP, Bruce AT, Ikeda H, Old LJ, Schreiber RD. Cancer immunoeediting: From immunosurveillance to tumor escape. *Nat Immunol* (2002) **3**:991–998. doi:10.1038/ni1102-991
24. Iwami S, Haeno H, Michor F. A race between tumor immunoescape and genome maintenance selects for optimum levels of (epi)genetic instability. *PLoS Comput Biol* (2012) **8**: doi:10.1371/journal.pcbi.1002370
25. Berraondo P. Mechanisms of action for different checkpoint inhibitors. *HemaSphere* (2019) **3**:28–30. doi:10.1097/HS9.0000000000000244
26. Andrews LP, Yano H, Vignali DAA. Inhibitory receptors and ligands beyond PD-1, PD-L1 and CTLA-4: breakthroughs or backups. *Nat Immunol* (2019) **20**:1425–1434. doi:10.1038/s41590-019-0512-0
27. Liu Q, Cai W, Zhang W, Li Y. Cancer immunotherapy using T-cell receptor engineered T cell. *Ann Blood* (2020) **5**:5–5. doi:10.21037/aob.2020.02.02
28. Barrett DM, Singh N, Porter DL, Grupp SA, June CH. Chimeric antigen receptor therapy for cancer. *Annu Rev Med* (2014) **65**:333–347. doi:10.1146/annurev-med-060512-150254

29. Govers C, Sebestyén Z, Roszik J, van Brakel M, Berrevoets C, Szöör Á, Panoutsopoulou K, Broertjes M, Van T, Vereb G, et al. TCRs Genetically Linked to CD28 and CD3 ϵ Do Not Mispair with Endogenous TCR Chains and Mediate Enhanced T Cell Persistence and Anti-Melanoma Activity. *J Immunol* (2014) **193**:5315–5326. doi:10.4049/jimmunol.1302074
30. Kalos M, Levine BL, Porter DL, Katz S, Stephan A, Bagg A, June CH. T cells with chimeric antigen receptors have potent antitumor effects. *Sci Transl Med* (2011) **3**:1–21. doi:10.1126/scitranslmed.3002842.T
31. Rafiq S, Hackett CS, Brentjens RJ. Engineering strategies to overcome the current roadblocks in CAR T cell therapy. *Nat Rev Clin Oncol* (2020) **17**:147–167. doi:10.1038/s41571-019-0297-y
32. Lee YH, Kim CH. Evolution of chimeric antigen receptor (CAR) T cell therapy: current status and future perspectives. *Arch Pharm Res* (2019) **42**:607–616. doi:10.1007/s12272-019-01136-x
33. Shin JH, Park HB, Oh YM, Lim DP, Lee JE, Seo HH, Lee SJ, Eom HS, Kim IH, Lee SH, et al. Positive conversion of negative signaling of CTLA4 potentiates antitumor efficacy of adoptive T-cell therapy in murine tumor models. *Blood* (2012) **119**:5678–5687. doi:10.1182/blood-2011-09-380519
34. Moeller M, Haynes NM, Trapani JA, Teng MWL, Jackson JT, Tanner JE, Cerutti L, Jane SM, Kershaw MH, Smyth MJ, et al. A functional role for CD28 costimulation in tumor recognition by single-chain receptor-modified T cells. *Cancer Gene Ther* (2004) **11**:371–379. doi:10.1038/sj.cgt.7700710
35. Oda SK, Anderson KG, Ravikumar P, Bonson P, Garcia NM, Jenkins CM, Zhuang S, Daman AW, Chiu EY, Bates BM, et al. A Fas-4-1BB fusion protein converts a death to a pro-survival signal and enhances T cell therapy. *J Exp Med* (2020) **217**: doi:10.1084/jem.20191166
36. Sukumaran S, Watanabe N, Bajgain P, Raja K, Mohammed S, Fisher WE, Brenner MK, Leen AM, Vera JF. Enhancing the potency and specificity of engineered T cells for cancer treatment. *Cancer Discov* (2018) **8**:972–987. doi:10.1158/2159-8290.CD-17-1298
37. Liu X, Ranganathan R, Jiang S, Fang C, Sun J, Kim S, Newick K, Lo A, June CH, Zhao Y, et al. A chimeric switch-receptor targeting PD1 augments the efficacy of second-generation CAR T cells in advanced solid tumors. *Cancer Res* (2016) **76**:1578–1590. doi:10.1158/0008-5472.CAN-15-2524
38. Hoogi S, Eisenberg V, Mayer S, Shamul A, Barliya T, Cohen CJ. A TIGIT-based chimeric co-stimulatory switch receptor improves T-cell anti-tumor function. *J Immunother cancer* (2019) **7**:243. doi:10.1186/s40425-019-0721-y
39. Roth TL, Li PJ, Blaeschke F, Nies JF, Apathy R, Mowery C, Yu R, Nguyen MLT, Lee Y, Truong A, et al. Pooled Knockin Targeting for Genome Engineering of Cellular Immunotherapies. *Cell* (2020) **181**:728-744.e21. doi:10.1016/j.cell.2020.03.039

40. Munroe ME, Bishop GA. A Costimulatory Function for T Cell CD40. *J Immunol* (2007) **178**:671–682. doi:10.4049/jimmunol.178.2.671
41. Grewal IS, Flavell RA. The Role of CD40 Ligand in Costimulation and T-Cell Activation. *Immunol Rev* (1996) **1**:85–106. doi:10.1111/j.1600-065x.1996.tb00921.x
42. Loskog ASI, Eliopoulos AG. The Janus faces of CD40 in cancer. *Semin Immunol* (2009) **21**:301–307. doi:10.1016/j.smim.2009.07.001
43. Hernandez MGH, Shen L, Rock KL. CD40-CD40 Ligand Interaction between Dendritic Cells and CD8 + T Cells Is Needed to Stimulate Maximal T Cell Responses in the Absence of CD4 + T Cell Help . *J Immunol* (2007) **178**:2844–2852. doi:10.4049/jimmunol.178.5.2844
44. Koguchi Y, Thauland TJ, Slifka MK, Parker DC. Preformed CD40 ligand exists in secretory lysosomes in effector and memory CD4+ T cells and is quickly expressed on the cell surface in an antigen-specific manner. *Blood* (2007) **110**:2520–2527. doi:10.1182/blood-2007-03-081299
45. Koguchi Y, Buenafe AC, Thauland TJ, Gardell JL, Bivins-Smith ER, Jacoby DB, Slifka MK, Parker DC. Preformed CD40L is stored in Th1, Th2, Th17, and T follicular helper cells as well as CD4 +8 - thymocytes and invariant NKT cells but not in Treg cells. *PLoS One* (2012) **7**: doi:10.1371/journal.pone.0031296
46. Daoussis D, Andonopoulos AP, Liossis SNC. Targeting CD40L: A promising therapeutic approach. *Clin Diagn Lab Immunol* (2004) **11**:635–641. doi:10.1128/CDLI.11.4.635-641.2004
47. Hancock WW, Sayegh MH, Zheng XG, Peach R, Linsley PS, Turka LA. Costimulatory function and expression of CD40 ligand, CD80, and CD86 in vascularized murine cardiac allograft rejection. *Proc Natl Acad Sci U S A* (1996) **93**:13967–13972. doi:10.1073/pnas.93.24.13967
48. Sun M, Fink PJ. A New Class of Reverse Signaling Costimulators Belongs to the TNF Family. *J Immunol* (2007) **179**:4307–4312. doi:10.4049/jimmunol.179.7.4307
49. Tong AW, Stone MJ. Prospects for CD40-directed experimental therapy of human cancer. *Cancer Gene Ther* (2003) **10**:1–13. doi:10.1038/sj.cgt.7700527
50. Loskog A, Totterman T. CD40L - A Multipotent Molecule for Tumor Therapy. *Endocrine, Metab Immune Disord Targets* (2007) **7**:23–28. doi:10.2174/187153007780059432
51. Law CL, Grewal IS. Therapeutic interventions targeting CD40L (CD154) and CD40: The opportunities and challenges. *Adv Exp Med Biol* (2009) **647**:8–36. doi:10.1007/978-0-387-89520-8_2

52. Bereznyaya NM, Chekhun VF. Expression of CD40 and CD40L on tumor cells: The role of their interaction and new approach to immunotherapy. *Exp Oncol* (2007) **29**:2–12.
53. Eliopoulos AG, Davies C, Knox PG, Gallagher NJ, Afford SC, Adams DH, Young LS. CD40 Induces Apoptosis in Carcinoma Cells through Activation of Cytotoxic Ligands of the Tumor Necrosis Factor Superfamily. *Mol Cell Biol* (2000) **20**:5503–5515. doi:10.1128/mcb.20.15.5503-5515.2000
54. Elmetwali T, Young LS, Palmer DH. CD40 ligand-induced carcinoma cell death: a balance between activation of TNFR-associated factor (TRAF) 3-dependent death signals and suppression of TRAF6-dependent survival signals. *J Immunol* (2010) **184**:1111–1120. doi:10.4049/jimmunol.0900528
55. Piechutta M, Berghoff AS. New emerging targets in cancer immunotherapy: The role of Cluster of Differentiation 40 (CD40/TNFR5). *ESMO Open* (2019) **4**:e000510. doi:10.1136/esmoopen-2019-000510
56. Arch RH, Gedrich RW, Thompson CB. Tumor necrosis factor receptor-associated factors (TRAFs) - A family of adapter proteins that regulates life and death. *Genes Dev* (1998) **12**:2821–2830. doi:10.1101/gad.12.18.2821
57. Hellman LM, Foley KC, Singh NK, Alonso JA, Riley TP, Devlin JR, Ayres CM, Keller GLJ, Zhang Y, Vander Kooi CW, et al. Improving T Cell Receptor On-Target Specificity via Structure-Guided Design. *Mol Ther* (2019) **27**:300–313. doi:10.1016/j.ymthe.2018.12.010
58. Ibraheem K, Yhmed AMA, Qayyum T, Bryan NP, Georgopoulos NT. CD40 induces renal cell carcinoma-specific differential regulation of TRAF proteins, ASK1 activation and JNK/p38-mediated, ROS-dependent mitochondrial apoptosis. *Cell Death Discov* (2019) **5**: doi:10.1038/s41420-019-0229-8
59. Curran KJ, Seinstra BA, Nikhamin Y, Yeh R, Usachenko Y, Van Leeuwen DG, Purdon T, Pegram HJ, Brentjens RJ. Enhancing antitumor efficacy of chimeric antigen receptor T cells through constitutive CD40L expression. *Mol Ther* (2015) **23**:769–778. doi:10.1038/mt.2015.4
60. Higham EM, Wittrup KD, Chen J. Activation of Tolerogenic Dendritic Cells in the Tumor Draining Lymph Nodes by CD8 + T Cells Engineered to Express CD40 Ligand . *J Immunol* (2010) **184**:3394–3400. doi:10.4049/jimmunol.0903111
61. Elmetwali T, Salman A, Wei W, Hussain SA, Young LS, Palmer DH. CD40L membrane retention enhances the immunostimulatory effects of CD40 ligation. *Sci Rep* (2020) **10**:1–15. doi:10.1038/s41598-019-57293-y
62. Kuhn NF, Purdon TJ, van Leeuwen DG, Lopez A V., Curran KJ, Daniyan AF, Brentjens RJ. CD40 Ligand-Modified Chimeric Antigen Receptor T Cells Enhance Antitumor Function by Eliciting an Endogenous Antitumor Response. *Cancer Cell* (2019) **35**:473-488. doi:10.1016/j.ccell.2019.02.006

63. Boćko D, Kosmaczewska A, Ciszak L, Teodorowska R, Frydecka I. CD28 costimulatory molecule - Expression, structure and function. *Arch Immunol Ther Exp (Warsz)* (2002) **50**:169–177.
64. Karmann K, Hughes CCW, Schechner J, Fanslow WC, Pober JS. CD40 on human endothelial cells: Inducibility by cytokines and functional regulation of adhesion molecule expression. *PNAS* (1995) **92**:4342–4346.
65. Hamzah J, Nelson D, Moldenhauer G, Arnold B, Hämmerling GJ, Ganss R. Vascular targeting of anti-CD40 antibodies and IL-2 into autochthonous tumors enhances immunotherapy in mice. *J Clin Invest* (2008) **118**:1691–1699. doi:10.1172/JCI33201
66. Eriksson E, Moreno R, Milenova I, Liljenfeldt L, Dieterich LC, Christiansson L, Karlsson H, Ullenhag G, Mangsbo SM, Dimberg A, et al. Activation of myeloid and endothelial cells by CD40L gene therapy supports T-cell expansion and migration into the tumor microenvironment. *Gene Ther* (2017) **24**:92–103. doi:10.1038/gt.2016.80
67. Hess S, Engelmann H. A novel function of CD40: Induction of cell death in transformed cells. *J Exp Med* (1996) **183**:159–167.
68. Lee J, Seki N, Sayers TJ, Subleski J, Gruys EM, Murphy WJ, Wiltrout RH. Constitutive expression of functional CD40 on mouse renal cancer cells : Induction of Fas and Fas-mediated killing by CD40L &. (2005) **235**:145–152. doi:10.1016/j.cellimm.2005.08.029
69. Schlenker R. Chimeric co-stimulatory receptors as a strategy to improve the performance of T cells in the tumor environment. Turning PD-1-mediated inhibition into activation. (2015) Available at: https://edoc.ub.uni-muenchen.de/21381/1/Schlenker_Ramona.pdf
70. Schlenker R, Olguín-Contreras LF, Leisegang M, Schnappinger J, Disovic A, Ruhland S, Nelson PJ, Leonhardt H, Harz H, Wilde S, et al. Chimeric PD-1:28 receptor upgrades low-avidity T cells and restores effector function of tumor-infiltrating lymphocytes for adoptive cell therapy. *Cancer Res* (2017) **77**:3577–3590. doi:10.1158/0008-5472.CAN-16-1922
71. Leisegang M, Engels B, Meyerhuber P, Kieback E, Sommermeyer D, Xue SA, Reuß S, Stauss H, Uckert W. Enhanced functionality of T cell receptor-redirected T cells is defined by the transgene cassette. *J Mol Med* (2008) **86**:573–583. doi:10.1007/s00109-008-0317-3
72. Bürdek M, Spranger S, Wilde S, Frankenberger B, Schendel DJ, Geiger C. Three-day dendritic cells for vaccine development: Antigen uptake, processing and presentation. *J Transl Med* (2010) **8**:1–13. doi:10.1186/1479-5876-8-90
73. Lodish UH, Lodish H, Berk A, Kaiser CA, Kaiser C, Krieger M, Kaiser UCA, Scott MP, Bretscher A, Ploegh H, et al. *Molecular Cell Biology*. W. H. Freeman (2008). Available at: <https://books.google.de/books?id=K3JbjG1JiUMC>

74. Hombach A, Hombach AA, Abken H. Adoptive immunotherapy with genetically engineered T cells: Modification of the IgG1 Fc spacer domain in the extracellular moiety of chimeric antigen receptors avoids off-target activation and unintended initiation of an innate immune response. *Gene Ther* (2010) **17**:1206–1213. doi:10.1038/gt.2010.91
75. Razinia Z, Mäkelä T, Yläne J, Calderwood DA. Filamins in mechanosensing and signaling. *Annu Rev Biophys* (2012) **41**:227–246. doi:10.1146/annurev-biophys-050511-102252
76. Zhang T, Barber A, Sentman CL. Generation of antitumor responses by genetic modification of primary human T cells with a chimeric NKG2D receptor. *Cancer Res* (2006) **66**:5927–5933. doi:10.1158/0008-5472.CAN-06-0130
77. Johnson-Léger C, Christensen J, Klaus GGB. CD28 co-stimulation stabilizes the expression of the CD40 ligand on T cells. *Int Immunol* (1998) **10**:1083–1091. doi:10.1093/intimm/10.8.1083
78. Frentsch M, Stark R, Matzmohr N, Meier S, Durlanik S, Schulz AR, Stervbo U, Jürchott K, Gebhardt F, Heine G, et al. CD40L expression permits CD8+ T cells to execute immunologic helper functions. *Blood* (2013) **122**:405–412. doi:10.1182/blood-2013-02-483586
79. van Kooten C, Banchereau J. CD40-CD40 ligand. *J Leukoc Biol* (2000) **67**:2–17. doi:10.1016/j.molmed.2008.09.006
80. Kawabe T, Matsushima M, Hashimoto N, Imaizumi K, Hasegawa Y. CD40/CD40 ligand interactions in immune responses and pulmonary immunity. *Nagoya J Med Sci* (2011) **73**:69–78. doi:10.18999/nagjms.73.3-4.69
81. Wilde S, Sommermeyer D, Frankenberger B, Schiemann M, Milosevic S, Spranger S, Pohla H, Uckert W, Busch DH, Schendel DJ. Dendritic cells pulsed with RNA encoding allogeneic MHC and antigen induce T cells with superior antitumor activity and higher TCR functional avidity. *Blood* (2009) **114**:2131–2139. doi:10.1182/blood-2009-03-209387
82. Kretschmer B, Kühl S, Fleischer B, Breloer M. Activated T cells induce rapid CD83 expression on B cells by engagement of CD40. *Immunol Lett* (2011) **136**:221–227. doi:10.1016/j.imlet.2011.01.013
83. Gerlach AM, Steimle A, Krampen L, Wittmann A, Gronbach K, Geisel J, Autenrieth IB, Frick JS. Role of CD40 ligation in dendritic cell semimatururation. *BMC Immunol* (2012) **13**: doi:10.1186/1471-2172-13-22
84. Acuto O, Michel F. CD28-mediated co-stimulation: A quantitative support for TCR signalling. *Nat Rev Immunol* (2003) **3**:939–951. doi:10.1038/nri1248

85. Rao RR, Li Q, Odunsi K, Shrikant PA. The mTOR Kinase Determines Effector versus Memory CD8+ T Cell Fate by Regulating the Expression of Transcription Factors T-bet and Eomesodermin. *Immunity* (2010) **32**:67–78. doi:10.1016/j.immuni.2009.10.010
86. Frauwirth KA, Riley JL, Harris MH, Parry R V, Rathmell JC, Plas DR, Elstrom RL, June CH, Thompson CB. The CD28 Signaling Pathway Regulates Glucose Metabolism ability of resting cells to take up and utilize nutrients at levels sufficient to maintain viability (Rathmell et al in fat and muscle cells insulin induces glucose uptake in excess of that required. *Immunity* (2002) **16**:769–777.
87. Menk A V., Scharping NE, Moreci RS, Zeng X, Guy C, Salvatore S, Bae H, Xie J, Young HA, Wendell SG, et al. Early TCR Signaling Induces Rapid Aerobic Glycolysis Enabling Distinct Acute T Cell Effector Functions. *Cell Rep* (2018) **22**:1509–1521. doi:10.1016/j.celrep.2018.01.040
88. Pauken KE, Wherry EJ. Overcoming T cell exhaustion in infection and cancer. *Trends Immunol* (2015) **36**:265–276. doi:10.1016/j.it.2015.02.008
89. Butte MJ, Keir ME, Phamduy TB, Sharpe AH, Freeman GJ. Programmed Death-1 Ligand 1 Interacts Specifically with the B7-1 Costimulatory Molecule to Inhibit T Cell Responses. *Immunity* (2007) **27**:111–122. doi:10.1016/j.immuni.2007.05.016
90. Bour-Jordan H, Bluestone JA. CD28 function: A balance of costimulatory and regulatory signals. *J Clin Immunol* (2002) **22**:1–7. doi:10.1023/A:1014256417651
91. Boomer JS, Green JM. An enigmatic tail of CD28 signaling. *Cold Spring Harb Perspect Biol* (2010) **2**:1–21. doi:10.1101/cshperspect.a002436
92. Driessens G, Kline J, Gajewski TF. Costimulatory and coinhibitory receptors in anti-tumor immunity. *Immunol Rev* (2009) **229**:126–144. doi:10.1111/j.1600-065X.2009.00771.x
93. Redeker A, Arens R. Improving adoptive T cell therapy: The particular role of T cell costimulation, cytokines, and post-transfer vaccination. *Front Immunol* (2016) **7**:1–17. doi:10.3389/fimmu.2016.00345
94. Maude SL, Frey N, Shaw PA, Aplenc R, Barrett DM, Bunin NJ, Chew A, Gonzalez VE, Zheng Z, Lacey SF, et al. Chimeric Antigen Receptor T Cells for Sustained Remissions in Leukemia. *N Engl J Med* (2014) **371**:1507–1517. doi:10.1056/nejmoa1407222
95. Ankri C, Shamalov K, Horovitz-Fried M, Mauer S, Cohen CJ. Human T Cells Engineered To Express a Programmed Death 1/28 Costimulatory Retargeting Molecule Display Enhanced Antitumor Activity. *J Immunol* (2013) **191**:4121–4129. doi:10.4049/jimmunol.1203085

96. Figel A, Brech D, Prinz PU, Lettenmeyer UK, Eckl J, Turqueti-neves A, Mysliwietz J, Anz D, Rieth N, Muenchmeier N, et al. Human Renal Cell Carcinoma Induces a Dendritic Cell Subset That Uses T-Cell Crosstalk for Tumor-Permissive Milieu Alterations. *AJPA* (2011) **179**:436–451. doi:10.1016/j.ajpath.2011.03.011
97. Oda SK, Daman AW, Garcia NM, Wagener F, Schmitt TM, Tan X, Chapuis AG, Greenberg PD. A CD200R-CD28 fusion protein appropriates an inhibitory signal to enhance T-cell function and therapy of murine leukemia. *Blood* (2017) **130**:2410–2419. doi:10.1182/blood-2017-04-777052
98. Song J, Lei FT, Xiong X, Haque R. Intracellular signals of T cell costimulation. *Cell Mol Immunol* (2008) **5**:239–247. doi:10.1038/cmi.2008.30
99. Von Heijne G. Membrane-protein topology. *Nat Rev Mol Cell Biol* (2006) **7**:909–918. doi:10.1038/nrm2063
100. Golmohammadi SK, Kurgan L, Crowley B, Reformat M. Classification of cell membrane proteins. *Proc Front Conver Biosci Inf Technol FBIT 2007* (2007)153–158. doi:10.1109/FBIT.2007.21
101. Almåsbaek H, Walseng E, Kristian A, Myhre MR, Suso EM, Munthe LA, Andersen JT, Wang MY, Kvalheim G, Gaudernack G, et al. Inclusion of an IgG1-Fc spacer abrogates efficacy of CD19 CAR T cells in a xenograft mouse model. *Gene Ther* (2015) **22**:391–403. doi:10.1038/gt.2015.4
102. Yacoub D, Benslimane N, Al-Zoobi L, Hassan G, Nadiri A, Mourad W. CD154 is released from t-cells by a disintegrin and metalloproteinase domain-containing protein 10 (ADAM10) and ADAM17 in a CD40 protein-dependent manner. *J Biol Chem* (2013) **288**:36083–36093. doi:10.1074/jbc.M113.506220
103. Tyshchuk O, Völger HR, Ferrara C, Bulau P, Koll H, Mølhøj M. Detection of a phosphorylated glycine-serine linker in an IgG-based fusion protein. *MAbs* (2017) **9**:94–103. doi:10.1080/19420862.2016.1236165
104. Reddy Chichili VP, Kumar V, Sivaraman J. Linkers in the structural biology of protein-protein interactions. *Protein Sci* (2013) **22**:153–167. doi:10.1002/pro.2206
105. Popowicz GM, Schleicher M, Noegel AA, Holak TA. Filamins: promiscuous organizers of the cytoskeleton. *Trends Biochem Sci* (2006) **31**:411–419. doi:10.1016/j.tibs.2006.05.006
106. Dalton AC, Barton W a. Over-expression of secreted proteins from mammalian cell lines. *Protein Sci* (2014) **23**:517–25. doi:10.1002/pro.2439
107. Lord JM. Go outside and see the proteasome. Protein degradation. *Curr Biol* (1996) **6**:1067–1069.

108. Ford GS, Barnhart B, Shone S, Covey LR. Regulation of CD154 (CD40 ligand) mRNA stability during T cell activation. *J Immunol* (1999) **162**:4037–44. Available at: <http://www.ncbi.nlm.nih.gov/pubmed/10201926>
109. Chess L. “Blockade of The CD40L / CD40 Pathway,” in *Therapeutic Immunology 2nd edition*, 441–456.
110. Ma DY, Clark E a. The role of CD40 and CD40L in Dendritic Cells. *Semin Immunol* 2009 (2010) **21**:265–272. doi:10.1016/j.smim.2009.05.010.The
111. Elgueta R, Benson MJ, De Vries VC, Wasiuk A, Guo Y, Noelle RJ. Molecular mechanism and function of CD40/CD40L engagement in the immune system. *Immunol Rev* (2009) **229**:152–172. doi:10.1111/j.1600-065X.2009.00782.x
112. Prinz PU, Mendler AN, Masouris I, Durner L, Oberneder R, Noessner E. High DGK- α and Disabled MAPK Pathways Cause Dysfunction of Human Tumor-Infiltrating CD8 + T Cells That Is Reversible by Pharmacologic Intervention. *J Immunol* (2012) **188**:5990–6000. doi:10.4049/jimmunol.1103028
113. Salmond RJ, Emery J, Okkenhaug K, Zamoyska R. MAPK, Phosphatidylinositol 3-Kinase, and Mammalian Target of Rapamycin Pathways Converge at the Level of Ribosomal Protein S6 Phosphorylation to Control Metabolic Signaling in CD8 T Cells. *J Immunol* (2009) **jimmunol.0902294**. doi:10.4049/jimmunol.0902294
114. Sulić S, Panić L, Barkić M, Merćep M, Uzelac M, Volarević S. Inactivation of S6 ribosomal protein gene in T lymphocytes activates a p53-dependent checkpoint response. *Genes Dev* (2005) **19**:3070–3082. doi:10.1101/gad.359305
115. Stein PH, Fraser JD, Weiss A. The cytoplasmic domain of CD28 is both necessary and sufficient for costimulation of interleukin-2 secretion and association with phosphatidylinositol 3'-kinase. *Mol Cell Biol* (1994) **14**:3392–3402. doi:10.1128/mcb.14.5.3392
116. Kuiper HM, de Jong R, Brouwer M, Lammers K, Wijdenes J, van Lier RA. Influence of CD28 co-stimulation on cytokine production is mainly regulated via interleukin-2. *Immunology* (1994) **83**:38–44. Available at: <http://www.ncbi.nlm.nih.gov/pubmed/7821964><http://www.pubmedcentral.nih.gov/articlerender.fcgi?artid=PMC1415021>
117. Leisegang M, Turqueti-Neves A, Engels B, Blankenstein T, Schendel DJ, Uckert W, Noessner E. T-cell receptor gene-modified T cells with shared renal cell carcinoma specificity for adoptive T-cell therapy. *Clin Cancer Res* (2010) **16**:2333–2343. doi:10.1158/1078-0432.CCR-09-2897
118. Silacci M, Baenziger-Tobler N, Lembke W, Zha W, Batey S, Bertschinger J, Grabulovski D. Linker length matters, Fynomer-Fc fusion with an optimized linker displaying picomolar IL-17A inhibition potency. *J Biol Chem* (2014) **289**:14392–14398. doi:10.1074/jbc.M113.534578

119. Yee C, Thompson JA, Byrd D, Riddell SR, Roche P, Celis E, Greenberg PD. Adoptive T cell therapy using antigen-specific CD8+ T cell clones for the treatment of patients with metastatic melanoma: In vivo persistence, migration, and antitumor effect of transferred T cells. *Proc Natl Acad Sci U S A* (2002) **99**:16168–16173. doi:10.1073/pnas.242600099
120. Ribas A, Shin DS, Zaretsky J, Frederiksen J, Cornish A, Avramis E, Seja E, Kivork C, Siebert J, Kaplan-Lefko P, et al. PD-1 blockade expands intratumoral memory T cells. *Cancer Immunol Res* (2016) **4**:194–203. doi:10.1158/2326-6066.CIR-15-0210
121. Kalos M, June CH. Adoptive T Cell Transfer for Cancer Immunotherapy in the Era of Synthetic Biology. *Immunity* (2013) **39**:49–60. doi:10.1016/j.immuni.2013.07.002
122. Rakhmilevich AL, Alderson KL, Sondel PM. T-cell-independent antitumor effects of CD40 ligation. *Int Rev Immunol* (2012) **31**:267–278. doi:10.3109/08830185.2012.698337

Acknowledgements

This has been quite a journey and I'm very thankful with everybody that supported me during all this time.

First of all, I would like to thank Prof. Dr. Elfriede Nöβner. For her trust and support in every single step of the way, for giving me the chance to dive in in such an amazing project, for all the interesting talks and discussions, and most of all, for never losing hope, always believing in me and giving me great tools to be a better scientist.

There are not enough words to thank Anna Mendler, Petra Prinz, Giulia Longinotti and Ramona Schlenker, not only for all the things I learned from them, but for becoming part of my family and my main support whenever I needed it, you pushed me to not only be a great scientist, but to never forget that the best things in life are the ones we can share and enjoy with the people we care about.

Thanks to Ilias Masouris, an amazing and trustworthy friend, for all the great life experiences. There is no dark side, nor a light side, there is only the force!

I also wish to thank Anna Brandl and Barbara Mosetter for their tremendous help, assistance and collaboration during my work time in the lab.

Many thanks to Adam Slusarski, Anja Disovic and Michael Hagemann for their long hours of help and support during the *in vivo* experiments.

Special thanks to Matthias Leisegang and Kordelia Hummel for all their help and advice during my research stay in Berlin.

Thank you also to Grzegorz Popowicz for his valuable advice regarding our chimeric protein design strategy.

I'm really thankful with Susanne Wilde for all her help before and after I came to Germany, she was a key factor for me to join the team at Helmholtz Zentrum München back in 2013.

Thanks a lot to all the blood donors that contributed for my experiments, specially Julia Schorisch, who became my favorite donor, great cells Schori!.

I would also like to thank all the amazing people that I got to know during all my years in the Institute, Dorothee Brech, Julia Schnappinger, Julia Schorisch, Anja

Disovic, Nadja Sailer, Nadine Hömberg, Fatima Ahmetlic, Nina Deppisch, Andrew Flatley, Svenja Rühland, Julia Wolst and all bachelor and master students I met along the way. I've always said that doing what you love is not enough if you are not surrounded by a great team and colleagues. You all outmatched by far this point, with all the good times during work, extra hours and of course the time we all spent together outside work. Simply amazing!

But most important of all, I want to deeply thank my family.

To my parents that no matter what, they have always been there by my side, supporting me, loving me and pushing me to go out to the world and fulfill my dreams. To my mom who has always been my heart and soul, ready to go beyond anything whenever I needed her, she always knows how to calm my heart. To my dad, who unfortunately is no longer with us, he never hesitated to support each and every single one of my decisions, he was always my strength, my guide and partner of many adventures. To them I owe everything I am and everything I will ever be, that is why no matter where I am, every single achievement of my life goes to them. I love them with all my heart!

To my brother who has always been there through thick and thin, he is not only my partner in crime, but also my best friend. Life will always be a nice ride if he is on the co-pilot seat. Thanks for being such a great example, love you bro!

My family is my core, the source of all the good in me, my inspiration, my safe place and the reason to always keep moving forward. They taught me that knowledge is nothing without love, and that I should always be thankful for the simple things in life.

Mamá, gracias por nunca dejar de apoyarme y darme consuelo siempre que lo necesitaba, eres y siempre serás la fuerza en mi corazón.

Papá, siempre fuiste mi fuerza y mi brújula, siento tu abrazo lleno de orgullo y sé que nunca dejarás de estar a mi lado.

Juan, la vida me dio en ti al mejor compañero para enfrentar lo que venga, gracias por siempre estar.

¡LOS AMO CON TODO MI CORAZON!

List of publications

- Schlenker R., Olguin-Contreras L. F., Leisegang M., Schnappinger J., Disovic A., Rühland S., Nelson P.J., Leonhardt H., Harz H., Wilde S., Schendel D. J., Uckert W., Willimsky G., Noessner E. **Chimeric PD-1:28 receptor upgrades low-avidity T cells and restores effector function of tumor-infiltrating lymphocytes for adoptive cell therapy.** *Cancer Res.* **77**, 3577–3590 (2017).

Data of this thesis regarding the use of the CD40L:CD28 CCPs have been presented by me as first author in poster sessions of the international meetings mentioned below:

- 2016. 3rd Immunotherapy of Cancer Conference (ITOC-3) in Munich, March 21st -23rd. Olguin-Contreras Luis., Mendler Anna, Noessner Elfriede: **“Double strike approach for tumor attack: Improving T cell functionality and targeting tumor stroma.”**
- 2017. Keystone Symposia of Cancer Immunology and Immunotherapy: Taking a Place in Mainstream Oncology (C7) in Whistler, BC Canada, March 19th -23rd. Olguin-Contreras L., Mendler A., Schlenker R., Weisz S., Popowicz G., Noessner E.: **“Double strike approach for tumor attack: chimeric co-stimulatory receptors for enhanced tumor targeting.”**

The design of the different CD40L:CD28 CCPs are part of the patent WO2017/162797

The manuscript containing the data on this thesis has been accepted for publication in the journal *Frontiers in Immunology*.

Collaborations

- 2020. AACR Annual meeting. Collaboration presented by Dr. Nadja Sailer:

Sailer N., Salvermoser M., Gerget M., Thome S., Fischbeck A. J., Ruehland S., Olguin-Contreras L. F., Buerdek M., Ellinger C., Noessner E., Schendel D. J. & Kehler P. Abstract 3231: **“The chimeric co-stimulatory receptor PD1-41BB enhances the function of T cell receptor (TCR)-modified T cells targeting solid tumors.”** *Cancer Res.* **80**, 3231 LP – 3231 (2020).

Affidavit



Affidavit

Olguín Contreras Luis Felipe

Surname, first name

Street

Zip code, town, country

I hereby declare, that the submitted thesis entitled:

Double strike approach for tumor attack: Engineering T cells using CD40L:CD28 chimeric co-stimulatory proteins for enhanced tumor targeting in adoptive cell therapy.

is my own work. I have only used the sources indicated and have not made unauthorized use of services of a third party. Where the work of others has been quoted or reproduced, the source is always given.

I further declare that the submitted thesis or parts thereof have not been presented as part of an examination degree to any other university.

München, 12.11.2021

place, date

Luis Felipe Olguín Contreras

Signature doctoral candidate